DISEÑO E INTEGRACIÓN DE SENSORES ÓPTICOS EN INSTRUMENTACIÓN PORTÁTIL PARA ANÁLISIS DE GASES

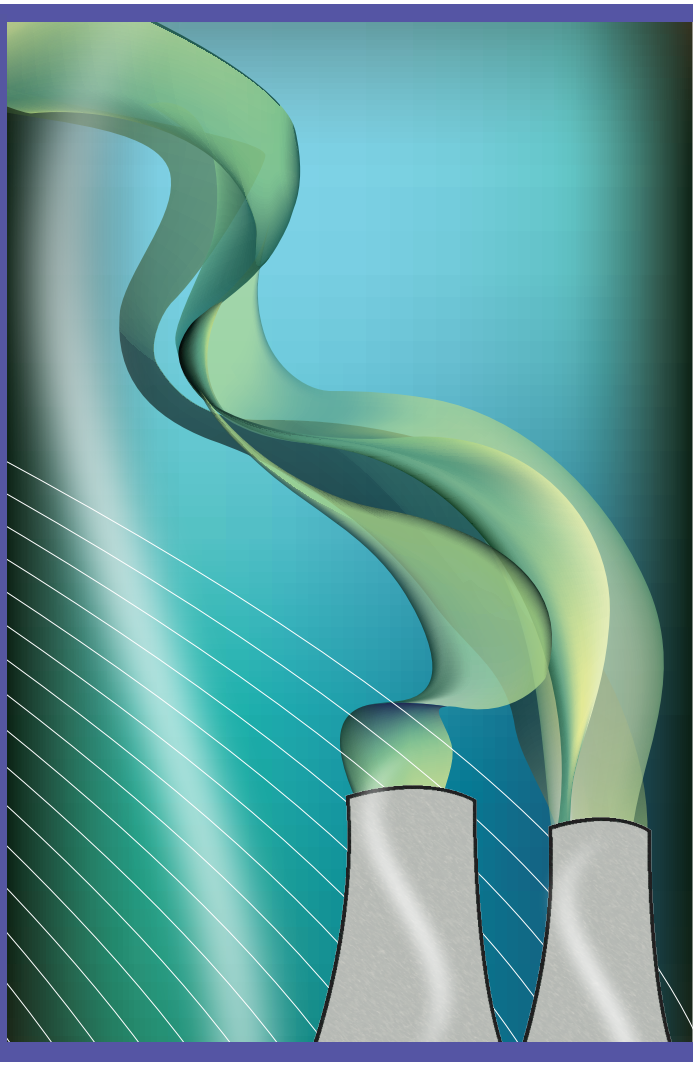

Tesis Doctoral

Isabel Mª Pérez de Vargas Sansalvador

Universidad de Granada
2011

UNIVERSIDAD DE GRANADA

DEPARTAMENTO DE QUÍMICA ANALÍTICA

DISEÑO E INTEGRACIÓN DE SENSORES ÓPTICOS EN INSTRUMENTACIÓN PORTÁTIL PARA ANÁLISIS DE GASES

TESIS DOCTORAL

Isabel Mª Pérez de Vargas Sansalvador

GRANADA, 2011

Editor: Editorial de la Universidad de Granada
Autor: Isabel María Pérez de Vargas Sansalvador
D.L.: GR 771-2012
ISBN: 978-84-694-5722-1

DISEÑO E INTEGRACIÓN DE SENSORES ÓPTICOS EN INSTRUMENTACIÓN PORTÁTIL PARA ANÁLISIS DE GASES

por

Isabel Mª Pérez de Vargas Sansalvador

Departamento de Química Analítica

Universidad de Granada

VISADO en Granada, a 5 de Mayo de 2011

Fdo.-
Prof. Dr. D. **Luis Fermín Capitán Vallvey**, Catedrático del Departamento de Química Analítica de la Universidad de Granada.

Prof. Dr. Dña. **Mª Dolores Fernández Ramos** Profesora Titular del Departamento de Química Analítica

Prof. Dr. D. **Alberto J. Palma López**, Profesor Titular del Departamento de Electrónica y Tecnología de Computadores de la Universidad de Granada.

MEMORIA presentada para aspirar al Grado de Doctor en Ciencias Químicas.
Granada, a 5 de Mayo de 2011

Fdo**.- Isabel Mª Pérez de Vargas Sansalvador**, Licenciada en Química.

A mis padres, mis hermanos y mi Yaya.

A Sergio.

Agradecimientos

En el transcurso de mi Tesis Doctoral, durante estos más de cuatro años, han pasado muchas cosas en mi vida, no sólo en el ámbito laboral sino también en el personal y no puedo terminarla sin mostrar mi agradecimiento a todas las personas que han estado conmigo durante este tiempo.

A mis directores, porque con nuestras discusiones y nuestro trabajo, con su ayuda, hemos conseguido sacar adelante esta Tesis.

A Fermín , de quien he aprendido tanto… que casi me quedo sin palabras para poder agradecérselo. Me ha demostrado que las cosas se consiguen con mucho trabajo y esfuerzo, que nada sale fácilmente, pero que con perseverancia, al final salen los resultados. Además es una persona humilde, a pesar de saber un montón; siempre se interesa por el trabajo, te da consejos y ayuda en todo lo posible y no sólo se ha preocupado por mi trabajo, sino también de mí. Da igual la hora a la que lo necesites, casi siempre lo encuentras en su despacho, ya sea tarde o temprano y siempre te atiende para lo que necesites. Muchas gracias por todo el tiempo que me ha dedicado, que es mucho; sin su ayuda, nada de esto hubiera sido posible.

A Loli, por animarme a continuar por este camino e intentar que viera las cosas un poco menos difíciles. Por estar pendiente de mis progresos y por contar conmigo. Por preocuparse por mi estancia en Dublín; siempre recibía correos de ánimo, diciendo que aprovechara y que era una experiencia inolvidable e interesándose por cómo me estaba yendo todo.

A Alberto, por la dedicación que le ha supuesto la dirección y supervisión de este trabajo.

A mis compañeros, con quienes he pasado muchos ratos (muchas más horas de las que correspondería) llegando a ser muchos de ellos más amigos que compañeros. Han sido muchas horas de trabajo, pero también de risas; con Enjuto (interneeeeeeet), Rocío Jurado… y muchas situaciones más.

En primer lugar quiero expresar mi agradecimiento a Miguel, que, aunque al principio no me hiciera caso, conseguí ganármelo comprándole unos Donuts; luego se convirtió en un gran amigo aunque a veces parecía mi jefe (ya sabes el porqué lo di-

go). Creo que me ha hecho una persona más responsable y nunca me podía imaginar lo que lo he echado de menos estos últimos meses que no ha estado en el laboratorio; muchas gracias por todo. A María, mi Enju, pues es mi niña del laboratorio (aunque Miguel en modo María Arenas también se nos acoplaba). Al principio no le hice caso alguno, pero poco a poco fue ganándome. Aparte de ser mi asesora personal para toda clase de eventos, es mi amiga, con la que siempre puedo contar. A Julio, el buenazo; he intentado enseñarle un poco de maldad pero es imposible, siempre dispuesto a ayudar en todo, anteponiendo lo de los demás a lo suyo. A Olga, que estuvo conmigo en los comienzos de esta andada y nos apoyamos mucho la una en la otra. A Antonio y Migue, mis electrónicos, que siempre han estado dispuestos a echar una mano y me han calmado en momentos de histeria cuando quería tirar los "cacharritos" por la ventana; no me podía haber tocado unos electrónicos mejores con los que trabajar. A Manuel, que aunque ha llegado hace poco, ya es uno más y me ha diseñado una portada muy chula. Mi agradecimiento también a Nuria, Sonia, Younes, Alfonso, Alejandro, Patri, Ismael y Joaquín.

A mis chicas de enfrente: Cristina, Carmen y Paulina, que siempre nos hemos tenido para cualquier cosa, para las alegrías y para las menos alegrías y donde dejamos esos gritos que nos damos de laboratorio a laboratorio, con los que supongo que debemos tener asustados a todo el Departamento.

A los profesores del Departamento, en especial a Alberto Navalón; cuántas veces he llamado a su puerta y siempre me he ido con una sonrisa. A Brigui, mi medio paisana, porque además de dejarme el cargador y contar conmigo en el proyecto de mentorización, tiene mucho arte y siempre me ha hecho reir. A Luis Cuadros, que siempre se interesa por cómo estás y además me ayudó con el límite de detección y a Mª Carmen Valencia, por su amabilidad y por permitirme tenerla frita con el árbol.

A Ignacio, por la llamada que me hizo un día, que estaba yo con mi familia en Tarifa, para saber qué era de mi vida y si me interesaría volver a la Universidad; sin esa llamada, yo no estaría hoy escribiendo esta Memoria, así que en gran parte es gracias a ti. Nunca has dejado de preocuparte por mí en este tiempo, incluso me has

regañado alguna vez que otra; lo importante es que siempre has estado pendiente de mi y dispuesto a ayudarme. Estas palabras son pocas para expresar mi gratitud.

I want to also thank Angela Tate, my English teacher, for helping me and because her classes are like a therapy, every Tuesday and Thursday I just looked at the time waiting for my class, wishing the time arrived because apart from learning a lot we laughed a lot every class.

And now that I'm writing in English, it reminds me of some wonderful people I met in Ireland. Dermot Diamond, thanks for giving me the opportunity to work there with such good people, for helping me and being interested in my work. Fernando Benito, you helped me a lot, you are such a funny person but at the same time so responsible and intelligent, thanks for looking after me during my stay there, all was easier with your help and I want to thank Lourdes also. Michele, Monika, Bartosz and Loli my "dream team" it was a gift to meet all of you, I miss you and the Spritz at Taste of Emilia and I have to admit that also the Guinness. I can't forgot Larissa (I remember the day we went to your house to have dinner, it was so funny) Andy (who tried to learn some Spanish, but just bad words), Vincenzo, Caroline, Simon C, Simon G, Clare, Cormac and Thomas. Mercedes, she is such a happy person and helpful, she spent lots of time speaking with Sergio about football. Loli, my Spanish friend in Ireland, we supported each other a lot and becacuse of that all was easier. I just want to say that I miss you all, our coffees in the Helix, Guinness at GraveDiggers and many more things.

A mis amigas de Algeciras, como a mis amigos granadinos, por los buenos ratos que pasamos juntos y lo mucho que me han ayudado, aunque no se dieran cuenta. Conchita, gracias por venirte conmigo la primera semana a Dublín y por ayudarme siempre que necesitaba una manilla en inglés y por otras muchas cosas.

A mi familia, en general, por preocuparse siempre de mí y de cómo iba mi Tesis.

A mis padres, que en gran medida gracias a ellos soy la persona que hoy soy. Siempre han estado conmigo en mis decisiones, me han aconsejado y apoyado. Re-

cuerdo a mi padre preguntándome por qué no estudiaba mejor Ingeniería Química en Algeciras, que para qué me iba a ir a Granada y yo responderle que a mí lo que me gusta es la Química, pura Química y bueno, pues para Granada. Al final acabamos Mamá, la Yaya y yo, bueno todos, llorando el día que me fui; mirad a dónde ha llevado todo (sí que era verdad que me gustaba, eh?). Os doy las gracias porque sois unos padres geniales y porque con sólo miraros sé que estáis orgullosos de mí y eso me hace muy feliz.

A mi Yaya, que aunque no está físicamente, sé que estás conmigo y siempre te llevaré en mi corazón. No hay día que no me acuerde de ti y muchas veces me acuesto deseando soñar contigo para poder verte otra vez.

A mis hermanos, Ignacito, Julita y Albertito, que siempre han cuidado de mí; es la ventaja de ser la peque, aunque también me han hecho alguna perrería. Siempre me están preguntando si he inventado algo para hacernos ricos y quitarlos así de trabajar; me parece a mí que tendrán que confiar en otra persona para ese propósito. Lo importante es que nos tenemos los unos a los otros y eso ya nos hace ricos.

A Montse, Juanma y Luci, que han pasado a formar parte de nuestra familia y no me imagino a unos cuñados mejores; bueno, mejor que Juanma sí, pero lo aceptamos.

A mis peques: José Alberto, Alvarito, Nico, Nacho (conocido también como Ignacito Iso) y Julisa. Siento haberme perdido muchas cosas por vivir lejos de vosotros y me hubiera gustado pasar más tiempo jugando con todos; aún así, hemos aprovechado muchos fines de semana en Algeciras, Madrid y también alguno en Granada.

A Sergio, mi niño, que ha soportado día a día los altibajos que he ido teniendo, que no han sido pocos. Me has animado a continuar. Has estado conmigo siempre y me has ayudado a superar etapas difíciles. Siempre me dices lo orgulloso que estás de mí y eso me da fuerzas. Me siento muy afortunada por tenerte a mi lado. Me siento débil cuando… (ya sabes como sigue). Gracias por todo, cariño.

Bueno, no sé si me olvido de alguien, pero como siga escribiendo agradecimientos, al final van a ser más largos que la propia Tesis. En definitiva, gracias a todos.

Índice

Capítulo 6

Objetivos

Esta Tesis Doctoral se centra en el estudio de sensores para gases e instrumentación portátil asociada. El objetivo general que persigue es el desarrollo de sensores ópticos para gases, en concreto para dióxido de carbono, que serán caracterizados mediante instrumentación de sobremesa para posteriormente ser implementados en instrumentación portátil con el objetivo de fácil uso y bajo coste. Se ensayarán diversos modos de transducción del reconocimiento de dióxido de carbono: fosforescencia y absorción de radiación; diversas aproximaciones instrumentales: LED-fotodetector y LED-LED; diversos modos: monoanalito y multianalito y diversas aplicaciones: gases atmosféricos y gases edáficos.

Para lograr el objetivo general se plantean un conjunto de objetivos específicos que pretenden ir desarrollando diferentes aspectos del mismo:

1. Preparar y caracterizar membranas sensoras ópticas para dióxido de carbono basadas en la medida de fosforescencia.

2. Desarrollar una instrumentación portátil optoelectrónica para la determinación de dióxido de carbono evaluando diferentes posibilidades de inclusión de las químicas de reconocimiento previamente estudiadas.

3. Caracterizar analíticamente los prototipos puestos a punto estableciendo y modelando la influencia de la temperatura.

4. Diseñar una instrumentación portátil multianalito para oxígeno y dióxido de carbono basándose en experiencias previas del grupo con el objetivo de usar el mismo principio de medida.

5. Explorar la técnica de medida PEDD para poner a punto un sistema instrumental para la medida de dióxido de carbono en gases.

6. Poner a punto una sonda para la medida de oxígeno edáfico y tras caracterizarla valorar su utilidad para la medida de oxígeno, humedad y temperatura en suelos cultivados.

Capítulo 1

Introducción

Gases y vapores

La palabra gas tiene su origen en la palabra griega *chaos* (estado primitivo del universo) usada por el químico flamenco Jan Baptist van Helmont (Bruselas, 1580 – Vilvorde, 1644) para designar el fluido que se origina por combustión de leña o carbón y modificada por la pronunciación en lengua flamenca de dicha palabra. Aunque van Helmont identifica a los gases como entidades químicas individuales diferentes del aire, la comparación con la idea actual de gas termina aquí.

Un gas es un estado de la materia que se encuentra entre los estados líquidos y plasma, siendo la gran separación entre las partículas individuales comparadas con su tamaño lo que los diferencia de líquidos y sólidos. Esto justifica que, en una primera aproximación, las propiedades físicas de un gas (volumen, presión, temperatura, número de moléculas) no dependan del gas particular. Están caracterizados por una densidad y viscosidad relativamente bajas y una gran capacidad para sufrir expansiones y contracciones con los cambios de temperatura y presión. Su capacidad para difundirse con facilidad justifica su tendencia espontánea a distribuirse uniformemente.

En el caso de que un fluido gaseoso tenga una temperatura inferior a su temperatura crítica, su presión no aumenta al ser comprimido, sino que se transforma parcialmente en líquido. En este caso, hablamos de vapor.

Actualmente la determinación de gases y vapores es una necesidad rutinaria en Química Analítica y existen multitud de situaciones en las que debe obtenerse información acerca de qué gases o vapores se encuentran presentes en una atmósfera determinada o disueltos en un líquido y en qué proporción.

Lo más inmediato es la atmósfera, especialmente la homosfera que ocupa los 100 km inferiores y tiene una composición constante y uniforme debido a fenómenos de mezcla convectiva y turbulenta. Está compuesta mayoritariamente por tres gases: nitrógeno (78%), oxígeno (21%) y argón (1%) y minoritariamente por otros gases como dióxido de carbono, monóxido de carbono,

metano, ozono y otros. Existiendo además vapores como el de agua en proporción muy variable, así como diversos sólidos y líquidos.

Un problema especialmente grave relacionado con ciertos gases lo constituye el llamado efecto invernadero, por el que se conoce a la subida de temperatura de la superficie terrestre y la atmósfera inferior debido a la presencia o aumento de concentración de ciertos gases -gases invernadero- en la atmósfera, así agua, dióxido de carbono, óxidos de nitrógeno, metano o hidrocarburos fluorados entre otros, que absorben radiación infrarroja que en otro caso escaparía al espacio. Este efecto invernadero es importante, pues sin él la Tierra no dispondría de suficiente calor para permitir la vida, pero si llega a ser demasiado intenso, como ha comenzado a ser el caso, se originan problemas para toda la biosfera. La importancia de este problema ha exigido la adopción de acuerdos internacionales como el Protocolo de Kyoto, realmente llamado Kyoto Protocol to the United Nations Framework Convention on Climate Change.

Las causas del incremento en la concentración de gases de efecto invernadero son muy variadas, siendo la más importante la de dióxido de carbono como consecuencia del empleo de combustibles fósiles (carbón, petróleo y derivados, gases, etc.) para la obtención de energía, aunque la deforestación y el cambio en el uso de la tierra también han contribuido.

Así, la cantidad de dióxido de carbono liberada a la atmósfera ha estado aumentando considerablemente durante los últimos 150 años. Como resultado, ha excedido la cantidad absorbible por la biomasa, los océanos y otros sumideros, por lo que ha habido un aumento en su concentración en la atmósfera de unos 280 mg/l en 1850 pasando a 316,38 mg/l en 1959 y a 391,76 mg/l en este año 2011.

Con objeto de comparar la capacidad de diferentes gases invernadero, se usa el concepto de potencial de calentamiento global (GWP) definido como el cociente entre el calor absorbido por unidad de masa de un gas dado y el de la unidad de masa del dióxido de carbono.

Otro gas de efecto invernadero de importancia es el óxido nitroso de larga persistencia en la atmósfera (120 años) y mucha mayor capacidad para absorber calor (GWP 310), el cual tiene su origen tanto en diversos procesos naturales como antropogénicos, así usos agrícolas, combustiones o producción de ácido nítrico. El metano es un gas de efecto invernadero originado en procesos biológicos que ocurren en ambientes anaerobios y es una importante fuente de energía. Aunque su vida media en la atmósfera es corta (12 años), su GWP es de 21.

Además de estos gases, existen otros de efecto invernadero más intenso, los cuales se pueden clasificar en tres grupos: los conocidos como hidrofluorocarbonos, realmente hidrocarburos fluorados, los perfluorocarbonos, realmente perfluorohidrocarburos, y el hexafluoruro de azufre.

Los hidrofluorocarbonos son un grupo de compuestos químicos de gran uso industrial, comercial y de consumo, muchos de los cuales se han desarrollado como alternativa a compuestos del tipo clorofluorocarbonos. Compuestos estos últimos que tienen gran incidencia en la disminución en la concentración de ozono en las capas altas de la atmósfera. El GWP de los hidrofluorocarbonos varia entre amplios márgenes que va desde 140 (HFC-152a) hasta 11.700 (HFC-23), con unos valores de vida media que oscilan entre un año para el HFC-152a a 260 años para el HFC-23.

Los perfluorocarbonos tienen su origen en diversos procesos industriales como la producción de aluminio y la fabricación de semiconductores, siendo los más habituales el tetrafluorometano y el hexafluoroetano (GWP 6.500 y 9.200 y una vida media de 50.000 y 10.000 años, respectivamente). El hexafluoruro de azufre es el gas invernadero más potente con un GWP de 23.900 y su concentración en la atmósfera se incrementa debido a su uso como aislante eléctrico, también en la fabricación de magnesio para aislarlo de la atmósfera cuando está fundido y en la industria de semiconductores.

Además de los gases que presentan el problema específico de actuar como gases de efecto invernadero, existen otra multitud de situaciones en las que se pueden generar gases que originan otros tipos de problemas.

Uno de ellos es el relativo a procesos de combustión que aparecen implicados en muy diversas situaciones y que generan diversos tipos de gases de los que algunos, principalmente dióxido de carbono, están implicados en el efecto invernadero. Se utilizan procesos de combustión principalmente en plantas de energía de combustión, vehículos, calefacciones industriales y domésticas, y los problemas que originan no son solo ambientales.

Por ejemplo, en procesos de combustión en el hogar que tienen su origen en cocinas y hornos tanto eléctricos como de gas o aceite y, en menor medida aunque no despreciable, leña o carbón. Como consecuencia de los procesos de cocinado y preparación de alimentos en general, se generan toda una serie de gases y vapores, algunos de los cuales presentan problemas para la salud, entre los que se encuentran monóxido de carbono, hidrocarburos, hidrocarburos aromáticos policíclicos, aldehídos, dióxido de azufre, sulfuro de hidrógeno, óxidos de nitrógeno y partículas en suspensión. El problema en este caso, no son los gases que escapen a la atmósfera sino los que permanezcan en el edificio por su incidencia sobre la salud a corto o largo plazo.

Un caso aparte lo constituyen los gases industriales cuyas principales usos se encuentran en la industria, medicina y aplicaciones ambientales. La razón del empleo de estos gases reside en su reactividad, en su inercia o bien como gases licuados por su capacidad para producir frío. Entre los primeros se encuentra el oxígeno, hidrógeno, metano, monóxido de carbono y dióxido de carbono usados en diferentes procesos industriales como procesados de metales o síntesis química. El nitrógeno y el argón son los más usados como gases inertes para el almacenamiento de productos inflamables bajo atmósfera de ellos o bien de productos degradables al aire como aceites vegetales o fragancias. Igualmente, el dióxido de carbono se usa por su inercia química para la extinción de incendios. Como gases licuados se usan nitrógeno y dióxido de carbono que combinan una frialdad intensa con gran inercia por lo que se usan para congelación industrial, así en alimentación o estudios biomédicos, de forma que no se altere la calidad del producto o se minimice el daño celular.

Por otro lado, en medicina tiene gran importancia la determinación de gases en sangre, principalmente en sangre arterial y más raramente en sangre venosa. Estos gases son oxígeno y dióxido de carbono. La determinación de la presión parcial de ambos gases, junto con el valor del pH, permite obtener información de gran interés acerca de las funciones respiratorias del paciente. El dióxido de carbono juega un papel esencial en la respiración celular y en la regulación del pH fisiológico, por lo que la monitorización del dióxido de carbono en pacientes se realiza de manera rutinaria en hospitales y especialmente en las unidades de cuidados intensivos. La medida de dióxido de carbono se ha utilizado para evaluar la microcirculación y las alteraciones microcirculatorias en pacientes críticos pues se ha sugerido que la hipercarbia es un indicador universal de perfusión reducida de forma crítica en tejidos [1], habiéndose propuesto la mucosa sublingual o la mucosa bucal como lugares apropiados para la medida de PCO_2 tisular y como medida de flujo de sangre microvascular [2,3].

Por las mismas razones anteriores es de gran importancia en muchos procesos industriales bioquímicos y microbiológicos, como pueden ser los procesos de fermentación, donde su control es crítico para obtener altos rendimientos y mínima formación de subproductos [4].

La mayor fuente de dióxido de carbono en la biosfera es la combustión generada por la industria, calentamientos domésticos, en incendios, por degradación de biomasa y fermentación. Los niveles de dióxido de carbono en los océanos son tan importantes como en la atmósfera. Los océanos ayudan a reducir el efecto del dióxido de carbono como gas de efecto invernadero y así disminuir el potencial del calentamiento global comportándose como una inmensa reserva de dióxido de carbono, sin embargo sus niveles en la atmósfera y en la hidrosfera no están en equilibrio, la relación de intercambio entre los dos depende de una gran variedad de parámetros como son presión atmosférica, viento, humedad y temperatura. La monitorización de los niveles de dióxido de carbono en la biosfera es de gran importancia en análisis medioambiental [5].

En la industria alimentaria, el envasado en atmósfera modificada es una técnica usada para prolongar la vida útil de productos frescos o mínimamente

procesados a través un cambio en la composición de la atmósfera que rodea el producto. Esta forma de envasado se usa de forma rutinaria en una amplia variedad de productos incluyendo pan, galletas, pasteles, pastas, dulces, café, té, alimentos secos, ahumados, productos lácteos, pastas precocinadas, etc.

El dióxido de carbono se usa habitualmente en este tipo de envasado pues es abundante y barato, fácilmente licuado (temperatura crítica = 31°C, presión critica = 72,9 atm), además niveles altos de dióxido de carbono tienen acción antimicrobiana reduciendo el metabolismo microbiano incluso si hay oxígeno presente.

El gas o mezcla de gases (oxígeno, dióxido de carbono, nitrógeno) usada depende del tipo de producto, material de envasado y temperatura de almacenamiento. En el caso de productos recién cortados o recogidos se usa la técnica de envasado en atmósfera con equilibrio modificado (*Equilibrium Modified Atmosphere Packaging*, EMAP), en la cual se suele disminuir el nivel de oxígeno y elevar el de dióxido de carbono, ralentizando la respiración normal del producto y aumentando de esta forma su vida útil [6]. La presión parcial de estos gases en la atmósfera del envasado sirve como indicador del estado de calidad del producto, valores que pueden cambiar en el tiempo influidos por el tipo de producto, respiración, material de envasado, tamaño del paquete, razón de volúmenes, condiciones de almacenamiento, integridad del embalaje, etc. [7].

Otro aspecto que no hay que olvidar es el empleo de multitud de productos químicos, muchos de los cuales no son en sí gases, aunque se vaporizan con facilidad o se usan en forma de aerosoles y que presentan gran incidencia en la salud. Así podemos citar el uso de plaguicidas en la agricultura, especialmente en la intensiva o la proyección de aislantes térmicos e impermeabilizantes en la construcción de edificios.

Un caso especial del empleo de gases y vapores es su uso en la guerra química y también para manejo y control de multitudes y en especial para control y represión de manifestaciones, donde encontramos desde gases letales

como los neurotóxicos, entre los que se encuentran los conocidos sarín y tabún, a incapacitantes como los lacrimógenos, estornudógenos o nauseosos.

Con este breve repaso se trata de poner de manifiesto que los gases y vapores están siempre presentes en nuestra sociedad y, como siempre, con una intencionalidad que depende del ser humano. Por ello, es necesario tanto el conocimiento como el control de estos compuestos.

Para el análisis tanto de gases como vapores y sus mezclas existen gran número de técnicas diferentes que no se van a referenciar en esta Introducción. Solo nos vamos a centrar en el empleo de sensores por el extraordinario desarrollo que han tenido, su amplio uso y el gran número de empresas que se dedican a ello y que constituyen por sí mismo un amplio campo de negocio.

Sensores químicos

Una de las tendencias actuales de la Química Analítica es la búsqueda de tecnologías que permitan desarrollar métodos de análisis rápidos, baratos, con instrumentación sencilla y a ser posible portátil que faciliten el análisis *in situ*, en tiempo real, simplificando todo el proceso analítico y descongestionando la realización de los análisis en el laboratorio que no sean realmente necesarios. Dentro de esta línea, la tecnología de sensores químicos ofrece un elevado potencial [8].

La primera cuestión que surge es establecer qué es un sensor. Desde hace bastante tiempo se vienen utilizando en el laboratorio sensores como puede ser el caso del electrodo de pH, que da lugar, mediante el uso del pH-metro, al mejor método que existe para su medida.

Los sensores pretenden de alguna manera emular o sustituir a los sentidos mediante los cuales los seres vivos interaccionan y se relacionan con el medio ambiente. Por ejemplo la nariz es un instrumento extremadamente selectivo y sensible, que es muy difícil de emular artificialmente. Lo que detectamos (olemos) por la nariz son pequeñas cantidades de partículas gaseosas. La consecución de una definición de sensor unánimemente aceptada ha dado lu-

gar a muchos debates y controversias por los muchos matices a que puede dar lugar. Una de las definiciones que en nuestra opinión mejor caracteriza el concepto y que se encuentra próxima a la definición de la IUPAC [9], es considerarlo un dispositivo capaz de registrar de forma directa, continua y reversible un parámetro físico (sensor físico) o la concentración o presencia de una especie química (sensor químico) [8,10-13].

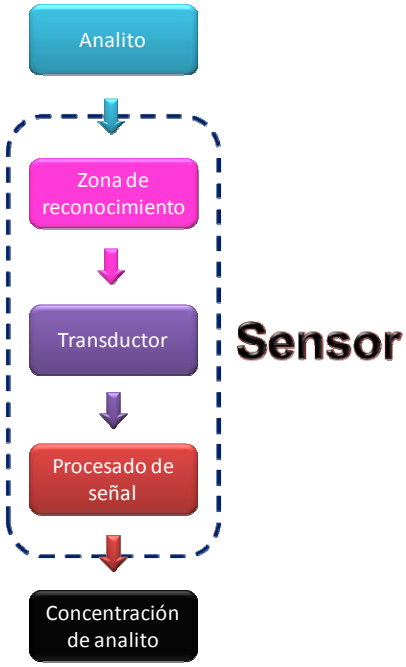

Figura 1. Modelo de sensor

Como vemos supone un cambio de paradigma en Química Analítica y aunque no siempre se cumple, tenemos que: 1) son dispositivos más que instrumentos; 2) suelen tener tamaño pequeño y ser portátiles; 3) integran detección y separación o reacción química, bioquímica o interacción biológica en la misma zona; y 4) se ponen en estrecho contacto con la muestra.

Los sensores químicos constan de un conjunto de elementos que se pueden agrupar en tres bloques básicos

1. Zona de reconocimiento: donde se produce la interacción selectiva con la especie o especies de interés. El elemento de reconocimiento es el componente clave de cualquier sensor. La interacción que allí se origina puede ser física, por ejemplo una radiación electromagnética con un analito capaz de absorberla o de generar luminiscencia o bien química o biológica, en los que se origina una reacción química entre el analito y los reactivos inmovilizados en ese elemento de reconocimiento originando como consecuencia de la variación negativa de energía libre que ha tenido lugar, variaciones en diversas propiedades físicas que servirán para su evaluación.
2. Sistema transductor: capaz de convertir la información química en una señal eléctrica que contenga información analítica útil
3. Sistema de amplificación y procesado de la señal, con lo que obtenemos los resultados en las unidades de interés.

El número de sensores químicos existentes es enorme y para dar una visión general y esquemática se puede recurrir a clasificarlos atendiendo a diferentes criterios [13,14].

1. Tipo de proceso: pasivo, donde se mide una propiedad del analito sin reacción ni separación o activo, donde ocurre en la zona de reconocimiento una reacción y/o una separación del analito.
2. Especies inmovilizadas en la zona receptora: de manera temporal o permanente se pueden inmovilizar especies intervinientes en una reacción química: analito, reactivos, productos de reacción, catalizadores.
3. Tipo de proceso de reconocimiento que tiene lugar. Los procesos de reconocimiento pueden basarse en diferentes tipos de reaccio-

nes e interacciones como: complejación, óxido-reducción, asociación, afinidad, adsorción, catálisis u otras dando lugar a interacciones tipo: anfitrión-huesped, ligando-metal, portador-ión, portador-molécula, óxido metálico-gas, enzima-sustrato, antígeno-anticuerpo, antígeno-hapteno o receptor-sustrato, entre otras [12].

4. Tipo de capa sensora: será de superficie activa cuando solo en la superficie se encuentren los reactivos inmovilizados y ocurran los procesos de adsorción del analito e interacción o bien de membrana completa (bulk membrane sensors) donde el analito se repartirá para producir la interacción en el interior de la misma que es donde se encuentran los reactivos necesarios distribuidos.

5. Proceso de separación: pueden ocurrir o no separación en la zona de reconocimiento. Esta puede ser por adsorción, extracción, difusión gaseosa, diálisis u otros mecanismos.

6. Tipo de señal generada. Se pueden medir un gran número de propiedades diferentes aunque en la práctica las más comunes [9] son: ópticas, electroquímicas, eléctricas, masa, magnéticas o termométricas.

7. Relación entre receptor y transductor: ambos elementos pueden estar conectados, de forma óptica o eléctrica, o bien integrados en un mismo dispositivo.

8. Forma de funcionamiento: reversible, es el sensor ideal, pues responde como un sensor físico sin consumir reactivo al interaccionar con el analito. Serán irreversibles si originan una respuesta como consecuencia de una reacción irreversible aunque podrán ser reutilizables a través de una etapa de regeneración o bien no reutilizables.

9. Disposición del sensor y forma de ponerlo en contacto con la muestra: 1) sonda, cuando adopta la forma de una varilla que se introduce en el problema y en la que la fase sensora está soportada sobre

una guía de ondas, comúnmente una fibra óptica [15,16]; 2) de flujo, cuando una muestra del problema se inyecta o aspira junto con los reactivos a una celda de flujo conectada o integrada en el sistema de medida, pudiendo ser tipo FIA [17,18] o bien microchip [19] y 3) de gota plana, donde el receptor es una zona plana donde se deposita un pequeño volumen de problema. Así tenemos los sensores de un solo uso, las tiras reactivas convencionales [20] y las tiras inmunocromatográficas o de flujo lateral [21].

10. Forma de operación: continua o discontinua.
11. Número de especies monitorizadas: una (sensor monoparamétrico) o varias (sensor multiparamétrico).

Las características generales de un sensor se pueden agrupar en cuatro tipos: analíticas, de funcionamiento, temporales y de fabricación. Dentro de las analíticas se encuentran precisión, exactitud, selectividad y sensibilidad; entre las características de funcionamiento: reversibilidad, reusabilidad y capacidad de simplificación del proceso analítico; las características temporales se refieren a velocidad de respuesta, respuesta en tiempo real y estabilidad tanto operacional como de almacenaje; y por último, entre las características de fabricación tenemos: simplicidad, coste, robustez y capacidad de integración, entre otras.

Jiří Janata [8] pone el acento en dos características de un sensor a las cuales considera fundamentales: robustez y reversibilidad. La primera entendida como la capacidad de un dispositivo para mantener sus características incluso en condiciones adversas de funcionamiento, condiciones que pueden ser físicas (choques, vibraciones, cambio de condiciones) o químicas (cambios en el ambiente químico, lo que a su vez está relacionado con la selectividad). Por su parte, la reversibilidad se refiere a que la respuesta del sensor sea capaz de seguir los cambios que tengan lugar en la concentración del analito y no a la reversibilidad termodinámica del proceso de reconocimiento. De hecho los sen-

sores pueden ser termodinámicamente reversibles (un electrodo selectivo de iones) o irreversibles (un electrodo enzimático) y mantener sus características de responder a aumento o disminución en la concentración de analito, esto es, de ser reversibles.

Sensores ópticos

Los sensores ópticos se basan en la medida del cambio de propiedades ópticas de la fase sensora que se origina como consecuencia del reconocimiento del analito. El interés acerca de este tipo de sensores ha ido en aumento especialmente en las tres últimas décadas por las ventajas que presentan [22-25]. Estas ventajas se refieren a diversos aspectos. De manera sintética: 1) no presentan interferencias eléctricas; 2) no requieren sistema de referencia como los electroquímicos, aunque este puede ser útil como luego se verá; 3) no tiene porqué existir contacto entre el sistema de reconocimiento y el sistema óptico; 4) la información relativa al analito se puede codificar de forma muy variada; en concreto en amplitud, fase, polarización o información espectral, lo que abre las puertas a la posibilidad de multiplexación; 5) pueden operar en condiciones extremas, así de temperatura, presión o radiación; 6) no hay consumo de analito; 7) pueden efectuar el análisis a distancia; 8) pueden ser esterilizables con el interés clínico que ello supone; y 9) son susceptibles de miniaturización.

Entre las desventajas que presentan pueden citarse: 1) problemas de fotodescomposición de reactivos inmovilizados; 2) reducción en la capacidad de reconocimiento de los reactivos por inmovilización; 3) interferencia de la luz ambiente; 4) tiempos de respuesta grandes, en algunas ocasiones; 5) funciones de calibrado con rango corto, en algunas ocasiones.

Sensores para gases

Tiene gran importancia la determinación de gases en diversas áreas como medicina, medioambiente, biología, agricultura, seguridad en el trabajo, defensa, transporte o industria, así en la industria automovilística, aeroespacial,

agroalimentaria, química o minera. De manera muy general y sin ser excluyente, se pueden clasificar en tres grandes grupos las necesidades de determinación de gases: a) sensores de oxígeno relacionados con atmósferas respirables (concentraciones del 21%) y con el control de procesos de combustión en calderas y motores de explosión interna (concentraciones entre 0 y 5%); b) sensores para gases inflamables que protejan de fuego o explosión y que deben operar por debajo del límite inferior de explosión, lo que supone la determinación de un bajo porcentaje de gas; c) sensores para gases tóxicos, capaces de determinar concentraciones por debajo de las dosis máximas admisibles (TLV), que frecuentemente se encuentran entre 1 y 100 ppm.

Los sensores para gases comerciales usados más habitualmente son los de estado sólido, los electroquímicos y los de infrarrojos. Dentro de los primeros, los sensores de estado sólido, hay tres tipos bien conocidos y de amplio uso: los de electrolito sólido, los catalíticos y los de óxidos semiconductores.

Los primeros de ellos emplean electrolitos sólidos que son materiales que permiten la conducción de iones pero no la de electrones, cumpliendo el papel de separar dos regiones de diferente actividad en el analito permitiendo una alta movilidad de iones del analito entre las dos regiones. La medida de potencial, intensidad o carga se usa como señal analítica, aunque los sensores más habituales son los potenciométricos de los cuales existen varios tipos [26].

Los sensores catalíticos se basan en el pellistor que es básicamente un microcalorímetro catalítico, consistente en una superficie catalítica situada sobre un sensor de temperatura, junto con un sistema de calentamiento, que frecuentemente es el mismo sensor de temperatura que mantiene el catalizador a una temperatura lo suficientemente alta (~500 ºC). Por ello, el pellistor suele ser un simple alambre de platino recubierto de una pasta catalítica de un material inerte, así alúmina, y un catalizador que acelera la oxidación. De esta forma, se asegura una rápida combustión de cualquier gas inflamable que se encuentre en las proximidades. La medida de las variaciones de resistencia como consecuencia del aumento de temperatura producido por la combustión permite la monitorización de cambios en la concentración [27].

El tercer grupo de sensores de gases de estado sólido utilizan óxidos metálicos semiconductores, como son ZnO_2, TiO_2, Cr_2TiO_3, WO_3 o SnO_2, basados en el cambio de resistencia eléctrica que experimentan por la adsorción de un gas en la superficie del mismo. Cambio en resistencia que se debe a la pérdida o ganancia de electrones superficiales como resultado de que el oxígeno adsorbido reacciona con el analito gaseoso. Si el óxido semiconductor es de tipo n, ocurrirá una ganancia de electrones, si el gas es reductor, o pérdida, si el gas es oxidante, desde la banda de conducción del semiconductor. Los óxidos tipo n aumentan su resistencia cuando el analito es un gas oxidante como NO_2 o O_3, mientras que la disminuyen si es reductor como ocurre para CO, CH_4 o C_2H_5OH. La inversa es cierta para óxidos tipo p como el Cr_2TiO_3 [28].

Los sensores electroquímicos de gases pueden ser de dos tipos: sensores basados en células de combustible y sensores de tipo galvánico. Los primeros son células de combustible miniaturizadas, pues consumen como combustible un gas, que es el analito, y como comburente oxígeno. Los sensores galvánicos consumen los electrodos o el electrolito presente, pudiendo ser usados para diferentes gases como oxígeno, gases ácidos, amoniaco o cianuro de hidrógeno, por ello, la vida de estos sensores está gobernada por la cantidad de gas que utiliza, lo que hace que, en general, sea corta. Los sensores electroquímicos pueden ser más selectivos que los anteriormente citados, aunque presentan problemas relacionados con el alto valor de la corriente residual, deriva y lentitud en la respuesta [8,29,30].

Los sensores de tipo óptico para gases pueden utilizar propiedades intrínsecas como es el caso de dióxido de carbono, metano, dióxido de azufre u otros, basado en su absorción infrarroja y menos frecuentemente en su absorción ultravioleta. La medida de absorción infrarroja por parte de gases da lugar a sensores simples, robustos, con tiempo de respuesta corto, inmune a envenenamiento y con buena estabilidad. Es habitual que las medidas utilicen un sistema de doble haz, un haz de radiación de frecuencia adecuada atraviesa una distancia fija en la atmosfera donde se puede encontrar el gas, mientras

que una frecuencia no absorbida por el gas en cuestión se usa en el haz de referencia [25].

Sensores para dióxido de carbono

La determinación habitual de dióxido de carbono, especialmente en disolución, en la industria, medicina y aplicaciones ambientales se ha llevado a cabo mediante el electrodo de Severinghaus [31]. Consiste en un electrodo de pH recubierto con una membrana de PTFE o silicona que lo aísla del exterior y que lo hace impermeable a iones y permeable a dióxido de carbono, detectando cambios en el pH de una disolución tampón interna de hidrógenocarbonato causados por ese gas. El cambio de pH se relaciona de forma simple con la presión parcial de dióxido de carbono. Tiene una serie de inconvenientes como interferencias por gases ácidos y básicos, tiempo de respuesta alto y efecto de presión osmótica causada por la variabilidad en la salinidad de las muestras, así como posible contaminación del electrodo de referencia y de las uniones líquidas.

Sin embargo, el método más utilizado para la determinación de dióxido de carbono en fase gaseosa es la espectroscopia infrarroja [25]. Se basa en las intensas bandas de rotación-vibración en la región 1–25 μm de moléculas poliatómicas como es el dióxido de carbono. En este caso presenta una intensa banda de absorción extendida desde 4,2 a 4,4 μm. Para ello es frecuente usar filtros de paso de banda elegidos de manera que sólo dejen pasar radiación de determinada frecuencia, evitando de este modo las bandas de absorción debidas a otros gases, siendo posible integrar todo estos elementos en instrumentación de pequeño tamaño.

Desde comienzo de la década de los 80 diversos instrumentos portátiles para dióxido de carbono, tanto en versión monoparámetro como multiparámetro, han sido comercializados por diversas empresas como Agiltron, Codel, Compur Monitors, Dräger, Edinburgh Instruments, LumaSense o RAE. La mayoría de los sensores de gases portátiles IR son de tipo no dispersivo, aunque se han intro-

ducido algunos instrumentos de tipo dispersivo y de transformada de Fourier [32,33].

Como ejemplo podemos citar un instrumento IR portátil para dióxido de carbono gaseoso basado en una estructura óptica de doble haz que no presenta partes móviles tales como *choppers* o bombas. Para mejorar la mala respuesta dinámica originada por la ausencia de una bomba que mueva el gas a la celda de medida, el diseño incluye un filtro de compensación dinámico y dos series de termopilas miniaturizadas usadas como detectores IR. La calibración se lleva a cabo mediante redes neuronales para corregir influencia de la temperatura, logrando llegar hasta un 3% de gas con una exactitud del 0,028% [34].

La absorción infrarroja está limitada en su aplicación a disoluciones acuosas debido a la intensa absorción intrínseca del agua y a las largas longitudes de onda requeridas.

En general, la determinación de dióxido de carbono mediante sensores ópticos extrínsecos es difícil debido a que es una molécula relativamente inerte. No se conocen datos de que un compuesto fluorescente sea sensible directamente a dióxido de carbono, en contraste con la gran variedad de cationes, aniones y gases que sí son capaces de modificar directamente las propiedades de distintos luminóforos. Esta molécula no actúa como atenuador colisional de fluorescencia y no hay complejos quelatos conocidos para dióxido de carbono. Debido a estas dificultades para su determinación óptica directa, la mayoría de los sensores de tipo óptico cuantifican dióxido de carbono indirectamente, a partir del cambio de pH producido, al igual que el electrodo de Severinghaus antes citado. Diversos artículos y capítulos de libro han revisado de forma total o parcial el estado del arte de los sensores ópticos para dióxido de carbono [15,35-40].

Principios básicos para el diseño de un sensor óptico de dióxido de carbono

El dióxido de carbono se disuelve en agua de acuerdo con el equilibrio:

$$CO_2(g) \Leftrightarrow CO_2(l) \qquad K_D = 3{,}3x10^{-2} \qquad \text{(ec. 1)}$$

siendo la solubilidad a temperatura ambiente de unos 90 cm^3 of CO_2/100 ml. Como cualquier gas soluble en agua, su solubilidad aumenta al disminuir la temperatura debido al cambio entrópico positivo que supone. Este efecto es especialmente intenso para gases como el dióxido de carbono que reaccionan con agua. Este compuesto actúa como ácido Lewis frente al agua que actúa como base Lewis compartiendo pares electrónicos y dando lugar al ácido carbónico:

$$CO_2(l) + H_2O \Leftrightarrow H_2CO_3 \qquad K_h = 2{,}6x10^{-3} \qquad \text{(ec. 2)}$$

a través de una reacción de cinética lenta. En el equilibrio sólo una pequeña fracción, entre el 0,2 y el 1%, del dióxido de carbono disuelto se convierte en ácido carbónico, quedando la mayor parte como dióxido de carbono solvatado.

El ácido carbónico es un ácido débil que se puede disociar en dos etapas:

$$H_2CO_3 + H_2O \Leftrightarrow HCO_3^- + H_3O^+ \qquad K_1 = 1{,}72x10^{-4} \qquad \text{(ec. 3)}$$

$$HCO_3 + H_2O \Leftrightarrow CO_3^{2-} + H_3O^+ \qquad K_2 = 5{,}59x10^{-11} \qquad \text{(ec. 4)}$$

Si una disolución contiene hidrógenocarbonato sódico, la presencia de dióxido de carbono por todos los equilibrios concurrentes citados origina una modificación de pH. La relación entre la presión parcial de dióxido de carbono P_{CO_2} y la concentración de protones en la disolución acuosa viene dada por la siguiente ecuación [41]:

$$\alpha P_{CO_2} = [H_2CO_3] = \frac{[H^+]^3 + [H^+]^2[Na^+] \quad K_w[H^+]}{K_1([H^+] + 2K_2)} \qquad \text{(ec. 5)}$$

donde $\alpha = K_D K_h [H_2O]$ y K_W es la constante de autoprotólisis del agua. El electrodo de Severinghaus antes citado [31] quizás es el más conocido de los que explotan este efecto para la determinación de dióxido de carbono. Si la concentración de hidrógenocarbonato es suficientemente alta en la disolución tampón interna (10^{-2} M) se puede simplificar la ecuación resultando la presión parcial del gas directamente proporcional a la concentración protónica:

$$\alpha P_{CO_2} = [H_2CO_3] \approx \frac{[H^+][Na^+]}{K_1} \qquad \text{(ec. 6)}$$

Sin embargo hay un gran número de sensores descritos en los que se pone de manifiesto la variación de pH no vía potenciométrica sino óptica utilizando indicadores ácido base que modifican su color o su emisión luminiscente al variar este.

En este caso, para un indicador HD ocurre:

$$\underset{\text{color 1}}{HD} \leftrightarrow H^+ + \underset{\text{color 2}}{D} \qquad \text{(ec. 7)}$$

caracterizado por una constante de acidez K_a que debe ser adecuada para modificar la posición de equilibrio en presencia del dióxido de carbono.

$$K_a = \frac{[D][H^+]}{[HD]} \qquad \text{(ec. 8)}$$

Si la concentración de indicador usada es pequeña comparada con la de hidrógenocarbonato sódico entonces la ecuación 6 resulta:

$$\alpha P_{CO_2} = [H_2CO_3] \approx \frac{K_a[HD][Na^+]}{K_1[D^-]} \qquad \text{(ec. 9)}$$

donde las concentraciones de las formas protonada y desprotonada del indicador se pueden estimar de forma óptica por medida de absorbancia, reflectancia difusa, fluorescencia o fosforescencia.

La ecuación 9 resulta en una dependencia de tipo hiperbólico [42] cuando la respuesta está controlada por la difusión del dióxido de carbono y medimos absorbancia o luminiscencia como parámetro analítico en presencia S o ausencia S_0 de analito como indica la ecuación 10.

$$\frac{S}{S_0} = 1 + K[CO_2] \qquad \text{(ec. 10)}$$

Este tipo de dependencia justifica el comportamiento asimétrico de los tiempos de respuesta y recuperación de este tipo de sensores ópticos.

Estrategias para el desarrollo de sensores para dióxido de carbono

Se han utilizado diversas estrategias para la preparación de membranas sensibles a dióxido de carbono basadas en el uso de indicadores ácido-base

[37]. Estas se pueden resumir en dos grandes grupos: a) sensores húmedos y b) sensores secos.

Sensores húmedos para dióxido de carbono

Estos sensores fueron los primeros que se describieron y consistían en una disolución acuosa del indicador ácido-base en una disolución de hidrógenocarbonato, denominada disolución tampón interna, aislada del exterior mediante una membrana permeable al gas e impermeable a especies iónicas especialmente protones evitando la interferencia de la acidez del medio [38].

De este modo, el gas puede entrar, modificar el pH del tampón interno y, por tanto, la absorbancia o fluorescencia del indicador. Como vemos, en muchos aspectos, son similares al electrodo de Severinghaus antes citado. La razón de emplear una membrana de recubrimiento, además de una razón funcional, es impedir la lixiviación del indicador y minimizar la pérdida de agua por evaporación, lo que impediría el funcionamiento del sensor.

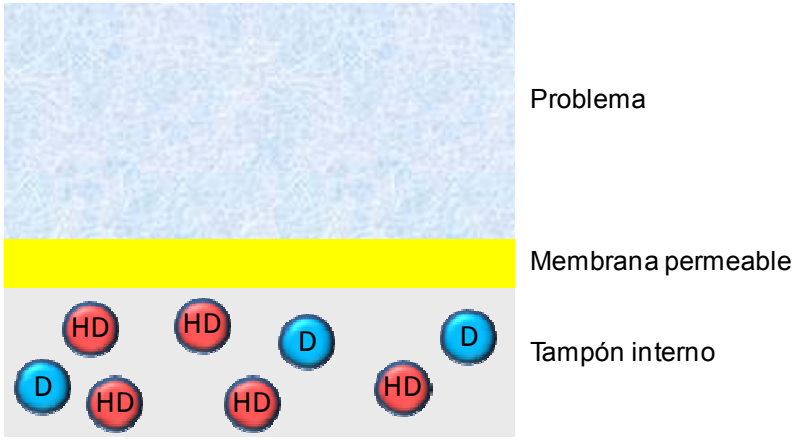

Figura 2. Esquema de un sensor húmedo para dióxido de carbono

Uno de los indicadores fluorescentes usados ha sido la β-metil umbiliferona ($\lambda_{exc\ D}$ = 357 nm; $\lambda_{em\ D}$ = 445 nm) disuelta en hidrógenocarbonato 5 mM con un 1% de agarosa para mejorar la estabilidad mecánica, todo ello separado de la disolución o gas mediante una membrana de PTFE [43]. El diseño presenta el inconveniente de un tamaño excesivamente grande lo que impide su uso para aplicaciones *in vivo*, razón por la cual han sido mucho más usados los diseños basados en fibra óptica. Así, un sensor similar, aunque colorimétrico en este caso, fue propuesto usando rojo fenol como indicador en una disolución de hidrógenocarbonato situada en el extremo de una fibra óptica mediante una membrana de silicona [44].

A partir del sensor desarrollado por Lubbers y Opitz, aparecieron diversas variantes tanto en formato de flujo como en formato sonda usando fibra óptica. Veamos algunos ejemplos: a) circular una disolución de rojo fenol en tampón hidrógenocarbonato por un tubo de silicona permeable a gases situado en un recipiente donde se hace llegar la sangre a analizar mediante una bomba peristáltica [45]; b) incorporar la disolución de hidrógenocarbonato conteniendo el indicador fluorescente 1-hidroxipireno-3,6,8-trisulfónico (HPTS) en cápsulas de poliacrilamida de 150-250 nm [46]; c) entrapar la disolución del indicador HPTS disuelto en tampón hidrógenocarbonato en una membrana de PTFE expandido (Gore-Tex™) [47]; d) adsorber la misma disolución anterior en gránulos de celulosa cohesionados mediante un hidrogel que forma la membrana [48]; e) Retener por cambio iónico del indicador HPTS en una membrana de cambio aniónico saturada de tampón [49]; f) Inmovilizar covalentemente el indicador en polihidroxietilmetacrilato y situarlo en el extremo de una fibra óptica que se cubre con una membrana permeable a gases, después de haber saturado la membrana indicadora con hidrógenocarbonato. Como indicador se ha usado acrilofluoresceina [50], fluoresceína y HPTS [51]; g) Inmovilizar el indicador diclorofluoresceina por adsorción en presencia de $LiNO_3$ para mantener un nivel constante de humedad en una microesfera de tamaño de poro controlado fijada en el extremo de una fibra óptica [52].

Una alternativa para preparar una membrana única que sea a la vez permeable a dióxido de carbono y responda a variaciones de pH consiste en la dispersión de la disolución acuosa del indicador junto con hidrógenocarbonato en un polímero de membrana, lo cual fue propuesto por primera vez por Wolfbeis *et al.* en 1986 [53]. De esta manera, la acción sensora de la membrana tiene lugar en las pequeñas gotas de disolución acuosa dispersas en el polímero.

De entre los sistemas descritos de este tipo podemos citar: a) uso de una emulsión de una disolución de HPTS e hidrógenocarbonato en silicona; presenta el inconveniente de que la deshidratación que sufre al exponerse a gas seco afecta de forma considerable a su estabilidad [36,53]. Una membrana similar se ha propuesto usando poliuretano como polímero de membrana [54]; b) empleo de una emulsión parecida para un sensor colorimétrico, en este caso usa rojo fenol como indicador, que junto con el tampón hidrógenocarbonato es preparado en una mezcla de un polímero tipo polimetilmetacrilato y de polietilenglicol de 600 D [55]; c) estabilización de las pequeñas gotas de la disolución acuosa formando micelas; así se ha usado polivinilpirrolidona para estabilizar micelas de hidrógenocarbonato y seminaftorodamina como indicador luminiscente, todo ello disperso en un polímero tipo siloxano [56]; d) uso de un material de membrana completamente soluble en agua como es el polietilenglicol junto con fluoresceína como indicador. En este caso, no añaden hidrógenocarbonato, sino que se ajusta el pH del polietilenglicol con NaOH antes de formar la membrana, de forma que la película final situada al extremo de una fibra óptica contiene pequeñas gotas de agua con el indicador al pH adecuado para responder al gas [57]. Evidentemente, el sensor no sirve para determinar dióxido de carbono en agua.

El inconveniente que presenta este tipo de membranas sensoras es que la respuesta del sensor varía si lo hace la tensión de vapor del problema en el caso de medidas en fase gas, o la presión osmótica para medidas de dióxido de carbono disuelto. Esto exige que la calibración del sensor se haga con disoluciones de presión osmótica o de vapor similares a las del sensor.

La medida en este tipo de sensores para dióxido de carbono es de absorción de radiación o de intensidad de luminiscencia, sin embargo existen alguna propuestas alternativas como la de Colin *et al.* [58] quienes proponen un sistema tipo dosímetro consistente en una lamina de ITO (óxido de estaño-indio) dispuesto sobre PVDF con una membrana de etilcelulosa con purpura de m-cresol en tampón hidrógenocarbonato depositada encima. Tras la equilibración del dosímetro en la atmosfera a monitorizar, se lee en un dispositivo que usa varios LED para iluminar la membrana. La absorción de radiación deforma el film piezoeléctrico ITO generando una carga que se mide permitiendo determinar hasta un 2,5% de dióxido de carbono.

Sensores secos para dióxido de carbono

Los sensores secos, sensores plásticos o de membrana homogénea presentan el indicador directamente entrapado en la membrana permeable a gases e impermeable a iones y responden a dióxido de carbono. El polímero de membrana actúa como una barrera a los protones reduciendo la sensibilidad cruzada al pH de la muestra. Estos sensores fueron descritos por primera vez en 1991 por Raemer y col., aunque con fines cualitativos, en una patente para la indicación visual de CO_2 para la correcta ubicación de tubos endotraqueales usados en anestesia [59]. Estudiaron la adición de un hidróxido de amonio cuaternario, al que denominaron agente de transferencia de fase, a las membranas con el indicador –rojo fenol o azul de bromotimol-, sugiriendo que su papel era acelerar el intercambio de dióxido de carbono con la fase líquida sensora.

El primer sensor al que realmente se puede considerar de membrana homogénea es el descrito por Mills *et al.* [41,60] en el que utilizan hidróxido de tetraoctilamonio (Q^+) para solubilizar el indicador de pH, púrpura de m-cresol, (In^-) en forma de par iónico en el material de membrana que es relativamente hidrófobo, así etilcelulosa o polivinilbutiral. Para ayudar a la difusión de dióxido de carbono en la membrana, se añade algún plastificante, como por ejemplo tributilfosfato mejorando de esta manera el tiempo de respuesta del sensor [61,62].

La capacidad de la membrana para responder al gas se justifica por la presencia de moléculas de agua de hidratación en el par iónico, las cuales permitirían la hidratación necesaria del dióxido de carbono para que actúe como ácido frente al agua en la forma:

$$Q^+In^- \cdot xH_2O + CO_2 \Leftrightarrow Q^+HCO_3^- \cdot (x-1)H_2O \cdot HIn \qquad \text{(ec. 11)}$$

Una de las ventajas de este tipo de sensores es que la membrana hidrófoba puede actuar por sí misma como una barrera a iones por lo que no se necesita utilizar ninguna membrana adicional. Por ello, también se han denominado sensores desnudos a este tipo de sensores de dióxido de carbono.

Se ha observado que la incorporación de una cierta cantidad de hidróxido de amonio cuaternario (Q^+OH^-) a la membrana conteniendo el par iónico (Q^+D^-) disuelto en un polímero incrementa el tiempo de vida y estabilidad de dicha membrana actuando como un sistema tampón lipofílico. La relación (Q^+D^-)/(Q^+OH^-) gobierna su sensibilidad así como su grado de linealidad [63].

Estos sensores de membrana homogénea son muy rápidos de respuesta en fase gas, pues no son raros valores de tiempos de respuesta y recuperación alrededor de 4 y 7 segundos, respectivamente [41].

Por otra parte, presentan ventajas en cuanto al mayor tiempo de vida en atmósferas secas, al perder el agua de hidratación con mayor dificultad. Para la determinación de este gas en disolución presentan la ventaja de ser menos sensibles a los cambios en presión osmótica que los sensores de disolución recubierta, aunque para un uso prolongado es necesario emplear una membrana de recubrimiento impermeable a iones [37].

Presentan el inconveniente del efecto irreversible que les originan gases ácidos como NO_2 y SO_2, debido a su reacción con el hidróxido de amonio cuaternario y con el indicador en forma básica. Con respecto a su estabilidad, se han descrito tiempos de vida de las membranas sensoras de hasta un año,

sobre todo si se conservan en bolsas selladas, refrigeradas y en la oscuridad, aunque lo habitual es que con un uso continuo su vida sea de pocas semanas, habiéndose señalado que la degradación de Hoffman del amonio cuaternario es lo que justifica su baja estabilidad [41].

Todos los problemas citados unidos a los que origina la lixiviación del indicador constituyen las principales limitaciones de estos sensores de dióxido de carbono. Una de las soluciones usadas en bibliografía consiste en usar un reservorio en el que se sumerge el extremo de la fibra óptica sensora, el cual contiene indicador en tampón, de forma que por difusión se regenere continuamente la membrana sensora [64].

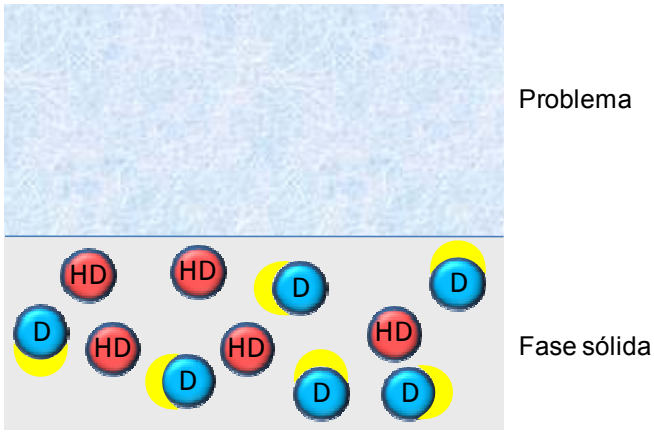

Figura 3. Esquema de un sensor seco para dióxido de carbono

Se han usado diferentes indicadores ácido-base para la preparación de sensores secos para dióxido de carbono, así para membranas colorimétricas el indicador dianiónico rojo cresol [63,65,66] y para membranas luminiscentes, el HPTS [67,68]. En ambos casos, se ha empleado además del hidróxido de tetraoctilamonio, etilcelulosa como polímero y tributilfosfato como plastificante. Con este mismo esquema químico se ha propuesto el empleo de Teflon AF 1600 como recubrimiento altamente permeable a gases para evitar interferencias iónicas; sistema que se ha aplicado como microsensor para la determinación en

agua de mar [69]. Otras alternativas empleando el mismo indicador luminiscente, han consistido en: a) fijar electrostáticamente el par iónico HPTS-tetraoctilamonio en la superficie de partículas de aminocelulosa que a continuación se dispersan en silicona formando la membrana. De esta manera se aumenta la estabilidad y el tiempo de vida [70]; b) la incorporación del par iónico en un vidrio hidrofóbico, en concreto en una sílice modificada orgánicamente (ormosil), que da lugar a un material sol-gel con buenas propiedades sensoras del gas [71-73]; La inclusión de partículas de TiO_2 (<5 μm diámetro) en el sol-gel para producir dispersión Mie e incrementar la interacción de la luz incidente con la película sensora lo que mejora la relación S/N, pudiendose determinar dióxido de carbono por debajo del nivel atmosférico (LOD 0,008%) [74]; c) inmovilización del par iónico azul de timol-tetrametilamonio en vidrio sol-gel a partir de tetraetoxisilano y metiltrietoxisilano [75]; d) el uso de silicona de dos componentes de alta hidrofobicidad que incorpora HPTS e hidróxido de cetiltrimetilamonio como agente de transferencia presenta ventajas en cuanto a menor lixiviación de indicador e interferencias [76].

Aunque se han propuesto diversos sensores para dióxido de carbono de tipo luminiscente [38], la gran mayoría utilizan el mismo indicador, el HPTS, pues no existen muchos indicadores fluorescentes que tengan características ácido-base (pK_a entre 8 y 10) y espectrales adecuadas.

Un ejemplo de indicador fluorescente diferente de HTPS usado para dióxido de carbono es el 4-[(p-N,N-dimetilamino)benciliden]-2-feniloxazol-5-ona que presenta un pKa de 6,97. Este indicador ha sido usado en una membrana para este gas conteniendo además de los reactivos habituales el perfluoroderivado ácido nonadecafluorodecanoico que actúa como transportador eficiente de dióxido de carbono lo que parece mejorar las características del sensor [77].

Alternativas en sensores secos para dióxido de carbono

Gran parte de la investigación realizada en estos últimos años ha pretendido buscar alternativas al problema del escaso número de indicadores fluo-

rescentes existentes que permitan el uso de medidas de tipo luminiscente [38]. Estas estrategias se refieren al uso de efectos como el de filtro interno y de transferencia de energía de resonancia a través de la incorporación de luminóforos adecuados en la membrana, aunque otros efectos como transferencia electrónica fotoinducida y transferencia protónica también han permitido la determinación de dióxido de carbono.

Otros problemas como la escasa fotoestabilidad de los indicadores, variabilidad de la fuente de excitación o lixiviación de reactivos han sido abordados a través de la medida de tiempos de vida en lugar de la medida de intensidad así como mediante los métodos de cocientes de señales o ratiométricos o la técnica de referenciación con doble luminóforo. Otro reciente abordaje de los problemas de fotoestabilidad junto con una serie de ventajas adicionales se logra mediante el empleo de técnicas basadas en *up-conversion*. Los problemas de estabilidad de membranas especialmente en lo que se refiere a la deshidratación se han abordado a través de la inclusión de nuevos aditivos entre los que destacan los líquidos iónicos. A continuación vamos a discutir de forma breve estas estrategias.

Una estrategia para ampliar las posibilidades de la medida de luminiscencia es el empleo del **efecto de filtro interno** de manera que se incorpore a la membrana un compuesto fluorescente que tenga la característica de emitir radiación a una longitud de onda correspondiente a una de las formas, ácida o básica, del indicador colorimétrico para dióxido de carbono. De esta manera, parte de la radiación emitida por el fluoróforo será absorbida por el indicador y la disminución de intensidad se relacionará con la concentración del gas. Se ha propuesto la α-naftoltaleina como indicador fijado como par iónico en una membrana de etilcelulosa en una cara de una lámina de cuarzo, mientras que en la opuesta se ha situado tetrafenilporfirina en poliestireno como fluoróforo [78]. De forma similar, se ha estudiado el uso del rojo cresol en combinación con el complejo tris(tenoiltrifluoroacetonato) de europio(III) dihidrato [79].

Hasta ahora hemos discutido sensores para dióxido de carbono basados en medida de intensidad bien de absorción de radiación o de fluorescencia

de un indicador ácido-base que modifica su posición de equilibrio como consecuencia de la presencia de dióxido de carbono. Por ello, la pérdida de indicador por fotooxidación o por lixiviación, da como resultado errores en las medidas y en la concentración de gas. Por esta razón, se ha buscado diversas soluciones al problema.

Una de ellas consiste en emplear **métodos de cocientes de señales o ratiométrico**s. Así el HPTS presenta dos máximos de excitación (405 y 459 nm) correspondientes a su forma protonada y desprotonada, respectivamente, y uno solo de emisión, por lo que se ha propuesto usar el cociente de intensidades de fluorescencia a 405 nm y 459 nm como parámetro analítico sensible a dióxido de carbono [76].

Otro planteamiento consiste en usar el tiempo de vida de luminiscencia como parámetro analítico en lugar de la intensidad por las ventajas que presenta: independencia de la variación de concentración de luminóforo, de la intensidad de la fuente, de la fotooxidación y lixiviación del indicador, así como de la sensibilidad del mismo.

El problema que presentan algunos indicadores fluorescentes es su corto tiempo de vida; así le ocurre al HPTS, lo que impide el uso de instrumentación de bajo precio para la medida de tiempos de vida como son las técnicas de modulación de fase. Una solución propuesta para resolver el problema es la **técnica de referenciación con doble luminóforo** (*Dual Luminophore Referencing*, DLR). Se trata de un método ratiométrico interno en el que la señal de intensidad de fluorescencia se convierte en señal de dominio de fase, coinmovilizando en la membrana un luminóforo de referencia que sea inerte, con largo tiempo de vida y similares propiedades espectrales al sensible a dióxido de carbono. El valor del ángulo de fase de la señal total medida se correlaciona con la concentración del gas. Se ha propuesto el uso del complejo tris(4,7-difenil-1,10-fenantrolina) rutenio(II) encapsulado en nanopartículas impermeables a oxígeno incorporado en una membrana sol-gel conteniendo HPTS como par iónico [80].

Una alternativa interesante para la medida de dióxido de carbono es el empleo de la luminiscencia por **transferencia de energía de resonancia** (RET). Para que se produzca fluorescencia por transferencia de energía de resonancia deben coexistir en la membrana dos fluoróforos o bien un fluoróforo y un colorante, donde el aceptor fluoróforo o bien el aceptor colorante atenúan la fluorescencia del donor fluoróforo.

La transferencia de energía ocurre sin la aparición de fotones, al contrario de lo que ocurre en filtro interno, y es el resultado de las interacciones dipolo-dipolo entre donor y aceptor [81]. La energía de resonancia depende del solapamiento de los espectros de emisión del donor y de absorción del aceptor y de la distancia, en concreto de la sexta potencia de la distancia según la ecuación de Förster, por lo que el proceso sólo es eficaz si la distancia entre ambas moléculas es inferior a 100 nm aproximadamente.

De esta manera, se convierten variaciones en absorción de radiación en variaciones en tiempo de vida del donor luminiscente, que es lo que se va a medir. Se han propuesto diversos sensores para dióxido de carbono basados en procesos RET como el que emplea Sudan III como aceptor sensible al gas, encapsulado en sol-gel conteniendo el complejo tris(4,7-difenil-1,10-fenantrolina) rutenio(II). Las medidas de tiempo de vida se realizan mediante técnicas de fluorimetría de fase [82]. Un sistema análogo ha sido estudiado con el fluoróforo 4, 4' difenil- 2, 2' bipiridil rutenio (II) aunque empleando azul timol como indicador en ese caso [83]. Lakowic et al. [84] han propuesto como luminóforo donor sulforodamina 101 que tiene un tiempo de vida pequeño y como indicador sensible a pH el púrpura de m-cresol o el azul timol para la determinación de dióxido de carbono en reactores de fermentación.

Otra forma de determinar dióxido de carbono en disolución, consiste en la medida de la atenuación de fluorescencia mediante **transferencia electrónica fotoinducida** (PET). Se ha demostrado que muchos hidrocarburos aromáticos en estado excitado interaccionan con aminas que atenúan la emisión del compuesto luminiscente, formándose un exciplejo entre la amina y el fluoróforo, mediante transferencia electrónica fotoinducida. Han sido estudiadas aminas

derivadas del naftaleno y antraceno, observándose que la emisión es particularmente atenuada por el grupo amino desprotonado y es menos atenuada cuando este grupo se encuentra protonado. Esta atenuación por PET depende de los pares electrónicos del grupo amino, por tanto una reacción en la que decrezca la densidad de electrones no enlazados, provocará un aumento en la intensidad de fluorescencia, y una posible reacción es la formación de carbamatos entre los grupos amino y el dióxido de carbono, lo cual justificaría los resultados encontrados por Herman *et al.* [85].

Otra alternativa es emplear la atenuación de **luminiscencia por transferencia protónica**, en concreto la transferencia protónica al catión en estado excitado tris[2-(2-pirazinil)tiazol)-rutenio(II) a partir de cualquier ácido Brönsted. Para ello, se utiliza el complejo inmovilizado en Sephadex CM saturado con tampón ftalato o fosfato y recubierto con una membrana de silicona en el extremo de una fibra óptica. La inclusión de la enzima anhidrasa carbónica a la capa indicadora aumenta la velocidad de respuesta del sensor luminiscente [40,86,87].

Una opción de gran interés es el empleo de **nanopartículas basadas en *upconversion***. La *up-conversion* se refiere a un efecto relacionado con la emisión de fluorescencia anti-Stokes en el rango del visible debido a excitación de luminóforos en el infrarrojo próximo (NIR). Estos luminóforos suelen ser sólidos dopados de tierras raras, compuestos con metales de transición dopados o bien mezcla de ambos y se debe a la absorción secuencial de dos o más fotones NIR por parte de los dopantes. Estos materiales presentan un potencial interés en sensores por diversas razones como el incremento de fotoestabilidad, y por tanto tiempo de vida, que logran al iluminar el sensor con radiación NIR, la disminución de señal de fondo o el bajo coste de las fuentes NIR que permite abaratar instrumentación [88].

Se ha propuesto un sensor para dióxido de carbono basado en una efecto de filtro interno basado en *up-conversion* entre nanopartículas de $NaYF_4$:Yb,Er en una membrana de poliestireno conteniendo azul de bromotimol.

Este sensor presenta un tiempo de respuesta de 10 s y un límite de detección del 0,11 % [89].

Como antes se ha señalado, los problemas de estabilidad de las membranas en lo referido a la deshidratación se han abordado a través de la inclusión de aditivos como son los **líquidos iónicos**. Los líquidos iónicos son fluidos constituidos exclusivamente por sales con temperatura de fusión por debajo del punto de ebullición del agua, a veces hidrolíticamente estables y compuestos por un catión orgánico y un anión inorgánico poliatómico. Presentan presiones de vapor no medibles por encima de su punto de descomposición térmica (> 300ºC) y además absorben y desorben gases de manera muy rápida [90].

Ertekin *et al.* [91] han propuesto un sensor espectrofotométrico para dióxido de carbono en el par iónico azul bromo timol/tetraoctilamonio disueltos en líquidos iónicos tipo imidazolio y en presencia de hidróxido de tetraoctilamonio. Poco después Wolfbeis *et al.* [92] han propuesto un sensor fluorimétrico basado en un método ratiométrico con un fluoróforo de referencia inerte emulsionando en indicador junto con el liquido iónico en una silicona. La estabilidad térmica de las membranas preparas es buena pero muestran una fotoestabilidad moderada y se deterioran rápidamente cuando se emplean para medidas en medios acuosos.

Por otra parte, el uso de materiales nanofibrosos preparados por técnicas de electrohilado conteniendo HPTS en presencia de polímeros como etilcelulosa y polimetilmetacrilato y líquidos iónicos tipo imidazolio, conduce a un material de gran área superficial con una buena estabilidad y sensibilidad mayor entre uno y dos órdenes de magnitud que las correspondientes membranas de análoga composición [93].

La **sustitución de la base lipofílica** presente se ha sugerido para aumentar la estabilidad de la membrana sensora cuya estabilidad se ve comprometida por la lenta degradación de Hoffman que sufre el amonio cuaternario. Para ello se ha sustituido el amonio cuaternario por una base neutra con un nitrógeno terciario como grupo básico, en concreto por un fosfaceno [94]. Aunque las membranas preparadas son capaces de responder a dióxido de carbo-

no, presentan una alta sensibilidad cruzada hacia la humedad así como cierta volatilidad del fosfaceno en forma neutra lo que impide su utilización para dióxido de carbono en fase gas sino solo en disolución.

Instrumentación para sensores ópticos de dióxido de carbono

La instrumentación utilizada para la medida de las señales originada por estos sensores puede ser instrumentación convencional de sobremesa tipo espectrofotómetros, fluorímetros o en general luminómetros, tanto para medida de intensidad como de tiempos de vida habitualmente a través de medidas de desplazamiento de fase. En esta introducción no vamos a tratar de ellos. Sí dedicaremos un breve comentario a algunas formas de medida no convencionales.

El empleo de dispositivos de imagen como pueden ser cámaras CCD permite obtener información espacial de analitos empleando membranas sensoras o bien matrices de sensores, así como la resolución de mezclas de analitos. Este es el caso del sensor propuesto para la determinación simultánea de oxígeno y dióxido de carbono basado en una única membrana sensora conteniendo simultáneamente la química para el reconocimiento de dióxido de carbono basada en HPTS y la de oxígeno basada en el complejo tris(4,7-difenil-1,10-fenantrolina) rutenio (II). El empleo de una cámara CCD como sistema de detección con ventanas de tiempo capaces de medir o discriminar entre tiempos de vida permite la resolución de ambos analitos [95].

El uso de sensores luminiscentes que emiten a longitudes de onda suficientemente separadas se ha utilizado para diseñar un sensor para la medida simultánea de dióxido de carbono, basada en HPTS, y temperatura, basada en el complejo tris(tenoiltrifluoroacetilacetonato)-(2-(4-dietilaminofenil)-4,6-bis(3,5-dimetilpirazol-1-il)-1,3,5-triazina) Eu(III), empleando una cámara CCD en blanco y negro. Para ello utiliza las diferentes señales que origina cada sistema sensor en cada uno de los tres filtros rojos, verdes y azules que constituyen el mosaico de Bayer de la cámara CCD [96]. El *review* de Mills y Hogden [38] examina la instrumentación comercial existente para dióxido de carbono.

Un tipo de instrumentación que queremos comentar es la de tipo portátil ya que ello constituirá un objetivo de esta Tesis Doctoral. Por definición un instrumento portátil (*handheld/portable instrument*) debe poder ser manejado con una mano o al menos debe ser lo suficientemente ligero y pequeño como para poder ser llevado o transportado con facilidad. Debe poseer la característica de poderlo llevar donde haya que recoger la información, lo que tiene gran importancia en diversos campos como puede ser monitorizar seguridad laboral y analizar muestras potencialmente peligrosas donde la obtención de datos en tiempo real y la monitorización es aconsejable u obligatoria para permitir una toma de decisiones rápida [97,98]. Entre las diferentes áreas que pueden requerir el empleo de instrumentación portátil se encuentra la industria química, análisis en atención primaria (*point-of-care testing*), defensa antiterrorista, protección ambiental, prospección geoquímica e higiene y seguridad en el trabajo, entre otras.

No obstante lo dicho, los instrumentos portátiles no solamente se usan para medidas en el exterior, pues como pesan menos, son menores de tamaño, habitualmente son más baratos y fáciles de manejar que sus equivalentes de sobremesa, son también apropiados para su uso en laboratorios de rutina.

Independientemente del tamaño del instrumento portátil, casi todos los basados en detección óptica contienen los siguientes subsistemas básicos: fuente de luz, guía de luz, dispositivos para seleccionar longitudes de onda, detector de luz o imagen y electrónica para el procesado y transmisión de señal. En todos estos módulos han tenido lugar grandes avances en las últimas décadas, lo que ha ayudado al desarrollo de instrumentación miniaturizada.

En lo que respecta a instrumentación portátil para dióxido de carbono podemos citar el dispositivo desarrollado por Hauser *et al.* [99] basado en un LED azul de alta intensidad como fuente de radiación para excitar la fluorescencia de una membrana basada en HPTS. La radiación emitida se lleva con fibra óptica de plástico a un fotodetector, discriminando longitudes de onda mediante un filtro de colorante y eliminando la interferencia de la luz ambiente con un amplificador *lock-in*.

La medida de tiempo de vida de fluorescencia también se ha utilizado en instrumentación portátil como la desarrollada por Lippitsch *et al.* [100,101] para la determinación de gases en sangre. La membrana sensora se sitúa en la pared interior de un capilar por el que circula la sangre y que actúa como guía de ondas. La fluorescencia de un complejo de rutenio es excitada por un LED y recogida por un fotodetector acoplado a un generador de retrasos, lo que permite recoger la curva de decaimiento y calcular el tiempo de vida.

MacCraith *et al.* [102] han presentado una plataforma sensora basada en la medida de intensidad de fluorescencia originada por un sustrato desechable conteniendo la membrana sensora. Más tarde han desarrollado una plataforma más eficiente consistente en una película sensora depositada en una guía de ondas de polimetilmetacrilato, la cual excita la fluorescencia con un LED azul midiendo la luminiscencia por fluorimetría de fase. Se ha utilizado para la monitorización de la calidad de ambientes interiores midiendo oxigeno, humedad relativa y dióxido de carbono [103].

Una aproximación reciente muy interesante es la propuesta por Mayr *et al.* [104] basada en electrónica impresa. Consiste en una plataforma que integra monolíticamente la membrana sensora conteniendo HPTS junto con el fotodetector en forma de anillo ambos impresos sobre un sustrato único de PET y ensamblado con un OLED de manera que no requiere el empleo de filtros para discriminar la emisión luminiscente.

Bibliografia

1. M.H. Weil, Y. Nakagawa, W. Tang, Y. Sato, F. Ercoli, R. Finegan, G. Grayman, J. Bisera, Sublingual capnometry: a new noninvasive measurement for diagnosis and quantitation of severity of circulatory shock, Crit Care Med 27 (1999) 1225.

2. J. Creteur, B.D. De, Y. Sakr, M. Koch, J. Vincent, Sublingual capnometry tracks microcirculatory changes in septic patients, Intensive Care Med 32 (2006) 516.

3. D. De Backer, G. Ospina-Tascon, D. Salgado, R. Favory, J. Creteur, J. Vincent, Monitoring the microcirculation in the critically ill patient: current methods and future approaches, Intensive Care Med 36 (2010) 1813.

4. D.G. Mou, Process dynamics: instrumentation and control, Biotech.Adv. 1 (1983) 229.

5. R. P. Wayne. Chemistry of Atmospheres, 3rd Edition ed., Oxford University Press, Oxford, 2000

6. I.J. Church, A.L. Parsons, Modified atmosphere packaging technology: A review, J.Sci.Food Agric. 67 (1995) 143.

7. J.P. Kerry, M.N. O'Grady, S.A. Hogan, Past, current and potential utilisation of active and intelligent packaging systems for meat and muscle-based products: A review, Meat Science 74 (2006) 113.

8. J. Janata. Principles of Chemical Sensors, 2 ed., Springer, 2009

9. A. Hulanicki, S. Geab, F. Ingman, Chemical sensors definitions and classification, Pure Appl.Chem. 63 (1991) 1247.

10. K. Cammann, G. G. Guilbault, H. Hal, R. Kellner, O. S. Wolfbeis. The Cambridge Definition of Chemical Sensors, Cambridge Workshop on Chemical Sensors and Biosensors, Cambridge University Press, New York, 1996

11. W. Göpel, T. A. Jones, I. Lundstrom, T. Seiyama. Sensors. Chemical and Biochemical Sensors Part I , Weinheim: VCH, 1991

12. U. E. Spichiger-Keller. Chemical Sensors and Biosensors for Medical and Biological Applications, 1 ed., Wiley-VCH, Weinheim, 1998 p. 1.

13. C. Perez Conde. Sensores ópticos, 1 ed., Servicio de Publicaciones Universidad de Valencia, Valencia, 1996

14. M. Valcarcel, M. D. Luque de Castro. Flow-Through (Bio)Chemical Sensors, Elsevier Science B.V., Amsterdam, 1994

15. F. Baldini, A. Giannetti, A.A. Mencaglia, C. Trono, Fiber optic sensors for biomedical applications, Curr.Anal.Chem. 4 (2008) 378.

16. M.D. Marazuela, M. Cruz Moreno-Bondi, Fiber-optic biosensors - An overview, Anal.Bioanal.Chem. 372 (2002) 664.

17. C. Bosch Ojeda, F. Sánchez Rojas, Recent Development in Optical Chemical Sensors Coupling with Flow Injection Analysis, Sensors 6 (2006) 1245.

18. M. Miro, W. Frenzel, Flow-through sorptive preconcentration with direct optosensing at solid surfaces for trace-ion analysis, TrAC, Trends Anal.Chem. 23 (2004) 11.

19. J. Wang, Microchip devices for detecting terrorist weapons, Anal.Chim.Acta 507 (2004) 3.

20. L. F. Capitan-Vallvey , in: Grimes, C. A.; Dickey, E. C.Pishko, M. V., Eds. (Ed.), Encyclopedia of Sensors, The Pennsylvania State University, Pennsylvania, USA, 2005, pp. 55-93 .

21. K. Faulstich, R. Gruler, M. Eberhard, D. Lentzsch, K. Haberstroh , in: Wong, R. C.; Tse, H. Y., Eds. (Ed.), Lateral Flow Immunoassay, Humana Press, New York, 2009, pp. 157-184 (Chapter 9.

22. F. Baldini, A. N. Chester, J. Homola. Optical Chemical Sensors, Springer, 2006

23. C. McDonagh, C.S. Burke, B.D. MacCraith, Optical Chemical Sensors, Chem.Rev. 108 (2008) 400.

24. Orellana, G. and Moreno-Bondi, M. C. Frontiers in Chemical Sensors: Novel Principles and Techniques. Wolfbeis, Otto S. [3]. 2005. Springer. Springer Series on Chemical Sensors and Biosensors.

25. O. S. Wolfbeis. Fiber optical sensors and biosensors, CRC Press, Ann Arbor, 1991 p. 1.

26. H.D. Wiemhofer, W. Gopel, Fundamentals and principles of potentiometric gas sensors based upon solid electrolytes, Sens.Actuators B 4 (1991) 365.

27. F. Oehme, Solid-state gas sensors, Sensorik 4 (1994) 47.

28. D.E. Williams, Semiconducting oxides as gas-sensitive resistors, Sens.Actuators, B B57 (1999) 1.

29. D. Ebeling, V. Patel, M. Findlay, J. Stetter, Electrochemical ozone sensor and instrument with characterization of the electrode and gas flow effects, Sens.Actuators B 137 (2009) 129.

30. G.A. Urban, G. Jobst, Sensor Systems, Top.Curr.Chem. 194 (1998) 189.

31. J.W. Severinghaus, A.F. BRADLEY, Electrodes for blood pO2 and pCO2 determination, J.Appl.Physiol. 13 (1958) 515.

32. K. Ashley, Analytical instrument performance criteria: field-portable spectroscopy, Appl.Occup.Environ.Hyg. 18 (2003) 10.

33. P.G. Zemek, S.V. Plowman, M.A. Druy, C.D. Brown, R.A. Crocombe, Portable open-path optical remote sensing (ORS) Fourier transform infrared (FTIR) instrumentation miniaturization and software for point and click real-time analysis, Proc.SPIE 7680 (2010) 76800Q/1.

34. G. Zhang, X. Wu, A novel CO2 gas analyzer based on IR absorption, Opt.Lasers Eng. 42 (2004) 219.

35. M. Ando, Recent advances in optochemical sensors for the detection of H2, O2, O3, CO, CO2 and H2O in air, TrAC, Trends Anal.Chem. 25 (2006) 937.

36. M.J.P. Leiner, Luminescence chemical sensors for biomedical applications: scope and limitations, Anal.Chim.Acta 255 (1991) 209.

37. A. Mills, K. Eaton, Optical sensors for carbon dioxide: an overview of sensing strategies past and present, Quim.Anal. 19 (2000) 75.

38. A. Mills, S. Hodgen, Fluorescent carbon dioxide indicators, Top.Fluoresc.Spectrosc. 9 (2005) 119.

39. G. Orellana, C. Cano-Raya, J. L£pez-Gejo, A. R. Santos , in: Peter, W., Ed. (Ed.), Treatise on Water Science, Elsevier, Oxford, 2011, pp. 221-261 .

40. G. Orellana, C.d. Dios, M.C. Moreno-Bondi, M.D. Marazuela, Intensity- and lifetime-based luminescence optosensing of carbon dioxide, Proc.SPIE-Int.Soc.Opt.Eng. 2508 (1995) 18.

41. A. Mills, Q. Chang, N. McMurray, Equilibrium Studies on Colorimetric Plastic Film Sensors for Carbon Dioxide, Anal.Chem. 64 (1992) 1383.

42. A. Mills, Q. Chang, Modelled diffusion-controlled response and recovery behaviour of a naked optical film sensor with a hyperbolic-type response to analyte concentration, Analyst 117 (1992) 1461.

43. D.W. Lubbers, N. Opitz, Quantitative fluorescence photometry with biological fluids and gases, Adv.Exp.Med.Biol. 75 (1976) 65.

44. G.G. Vurek, P.J. Feustel, J.W. Severinghaus, A fiber optic pCO2 sensor, Ann.Biomed.Eng. 11 (1983) 499.

45. C.G. Cooney, B.C. Towe, Intravascular carbon dioxide monitoring using micro-flow colorimetry, Biosensors Bioelectron. 12 (1997) 11.

46. D.W. Lubbers, N. Opitz, Blood gas analysis with fluorescence dyes as an example of their usefulness as quantitative chemical sensors, Analytical Chemistry Symposia Series 17 (1983) 609.

47. M. Uttamlal, D.R. Walt, A fiber-optic carbon dioxide sensor for fermentation monitoring, Bio/Technology 13 (1995) 597.

48. O.S. Wolfbeis, L.J. Weis, M.J.P. Leiner, W.E. Ziegler, Fiber-optics fluorosensor for oxygen and carbon dioxide, Anal.Chem. 60 (1988) 2028.

49. Z. Zhujun, W.R. Seitz, A carbon dioxide sensor based on fluorescence, Anal.Chim.Acta 160 (1984) 305.

50. J.A. Ferguson, B.G. Healey, K.S. Bronk, S.M. Barnard, D.R. Walt, Simultaneous monitoring of pH, CO2 and O2 using an optical imaging fiber, Anal.Chim.Acta 340 (1997) 123.

51. C. Munkholm, D.R. Walt, F.P. Milanovich, A fiber-optic sensor for carbon dioxide measurement, Talanta 35 (1988) 109.

52. T. Hirschfeld, F. Miller, S. Thomas, H. Miller, F. Milanovich, R. Gaver, Laser-fiber-optic "optrode" for real time in vivo blood carbon dioxide level monitoring, J.Lightwave Tech. 5 (1987) 1027.

53. H.J. Marsoner, H. Kroneis, O.S. Wolfbeis, Austrian Patent 386.078, 1986.

54. S. Hahn, A. Nelson, M. Bennett, H.K. Hui, CO2 Sensor using a hydrophilic polyurethane matrix, EP 0601816, 1994.

55. J.B. Yim, T.W. Hubbard, L.D. Melkerson, M.A. Sexton, B.M. Fieggen, Configuration fiber-optic blood gas sensor bundle and method of making, US 5,047,627, 1991.

56. J.W. Parker, O. Laksin, C. Yu, M.L. Lau, S. Klima, R. Fisher, I. Scott, B.W. Atwater, Fiber-optic sensors for pH and carbon dioxide using a self-referencing dye, Anal.Chem. 65 (1993) 2329.

57. Y. Kawabata, T. Kamichika, T. Imasaka, N. Ishibashi, Fiber-optic sensor for carbon dioxide with a pH indicator dispersed in a poly(ethylene glycol) membrane, Anal.Chim.Acta 219 (1989) 223.

58. F. Colin, T.J.N. Carter, J.D. Wright, Modification of a piezo-optical gas dosimeter system towards continuous gas sensing: a feasibility study with carbon dioxide, Sens.Actuators, B 90 (2003) 216.

59. D.B. Raemer, D.R. Walt, C. Munkholm, CO2 indicator and the use thereof to evaluate placement of tracheal tubes, US 5,005,572, 1991.

60. A. Mills , N. McMurray, Carbon dioxide monitor, US 5,472,668, 1995.

61. A. Mills, L. Monaf, Thin Plastic Film Colorimetric Sensors for Carbon Dioxide: Effect of Plasticizer on Response, Analyst 121 (1996) 535.

62. A. Mills, A. Lepre, L. Wild, Breath-by-breath measurement of carbon dioxide using a plastic film optical sensor, Sens.Actuators B 39 (1997) 419.

63. B.H. Weigl, O.S. Wolfbeis, Sensitivity studies on optical carbon dioxide sensors based on ion pairing, Sens.Actuators B 28 (1995) 151.

64. K. Ertekin, I. Klimant, G. Neurauter, O.S. Wolfbeis, Characterization of a reservoir-type capillary optical microsensor for pCO2 measurements, Talanta 59 (2003) 261.

65. F. Baldini, A. Falai, A.R. De Gaudio, D. Landi, A. Lueger, A. Mencaglia, D. Scherr, W. Trettnak, Continuous monitoring of gastric carbon dioxide with optical fibres, Sens.Actuators B 90 (2003) 132.

66. B.H. Weigl, O.S. Wolfbeis, New hydrophobic materials for optical carbon dioxide sensors based on ion pairing, Anal.Chim.Acta 302 (1995) 249.

67. A. Mills, Q. Chang, Fluorescence plastic thin-film sensor for carbon dioxide, Analyst 118 (1993) 839.

68. B. Müller, P.C. Hauser, Fluorescence Optical Sensor for Low Concentrations of Dissolved Carbon Dioxide, Analyst 121 (1996) 339.

69. G. Neurauter, O. Kilmant, O.S. Wolfbeis, Fiber-optic microsensor for high resolution pCO2 sensing in marin environment, Fresenius J.Anal.Chem. 366 (2000) 481.

70. O.S. Wolfbeis, B. Kovacs, K. Goswami, S.M. Klainer, Fiber optic fluorescence carbon dioxide sensor for environmental monitoring, Mikrochim.Acta 129 (1998) 181.

71. C. Malins, B.D. MacCraith, Dye-doped organically modified silica glass for fluorescence based carbon dioxide gas detection, Analyst 123 (1998) 2373.

72. C.S. Chu, Y.L. Lo, Fiber-optic carbon dioxide sensor based on fluorinated xerogels doped with HPTS, Sens.Actuators B 129 (2008) 120.

73. C.S. Chu, Y.L. Lo, Highly sensitive and linear optical fiber carbon dioxide sensor based on sol-gel matrix doped with silica particles and HPTS, Sens.Actuators, B B143 (2009) 205.

74. R.N. Dansby-Sparks, J. Jin, S.J. Mechery, U. Sampathkumaran, T.W. Owen, B.D. Yu, K. Goswami, K. Hong, J. Grant, Z.L. Xue, Fluorescent-Dye-Doped Sol- Gel Sensor for Highly Sensitive Carbon Dioxide Gas Detection below Atmospheric Concentrations, Anal.Chem. 82 (2009) 593.

75. H. Segawa, E. Ohnishi, Y. Arai, K. Yoshida, Sensitivity of fiber-optic carbon dioxide sensors utilizing indicator dye, Sens.Actuators B 94 (2003) 276.

76. X. Ge, Y. Kostov, G. Rao, High-stability non-invasive autoclavable naked optical CO2 sensor, Biosensors Bioelectron. 18 (2003) 857.

77. K. Ertekin, S. Alp, Enhanced emission based optical carbon dioxide sensing in presence of perfluorochemicals (PFCs), Sens.Actuators, B 115 (2006) 672.

78. Y. Amao, N. Nakamura, Optical CO2 sensor with the combination of colorimetric change of [alpha]-naphtholphthalein and internal reference fluorescent porphyrin dye, Sens.Actuators B 100 (2004) 351.

79. N. Nakamura, Y. Amao, Optical sensor for carbon dioxide combining colorimetric change of a pH indicator and a reference luminescent dye, Anal.Bioanal.Chem. 376 (2003) 642.

80. C.v. Bültzingslöwen, A.K. McEvoy, C. McDonagh, B.D. MacCraith, I. Klimant, K. Christian, O.S. Wolfbeis, Sol-gel based optical carbon dioxide sensor employing dual luminophore referencing for application in food packaging technology, Analyst 127 (2002) 1478.

81. J. R. Lakowicz. Principles of Fluorescence Spectroscopy, 3rd ed., Springler, 2006

82. C.v. Bültzingslöwen, A.K. McEvoy, C. McDonagh, B.D. MacCraith, Lifetime-based optical sensor for high-level pCO_2 detection employing fluorescence resonance energy transfer, Anal.Chim.Acta 480 (2003) 275.

83. G. Neurauter, I. Klimant, O.S. Wolfbeis, Microsecond lifetime-based optical carbon dioxide sensor using luminescence resonance energy transfer, Anal.Chim.Acta 382 (1999) 67.

84. Q. Chang, L. Randers-Eichhorn, J.R. Lakowicz, G. Rao, Steam-sterilizable, fluorescence-lifetime-based, sensing film for dissolved carbon dioxide, Biotechnol.Prog. 14 (1998) 326.

85. P. Herman, Z. Murtaza, J.R. Lakowicz, Sensing of Carbon Dioxide by a Decrease in Photoinduced Electron Transfer Quenching, Anal.Biochem. 272 (1999) 87.

86. M.D. Marazuela, M.C. Moreno-Bondi, G. Orellana, Enhanced performance of a fiber-optic luminescence CO2 sensor using carbonic anhydrase, Sens.Actuators B 29 (1995) 126.

87. G. Orellana, M.C. Moreno-Bondi, E. Segovia, M.D. Marazuela, Fiber-optic sensing of carbon dioxide based on excited-state proton transfer to a luminescent ruthenium(II) complex, Anal.Chem. 64 (1992) 2210.

88. D.E. Achatz, R. Ali, O.S. Wolfbeis, Luminescent Chemical Sensing, Biosensing, and Screening Using Upconverting Nanoparticles, Top.Curr.Chem. DOI: 10-1007/128_2010_98 (2010) .

89. R. Ali, S.M. Saleh, R.J. Meier, H.A. Azab, I.I. Abdelgawad, O.S. Wolfbeis, Upconverting nanoparticle based optical sensor for carbon dioxide, Sens.Actuators, B 150 (2010) 126.

90. C. Cadena, J.L. Anthony, J.K. Shah, T.I. Morrow, J.F. Brennecke, E.J. Maginn, Why Is CO2 So Soluble in Imidazolium-Based Ionic Liquids?, J.Am.Chem.Soc. 126 (2004) 5300.

91. O. Oter, K. Ertekin, D. Topkaya, S. Alp, Room temperature ionic liquids as optical sensor matrix materials for gaseous and dissolved CO2, Sens.Actuators, B 117 (2006) 295.

92. S.M. Borisov, M.C. Waldhier, I. Klimant, O.S. Wolfbeis, Optical Carbon Dioxide Sensors Based on Silicone-Encapsulated Room-Temperature Ionic Liquids, Chem.Mater. 19 (2007) 6187.

93. S. Aydogdu, K. Ertekin, A. Suslu, M. Ozdemir, E. Celik, U. Cocen, Optical CO2 Sensing with Ionic Liquid Doped Electrospun Nanofibers, J.Fluor. (2010) 1.

94. C.R. Schroeder, I. Klimant, The influence of the lipophilic base in solid state optical pCO2 sensors, Sens.Actuators, B 107 (2005) 572.

95. C.R. Schroeder, G. Neurauter, I. Klimant, Luminescent dual sensor for time-resolved imaging of pCO2 and pO2 in aquatic systems, Microchim.Acta 158 (2007) 205.

96. M.I.J. Stich, S.M. Borisov, U. Henne, M. Schaeferling, Read-out of multiple optical chemical sensors by means of digital color cameras, Sens.Actuators, B 139 (2009) 204.

97. G. McMahon. Analytical Instrumentation A Guide to Laboratory, Portable and Miniaturized Instruments, 1st ed., John Wiley & Sons, Chichester, 2007

98. C.C. Coffey, T.A. Pearce, Direct-reading methods for workplace air monitoring, J.Chem.Health Saf. 17 (2005) 10.

99. P.C. Hauser, A solid-state instrument for fluorescence chemical sensors using a blue light-emitting diode of high intensity, Meas.Sci.Technol. 6 (1995) 1081.

100. D. Kieslinger, K. Trznadel, K. Oechs, S. Draxler, M.E. Lippitsch, Lifetime-based portable instrument for blood gas analysis, Proc.SPIE-Int.Soc.Opt.Eng. 2976 (1997) 71.

101. M.E. Lippitsch, D. Kieslinger, S. Draxler, Luminescence lifetime-based sensing: New materials, new devices, Sens.Actuators B 38 (1997) 96.

102. C. Malins, M. Niggemann, B.D. MacCraith, Multi-analyte optical chemical sensor employing a plastic substrate, Meas.Sci.Technol. 11 (2000) 1105.

103. O. McGaughey, R. Nooney, A.K. McEvoy, C. McDonagh, B.D. MacCraith, Development of a multi-analyte integrated optical sensor platform for indoor air-quality monitoring, Proc.SPIE-Int.Soc.Opt.Eng. 5993 (2005) 59930R/1.

104. T. Mayr, T. Abel, E. Kraker, S. K÷stler, A. Haase, C. Konrad, M. Tscherner, B. Lamprecht, An optical sensor array on a flexible substrate with integrated organic opto-electric devices, Procedia Engineering 5 (2010) 1005.

Capítulo 2

Sensor fosforescente para dióxido de carbono basado en filtro interno secundario

Planteamiento

La determinación de gases y vapores es en la actualidad una necesidad rutinaria en Química Analítica y existen multitud de situaciones en las que se debe obtener información acerca de qué gases o vapores se encuentran presentes en una atmósfera determinada o disueltos en un líquido dado y en qué proporción.

Como antes se ha señalado, uno de los objetivos de esta Tesis doctoral es desarrollar un sensor óptico para dióxido de carbono compatible con el sensor para oxígeno incluido en un sistema instrumental portátil previamente desarrollado dentro de nuestro equipo de investigación. Con el término compatible entendemos que se base en unos principios de medida similares de forma que puedan ser compartidos con vistas a su integración en una plataforma instrumental común.

En el caso del sensor de oxígeno nos basamos en que origina atenuación dinámica de la fosforescencia emitida por un luminóforo de alto tiempo de vida, la octaetilporfirina de platino [1,2]. Para poder utilizar la medida de fosforescencia para la determinación de dióxido de carbono nos basamos en su carácter ácido-base para seleccionar un indicador ácido-base que presente un valor adecuado de constante de acidez y compatibilidad espectral para así poder transducir el cambio de color en un cambio de emisión luminiscente.

En este capítulo y como primer paso hacia el desarrollo de un sensor y de una instrumentación portátil asociada para determinación de dióxido de carbono, se estudiará y caracterizará una membrana para este gas.

Un aspecto básico para poder usar el mismo tipo de medida que la empleada en el sensor para oxígeno antes citado, es evitar la atenuación de luminiscencia del luminóforo por parte del oxígeno atmosférico. Para ello será necesario ensayar diversas estrategias basadas en polímeros impermeables a oxígeno.

Para la preparación de membranas sensoras a dióxido de carbono que contengan todos los materiales necesarios para la química de reconocimiento

utilizada, se estudiarán y valorarán cuatro configuraciones diferentes: membrana simple, doble capa, membrana sándwich y membrana en caras opuestas. También se planteará la inclusión del luminóforo en micropartículas preparadas mediante la técnica de *flow focusing*.

La técnica de *flow focusing* [3,4] permite la preparación de gotas controladas de tamaño nanométrico como resultado de la combinación de fuerzas hidrodinámicas con una geometría específica. El *flow focusing* consiste en la entrada del líquido enfocante, que normalmente es agua, en la cámara presurizada a un caudal constante mientras que la entrada del líquido enfocado se realiza por otro orificio también a flujo constante y suele ser una disolución orgánica del polímero que se va a utilizar para la preparación de las partículas. Al ser los dos líquidos inmiscibles entre sí, el agua produce una disminución en el diámetro del caudal de la disolución orgánica, dando lugar a un microchorro estacionario de forma controlada. El fluido enfocante moldea al menisco de flujo originándose una especie de micro o nano-reactor en el orificio de salida de la cámara, siendo el diámetro de este reactor mucho menor que el orificio de salida. La inestabilidad capilar rompe el chorro estacionario en gotitas homogéneas. Estas gotas así formadas caen sobre un recipiente abierto que contiene una disolución acuosa de un agente estabilizante, y por evaporación del disolvente orgánico se producen las micro o nanopartículas.

La técnica de *flow flocusing* asegura una producción extremadamente rápida de millones de gotitas por segundo, lo que es una velocidad mucho mayor que en otras técnicas de microgoteo.

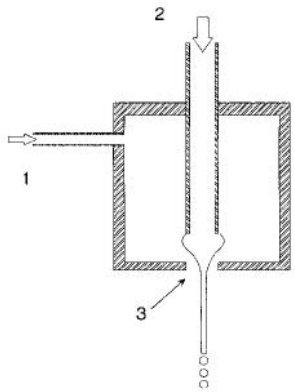

Figura 1. Esquema de la configuración experimental para *flow-focusing*: 1) fluido enfocante, 2) fluido enfocado, 3) menisco.

En lo que respecta al proceso de reconocimiento usado para dióxido de carbono, existen dos posibles mecanismos que pueden explicar su influencia sobre la señal luminiscente: filtro interno y transferencia de energía de resonancia. Como posteriormente veremos habrá que dilucidar cuál es el mecanismo responsable de la respuesta. Ahora vamos a comentar brevemente ambos mecanismos.

Transferencia de energía de resonancia

La transferencia de energía de resonancia (RET) es un proceso de atenuación de fluorescencia bimolecular que tiene lugar entre el estado excitado de una especie donora fluorescente y el estado fundamental de un especie aceptora, transfiriéndose la energía por un proceso no radiativo de acoplamiento dipolo-dipolo [5]. Este proceso supone una vía extra de relajación del estado excitado de la especie donora además del habitual proceso de emisión de fluorescencia intrínseca y de otros procesos no radiativos, y modifica la ley de decaimiento de intensidad de fluorescencia del donor. Para que tenga lugar el proceso RET es necesario que ocurra solapamiento entre el espectro de emisión del donor y el espectro de absorción del aceptor, dependiendo en gran medida la eficiencia del proceso del grado de solapamiento que tenga lugar y de la distancia entre donor y aceptor, según la teoría de Förster [6].

La extensión de la energía transferida se determina mediante la distancia aceptor-donor y por la extensión del solapamiento espectral. El solapamiento espectral se describe en términos de distancia de Föster (R_0) calculada a partir de las características espectrales del donor y del aceptor y del rendimiento cuántico del donor Φ_D utilizando la siguiente expresión:

$$R_0 = \frac{0.0211 \cdot \kappa^{1/3} \cdot \phi_D{}^{1/6} \cdot J(\lambda)^{1/6}}{n^{2/3}} \qquad \text{(ec. 1)}$$

en la que k es el factor de orientación, para el que se acepta un valor de $\sqrt{2/3}$ suponiendo que tiene lugar una rotación libre de las moléculas de donor y aceptor y n es el índice de refracción de la membrana para el que calculamos un valor de 1,46 y J(λ) es la integral de solapamiento, que indica el grado de solapamiento entre el espectro de emisión del donor y el espectro de absorción del aceptor.

La velocidad de transferencia de energía $K_T(r)$ viene dada por:

$$K_T(r) = \frac{1}{\tau_D}\left(\frac{R_0}{r}\right)^6 \qquad \text{(ec. 2)}$$

donde r es la distancia entre el donor y el aceptor, R_0 la distancia de Förster –definida como la distancia a la cual la velocidad de transferencia $K_T(r)$ es igual a la velocidad de decaimiento el donor en ausencia de aceptor- y τ_D es el tiempo de vida del donor en ausencia de transferencia de energía. La eficiencia de la transferencia de energía, definida como la fracción de fotones absorbidos por el donor que son transferidos al aceptor viene dada por la ecuación 3:

$$E = \frac{R_0^6}{R_0^6 + r^6} \qquad \text{(ec. 3)}$$

Por lo tanto, los procesos de transferencia de energía de resonancia dependen considerablemente de:

1. La distancia entre donor y aceptor (habitualmente ocurre a distancias de entre 10 y 100 Å).

2. La orientación de los dipolos de ambas moléculas que debe ser aproximadamente paralela.

3. El grado de solapamiento entre el espectro de emisión del donor y el espectro de absorción del aceptor, lo que se calcula mediante la integral de solapamiento J

En consecuencia, cuando se de un proceso de transferencia de energía de resonancia se va a observar una disminución tanto de la intensidad de luminiscencia como del tiempo de vida de la sustancia donora [6].

Filtro interno

Este proceso, al igual que el de transferencia de energía de resonancia, requiere de la existencia de un donor y un aceptor. Sin embargo, en esta ocasión viene causado por la absorción de radiación por el fluoróforo o bien por otro componente de la muestra.

Existen dos tipos de filtro interno [7]:

1. Filtro interno primario, que implica la absorción de la radiación de excitación por parte de la sustancia aceptora.
2. Filtro interno secundario, en el que se produce la absorción de la radiación luminiscente emitida por un luminóforo (donor).

Si nos centramos en el efecto de filtro interno secundario, ha de cumplirse que la sustancia donora sea luminiscente y que los espectros de emisión de la sustancia donora y el de absorción de la sustancia aceptora solapen.

Al contrario del proceso de transferencia de energía de resonancia, aquí sí hay proceso radiante, el donor va a emitir radiación que será absorbida en mayor o menor grado por la sustancia aceptora dependiendo del grado de solapamiento entre sus espectros. En este proceso vamos a observar una variación en la intensidad de luminiscencia, pero no en el tiempo de vida.

El factor de atenuación de la intensidad de luminiscencia debido al efecto de filtro interno se puede calcular mediante la ecuación propuesta por Leese y Wehry [8]:

$$\frac{I}{I_0} = \frac{1-10^{-\varepsilon[Q]b}}{2.303\varepsilon[Q]b} \qquad \text{(ec. 4)}$$

donde ε es el coeficiente de absortividad molar del aceptor Q a la longitud de onda de emisión y b es el paso efectivo del haz procedente de la fuente de radiación.

Estos efectos de filtro interno se han utilizado en diversas ocasiones, así para aumentar la sensibilidad de las medidas de fluorescencia usando un conjunto de indicadores con perfiles de pH complementarios, en concreto, indicadores colorimétricos junto con indicadores fluorimétricos que muestren valores de pK_a complementarios y solapamiento espectral [9]. También se han utilizado para el sensado de diferentes compuestos como ejemplo podemos citar: 1) etanol basado en un colorante tipo trifluoroacetilazobenzeno y un fluoróforo [10]; 2) de sodio usando ahora un ionóforo tipo calixareno terminado en un éter corona junto con indicadores de pH fluorescentes derivados del azul Nilo [11]; 3) de sodio utilizando la membrana conteniendo el ionoforo (un calix[4]areno derivado) y el cromoionoforo ETH5294 en presencia del compuesto fluorescente 5,10,15,20-tetrafenilporfina [12]; 4) de amoniaco mediante azul de bromofenol y partículas fluorescentes conteniendo Fluorescent Magenta [13] y 5) para dióxido de carbono basado en el indicador α-naftolftaleina y el fluoróforo tetrafenilporfina [14].

Analytica Chimica Acta 655 (2009) 66–74

Contents lists available at ScienceDirect

Analytica Chimica Acta

journal homepage: www.elsevier.com/locate/aca

Phosphorescent sensing of carbon dioxide based on secondary inner-filter quenching

I.M. Pérez de Vargas-Sansalvador[a], M.A. Carvajal[b], O.M. Roldán-Muñoz[a], J. Banqueri[b], M.D. Fernández-Ramos[a], L.F. Capitán-Vallvey[a,*]

[a] Department of Analytical Chemistry, Campus Fuentenueva, Faculty of Sciences, University of Granada, E-18071 Granada, Spain
[b] Department of Electronics and Computer Technology, Campus Fuentenueva, Faculty of Sciences, University of Granada, E-18071 Granada, Spain

ARTICLE INFO

Article history:
Received 26 June 2009
Received in revised form
22 September 2009
Accepted 24 September 2009
Available online 30 September 2009

Keywords:
Carbon dioxide
Gas sensor
Phosphorescence
Secondary inner-filter quenching
Microparticles

ABSTRACT

A study of different strategies to prepare phosphorescence-based sensors for gaseous CO_2 determina tion has been performed. It includes the characterization of different configurations tested, a discussion of the results obtained and possibilities for the future. The optical sensor for gaseous CO_2 is based on changes in the phosphorescence intensity of the platinum octaethylporphyrin (PtOEP) complex trapped both on oxygen-insensitive poly(vinylidene chloride-co-vinyl chloride) (PVCD) membranes and PVCD microparticles, due to the displacement of the α-naphtholphthalein acid–base equilibrium with CO_2 concentration. A secondary inner-filter mechanism was tested for the sensor and a full range linearized calibration was obtained by plotting $(I_{100} - I_0)/(I - I_0)$ versus the inverse of the CO_2 concentration, where I_0 and I_{100} are the detected luminescence intensities from a membrane exposed to 100% nitrogen and 100% CO_2, respectively, and I at a defined CO_2 concentration. The different configurations tested included the use of membranes containing luminophore and pH-sensitive dye placed on two opposite sides of a transparent support to prevent the observed degradation of the PtOEP complex in the presence of the tetraoctylammonium hydroxide (TOAOH) phase transfer agent, which produced better results regarding stability and sensitivity. The CO_2 gas sensor based on PtOEP homogeneous membranes presented better properties in terms of response time and sensitivity than that based on PtOEP microparticles. With a detection limit of 0.02%, the response time (10–90% maximum signal) is 9 s and the recovery time (90–10%) is 115 s. The lifetime of the membranes for CO_2 sensing preserved in a 94% RH atmosphere and dark conditions is longer than at least 4 months.

1. Introduction

The determination of CO_2, both in gas and in solution, is of considerable interest in different areas including clinical [1,2], environmental [3], biological [4], biochemical and industrial fields [5], such as wastewater treatment, control of biotechnological processes and modified atmosphere packaging [6]. Optical sensing of CO_2 takes advantage of its acidic nature, monitoring the CO_2 concentration via pH changes through different strategies it induces in acid–base indicators located in a membrane [7]. Obviously, in addition to CO_2, this sensing scheme is sensitive to different gases with acid–base properties. However, in different processes and applications, CO_2 is the only acidic gas present at a discernible level, such as in oxidative respiration and photosynthesis processes in bioreactors [8] and in marine sediments [3]; and in modified atmosphere packaging applications [9] and point-of-care testing in biomedicine [1].

Apart from infrared sensors, the first optical sensors for CO_2 were based on the interrogation of either an absorbance or fluorescence-based pH indicator in an aqueous hydrogen carbonate buffer, for example, a solution covered by a gas-permeable membrane [10] and a dye-doped layer of hydrophilic materia maintained beneath a gas-permeable hydrophobic membrane [11]. Later, the limitations of this design due to the need to maintain the moisture level in the membrane led to the appearance of so-called solid sensor membranes that replaced the aqueous buffer system by a quaternary ammonium hydroxide. This base was used for different functions: (1) ion pairing of the basic form of the pH indicator at least, depending on the charged groups of indicator and (2) providing needed water from the hydrated ionic pair for the uptake of CO_2 from the atmosphere by forming a lipophilic hydrogencarbonate buffer [12]. An alternative was the replacement of a quaternary ammonium cation by room-temperature ionic liquids [13,14].

The membrane polymer used plays an important role in sensitivity and stability of gas sensors, with ethyl cellulose [15], sol–gels [16], silicones [4] and composite materials being common [8]. On the other hand, the sensing material can be placed on a rigid and

* Corresponding author. Tel.: +34 958248436; fax: +34 958 243 328.
E-mail address: lcapitan@ugr.es (L.F. Capitán-Vallvey).

0003-2670/$ – see front matter © 2009 Elsevier B.V. All rights reserved.
doi:10.1016/j.aca.2009.09.037

PHOSPHORESCENT SENSING OF CARBON DIOXIDE BASED ON SECONDARY INNER-FILTER QUENCHING

I. M. Pérez de Vargas-Sansalvador [a], M.A. Carvajal [b], O.M. Roldán-Muñoz [a], J. Banqueri [b], M.D. Fernández-Ramos [a] and L.F. Capitán-Vallvey [a]*

ECsens. [a] Department of Analytical Chemistry. [b] Department of Electronics and Computer Technology.Campus Fuentenueva, Faculty of Sciences, University of Granada, E-18071 Granada, Spain.

Abstract

A study of different strategies to prepare phosphorescence-based sensors for gaseous CO_2 determination has been performed. It includes the characterization of different configurations tested, a discussion of the results obtained and possibilities for the future. The optical sensor for gaseous CO_2 is based on changes in the phosphorescence intensity of the platinum octaethylporphyrin (PtOEP) complex trapped both on oxygen-insensitive poly(vinylidene chloride-co-vinyl chloride) (PVCD) membranes and PVCD microparticles, due to the displacement of the α-naphtholphthalein acid-base equilibrium with CO_2 concentration. A secondary inner-filter mechanism was tested for the sensor and a full range linearized calibration was obtained by plotting $(I_{100} - I_0)/(I - I_0)$ versus the inverse of the CO_2 concentration, where I_0 and I_{100} are the detected luminescence intensities from a membrane exposed to 100% nitrogen and 100% CO_2, respectively, and I at a defined CO_2 concentration. The different configurations tested included the use of membranes containing luminophore and pH-sensitive dye placed on two opposite sides of a transparent support to prevent the observed degradation of the PtOEP complex in the presence of the tetraoctylammonium hydroxide (TOAOH) phase transfer agent, which produced better results regarding stability and sensitivity. The CO_2 gas sensor based on PtOEP homogeneous membranes presented better properties in terms of response time and sensitivity than that based on PtOEP microparticles. With a detection limit of 0.02%, the re-

sponse time (10% to 90% maximum signal) is 9 s and the recovery time (90% to 10 %) is 115 s. The lifetime of the membranes for CO_2 sensing preserved in a 94% RH atmosphere and dark conditions is longer than at least 4 months.

Key words. Carbon dioxide; gas sensor; phosphorescence; secondary inner-filter quenching; microparticles.

* Corresponding author; *e-mail: lcapitan@ugr.es*

Introduction

The determination of CO_2, both in gas and in solution, is of considerable interest in different areas including clinical [15,16], environmental [17], biological [18], biochemical and industrial fields [19], such as wastewater treatment, control of biotechnological processes and modified atmosphere packaging [20]. Optical sensing of CO_2 takes advantage of its acidic nature, monitoring the CO_2 concentration via pH changes through different strategies it induces in acid - base indicators located in a membrane [21]. Obviously, in addition to CO_2, this sensing scheme is sensitive to different gases with acid-base properties. However, in different processes and applications, CO_2 is the only acidic gas present at a discernible level, such as in oxidative respiration and photosynthesis processes in bioreactors [22] and in marine sediments [17]; and in modified atmosphere packaging applications [23] and point-of-care testing in biomedicine [15].

Apart from infrared sensors, the first optical sensors for CO_2 were based on the interrogation of either an absorbance or fluorescence-based pH indicator in an aqueous hydrogen carbonate buffer, for example, a solution covered by a gas-permeable membrane [24] and a dye-doped layer of hydrophilic material maintained beneath a gas-permeable hydrophobic membrane [25]. Later, the limitations of this design due to the need to maintain the moisture level in the membrane led to the appearance of so-called solid sensor membranes that replaced the aqueous buffer system by a quaternary ammonium hydroxide. This base was used for different functions: 1) ion pairing of the basic form of the pH indicator, at least, depending on the charged groups of indicator; and 2) providing needed water from the hydrated ionic pair for the uptake of CO_2 from the atmosphere by forming a lipophilic hydrogencarbonate buffer [26]. An alternative was the replacement of a quaternary ammonium cation by room-temperature ionic liquids [27,28].

The membrane polymer used plays an important role in sensitivity and stability of gas sensors, with ethyl cellulose [29], sol-gels [30], silicones [18] and composite materials being common [22]. On the other hand, the sensing mate-

rial can be placed on a rigid and optically transparent support [23] or directly attached to the tip, at the end or in the core of an optical fibre [15].

The optical sensing element can be a colorimetric indicator entrapped [31] or covalently immobilized on a polymeric support [32]. The advantages of luminescence measurements favor the use of fluorescent indicators, although the limited number of fluorescent pH indicators with appropriate pKa, brightness, and photostability [27,31] has made it necessary to try different solutions. The most common of these relies on fluorescence intensity or quantum yield variation by quenching by a luminescent inert dye with one of the forms of the colorimetric pH indicator by resonance energy transfer (RET) [30] or inner-filter effects [14].

Fluorescence intensity is the most common parameter, although it suffers from different drawbacks such as photobleaching or drifts of the opto-electronic system[22]. One strategy for overcoming some of these problems is the steady-state ratiometric approach, using, for example, two excitation wavelengths of luminophore [18,33]. The measurement of decay time is a good alternative that requires more complex instrumentation in the case of short-lived luminophores [26,32], and thus the long-lived ones are more useful [34]. The measurement of the phase shift by different methods [30,34] is another strategy used to obtain lifetime information.

The use of room-temperature phosphorescence measurement in chemical sensing offers advantages over other luminescent signals [35]. In our opinion, the most interesting advantage is that which appears as a consequence of spin-forbidden transitions, which generates long lifetime emissions and facilitate the design of portable instrumentation [1,2].

In this paper, we report on the development of a phosphorescent inner filter-based membrane for CO_2 sensing. As an analyte-sensitive pH indicator, α-naphtholphthalein was used in combination with the long-lifetime luminophore platinum octaethylporphyrin (PtOEP) immobilized both on homogeneous PVCD membranes and PVCD microspheres and with TOAOH tetraoctylammonium hydroxide as the phase transfer.

2. Experimental section

2.1. Materials

Platinum octaethylporphyrin complex (PtOEP) was obtained from Porphyrin Products Inc. (Logan, UT, USA). The polymers used were: polyurethane hydrogel D4 and D6 from Tyndale Plains-Huter L.D. (Lawrenceville, NJ, USA), poly(vinylidene chloride-co-vinyl chloride) (PVCD, particle size 240-320 μm), polystyrene (PS, average MW 280,000, Tg:100 ºC, GPC grade), ethylcellulose (EC, ethoxyl content 49%) and Nafion from Sigma–Aldrich Química S.A. (Madrid, Spain), ethylene vinyl alcohol copolymer (EVAL, F104A, EVAL Europe, Zwijndrecht, Belgium) and polyacrylonitrile (PAN, Goodfellow, Cambridge, UK). Tetrahydrofuran (THF), tributyl phosphate (TBP), toluene, ethanol and poly(vinyl alcohol) (PVA, average molecular weight 70,000-100,000) were supplied by Sigma.

Other reagents used were thymol blue, α-naphtholphthalein, Sudan III, and tetraoctyl ammonium hydroxide (TOAOH) (0.335 M in methanol), all from Sigma. Sheets of Mylar-type polyester from Goodfellow (Cambridge, UK) were used as a support for membranes. The CO_2, O_2 and N_2 gases used were of a high purity (>99%) and were supplied in gas cylinders by Air Liquid S.A. (Madrid, Spain). The water used was reverse-osmosis type quality from Milli-RO 12 plus a Milli-Q purification system (Millipore, Bedford, MA, USA).

Luminescent microparticles containing PtOEP were produced by Flow Focusing technology [3,4] using a standard Avant Flow Focusing nozzle (Ingeniatrics, Sevilla, Spain) in a liquid–liquid configuration. The oil phase was 4.0% in PVCD in cyclohexanone containing 1.0 mM PtOEP injected through a syringe pump (1 $mL \cdot h^{-1}$) and the aqueous phase was water injected with an HPLC pump (2 $mL \cdot min^{-1}$). The continuous phase was water containing 0.25% poly(vinyl alcohol) to prevent the formation of aggregates and stirred at 350 rpm. Afterwards, the particles were washed with water and ethanol and were air-dried. Particle size distributions were determined by dynamical light scattering (DLS) and characterized by transmission electron microscope (TEM) and fluorescence microscopy.

2.2. Instrumentation

For the characterisation of the sensing membranes, steady-state measurements were performed using a Hewlett Packard diode array spectrophotometer (model 8453; Nortwalk, CT, US) for absorption measurement and a Cary Eclipse fluorescence spectrometer (Varian Australia Pty Ltd.) for luminescence measurements.

Figure 2. Cary Eclipse fluorescence spectrometer used for luminescence measurements.

Luminescence decay measurements were obtained using the time-correlated single photon counting technique with an OB 920 spectrometer with a μF 900-HP microsecond flash lamp and S900 single photon photomultiplier detection system (Edinburgh Instruments Ltd, Livingston, UK). The absorbance and luminescence measurements of the sensing films were performed using homemade cell holders for each type of spectrophotometer[36,37]. In the case of steady-state luminescence experiments, the membranes were measured at a

45° angle in the cell to minimise light scatter from the sample and substrate; additionally, the excitation and emission slits used were 5.0/5.0 nm and 5.0/10.0 for membranes containing microparticles. In the case of double membranes on the same or opposite sides of the plastic support, the membranes were irradiated with excitation light from the PtOEP side and the luminescence was collected from the α-naphtholphthalein side.

The standard mixtures of CO_2 (in the range 0–100%) in N_2 and CO_2 and O_2 in N_2 were produced using N_2 as the inert gas component and O_2 by controlling the flow rates of different high purity gases, CO_2, N_2 and O_2, in each case, which entered a mixing chamber using a computer-controlled mass flow controller (Air Liquid España S.A., Madrid, Spain) operating at a total pressure of 760 Torr and a flow rate between 100 and 500 $cm^3 \cdot min^{-1}$.

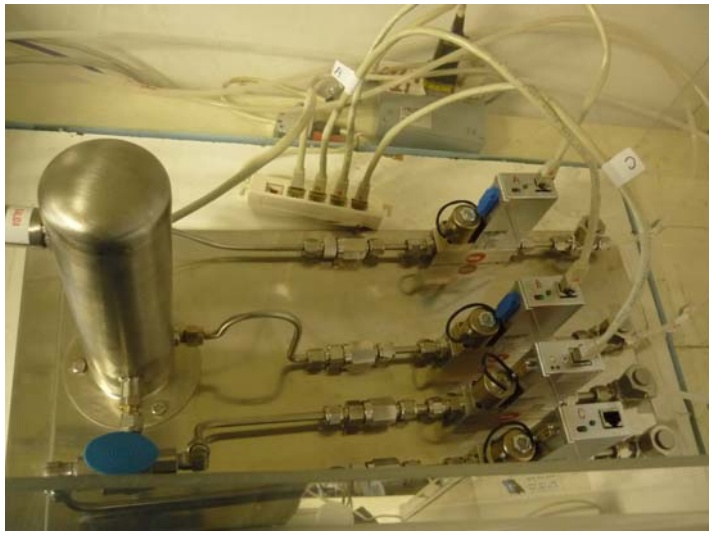

Figure 3. Mass flow controllers system for calibrated gas mixture preparation.

For the preparation of the gas mixtures with a concentration lower than 0.40% CO_2 a standard of 5% CO_2 in nitrogen was used, with lowest CO_2 con-

centration tested being 0.02%. To study the effect caused by other gases and vapors such as SO_2, He, Ar, NO_2, CO, HCl and CH_3COOH, a constant concentration of CO_2 was mixed with different flows of the cited gases or vapors using the mass flow controller cited above or an exponential dilution system [38].

All the emission intensity and decay measurements were carried out at room temperature. All measurements were made in triplicate, except when stated otherwise, to check for experimental errors.

2.3. Procedures

2.3.1. Sensing membrane preparation

The membranes were produced on a non-luminescent Mylar polyester substrate using a spin-coating technique. Sensing films were prepared from cocktails A and B; with cocktail A containing 100 mg PVCD dissolved in 1 mL of freshly distilled THF using an ultrasonic bath and then 0.5 mg PtOEP. Cocktail B is composed of 64 µL TBP, 320 µL of a α-naphtholphthalein solution (2.2 mg of α-naphtholphthalein in 2 mL of toluene/EtOH 80:20 v/v), 60 mg of EC previously dissolved in 1 mL of toluene and finally 200 µL of 0.335 M TOAOH were added. All cocktails were prepared weighing the chemicals in a 4 mL flask with a DV215CD balance (Ohaus Co., Pine Brook, NJ, USA) with a precision of ±0.01 mg.

Different configurations were tested for the sensing film preparation (Figure 1): 1) Single-membrane configuration: prepared by mixing 120 and 150 µL, respectively, of cocktails A and B and casting 20 µL of the mixture on a 0.5 mm thick transparent polyester sheet of 12 x 35 mm using a homemade spin-coater rotating at 180 rpm. After spinning for 2 min, the support was removed from the spin coater and dried in a dryer with a saturated THF atmosphere for 12 h at room temperature. 2) Double-membrane configuration: prepared with 20 µL of cocktail A using the above spin coater and after drying in a saturated THF atmosphere for 1 h, deposit of 25 µL of cocktail B on the top film and drying under vacuum for 12 h. 3) Sandwich membrane configuration: prepared in the

same way as number 2, but including a polymeric layer between them. As polymers for that layer polyurethane D4 and D6, PVCD and Nafion were tested. 4) Double membrane on opposite side configuration: this was prepared using the same volume of cocktails A and B as in the double-membrane configuration but on opposite sides of the Mylar support. 5) Membranes containing PtOEP microparticles. A new cocktail A was prepared containing 1.5 mg of PtOEP microparticles suspended in a mixture of 40 µL of toluene/EtOH mixture (80/20 v/v) and 200 µL of another solution containing 60 mg of EC dissolved in 1 mL of toluene, and stirred by a tube shaker. Using this cocktail and the previous cocktail B, different sensing membranes were cast using the same configurations indicated above. The membranes containing PtOEP in PVCD were stored for curing in darkness for 9 days before their use.

2.3.2. Operational lifetime.

All membranes, including those containing microparticles, displayed mechanical stability and good adhesion to the support. Short term stability was studied by continuous measurement for 12 h of the double membrane placed in the sample holder of the luminometer and irradiated at 537 nm in an atmosphere of 6.25% CO_2. The long-term stability of both the indicator and luminophore membranes was studied separately by storing the membranes in darkness in the case of luminophore and indicator membranes both in a 33% relative humidity (RH) atmosphere (25±0.5ºC) and 94% RH atmosphere (25±0.5ºC) using a desiccator. The effect of light on the stability was studied placing membranes in a desiccator exposed to indirect lab lighting. In all cases, the desiccators contained sodium carbonate to protect the membranes from acidic gases in the lab. The stability was studied by periodically performing a short calibration for CO_2 with 5 gas standards covering the whole range.

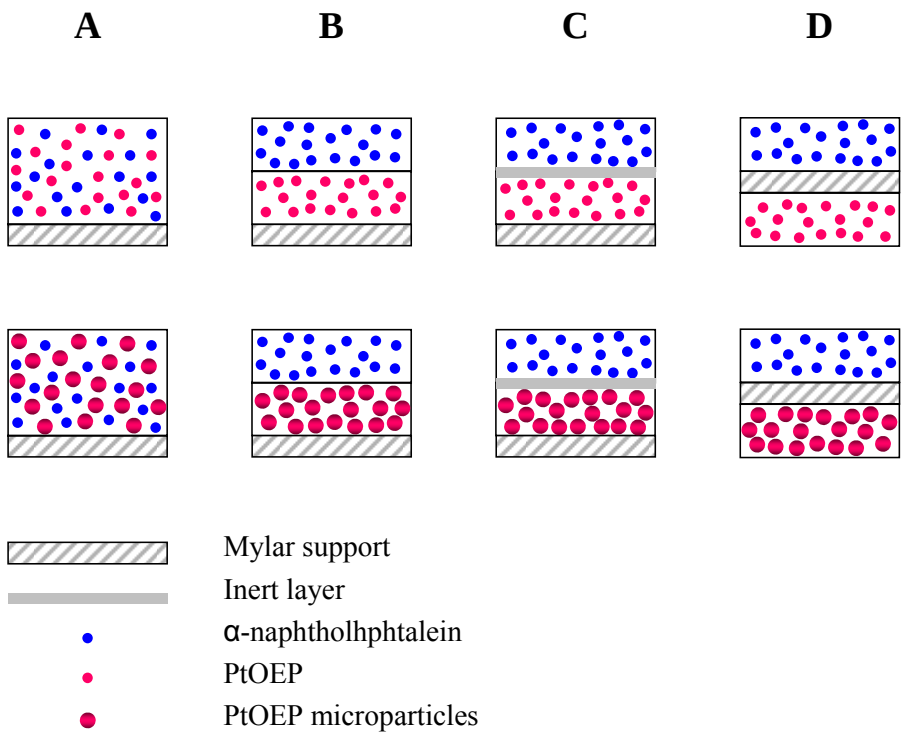

Figure 4. Cross section of the different configurations tested for the sensor layer used for optical sensing of CO_2. A: single-membrane configuration; B: double-membrane configuration; C: sandwich membrane configuration; D: double membrane on opposite sides.

3. Results and discussion

3.1. *Sensing chemistry*

The sensing chemistry for CO_2 that we study in this paper is based on plastic solid state sensor membranes that work by quenching a luminescent dye by one of the chemical forms of a non-fluorescent pH indicator [21]. In this system, a lipophilic or lipophilized acid-base indicator is included in a CO_2 permeable membrane containing an ammonium quaternary hydroxide as an internal buffering system to both turn the indicator into the deprotonated form and stabi-

lize its basic form as a hydrated ionic pair and to enable the uptake of CO_2 from the atmosphere by forming a lipophilic hydrogencarbonate buffer. The change in the position of the acid-base equilibrium by CO_2 in the membrane and the consequent change in colour is transduced into a change in luminescence due to the overlapping of the absorbance spectrum of the pH indicator and the emission of PtOEP.

3.2. *Choice of materials and membrane configurations*

The selected luminophore was the PtOEP complex because of its very long lifetime (τ_0 ~ 100-200 µs depending on the chemical nature of the polymeric matrix), visible absorption (B(0) at 380 nm and Q(0) at 533 nm), Stokes displacement (emission at 650 nm), phosphorescence quantum yield (~0.2 under ambient conditions) [39] and non-influence of CO_2 on luminescence, although it is not very photostable [40]. To the best of our knowledge, the PtOEP luminophore has not been used for CO_2 sensing chemistry probably due to its instability in the basic medium needed to adjust the equilibrium of the acid-base indicator.

A preliminary test performed with different acid-base indicators showed that the preparation of a single membrane from a cocktail containing luminophore (cocktail A) and any pH indicator (cocktail B) was not possible, due to the reaction of the PtOEP complex, which that leads to a strong quenching in luminescence (78.7% for membranes prepared with cocktail B without any indicator). The mix of both cocktails produced a quick change in the colour of membrane from pink to orange that changed with a black lump appearing when the amount of TOAOH added increased (Figure 2). The visible spectra of the above membranes were the same as that of membranes only containing PtOEP (from cocktail A), although with a considerable increase in background. That reaction can be ascribed to a reduction of Pt(II) present in PtOEP to metallic platinum by amines coming from the Hofmann elimination reaction by tetra octhyl ammonium salt (TOAOH) in the basic medium.

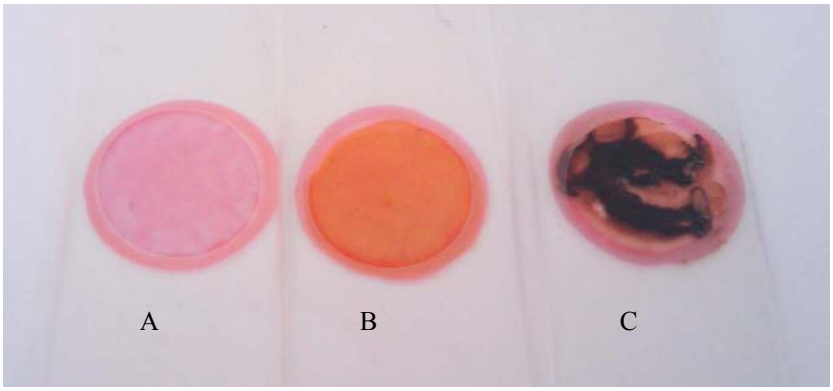

Figure 5. Sensing membranes prepared for CO_2. (A) Membrane containing only PtOEP (20 µL of cocktail A); (B) Membrane similar to A after the addition of 20 µL of cocktail B without the pH indicator; and (C) The same as B but increasing the concentration of TOAOH in the cocktail B.

To prevent the reduction in luminescence intensity and the lifetime of PtOEP emission by oxygen [41], we studied the membrane making different polymers with low oxygen permeability (EVAL, PAN and PVCD) but permeable for CO_2 while not changing the PtOEP spectral characteristics. The best suited was PVCD, due to its low oxygen permeability (0.10 cc.20µm/m^2.day.atm) [42] and the resulting spectral characteristics of PtOEP (λ_{exc} 537 nm; λ_{em} 650 nm; τ in N_2 96.0 µs). The luminescence intensity of a PVCD film containing PtOEP only decreases 3.3% at 30% O_2 and 40% at 100% O_2.

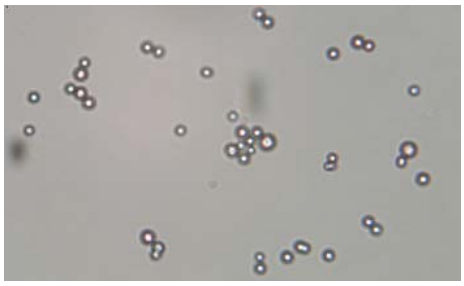

Figure 6. Picture of microparticles obtained using an optical microscope

Additionally, the inclusion of the PtOEP complex in microparticles was studied as a way to avoid their incompatibility with TOAOH and any quenching by oxygen. Using flow focusing technology [3,4] we produced PVCD microparticles. The solvent used for the PVCD was cyclohexanone because of the solubility of this polymer and its immiscibility with water, which is required for the flow focusing technique. Its higher boiling point (155.6 °C) than water made it necessary to maintain the solution obtained under vacuum for 24 h after mixing the two phases, followed by three centrifugation steps (13,500 rpm; 10 min) and washing with water before the lyophilisation of the obtained microparticles. Different influential factors on flow focusing methodology were optimized such as polymer, PtOEP and particle stabilizer (poly(vinyl alcohol)) concentrations, oil phase and aqueous phase flows and stirring rate. The obtained microparticles had a monomodal distribution when using a 1.0 mM PtOEP solution. The 5 µm mean diameter microparticles obtained were spherical and non-aggregated with a very reproducible size distribution showing the same spectral properties as PtOEP membranes in PVCD.

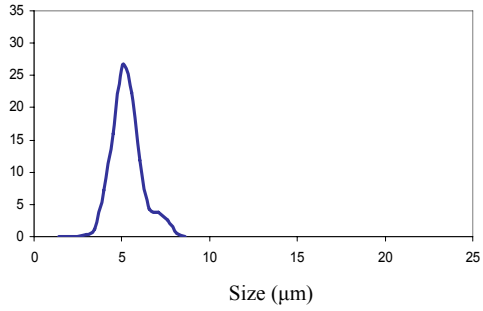

Figure 7. Size particle distribution by DLS.

To corroborate that the luminophore has been encapsulated a confocal miscroscope was used. The results are shown in figure 8.

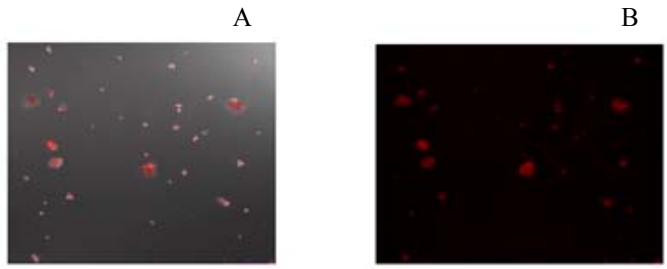

Figure 8. Confocal fluorescence microscopic images of the PVCD-PtOEP microparticles. Picture B is an enlargement of picture A.

As an acid-base indicator, we tested different compounds, namely Sudan III, thymol blue and α-naphtholphthalein, which shows adequate pKa values in water and absorption spectra to act as an acceptor of PtOEP luminescence. As membrane polymer, ethyl cellulose was used, which is usual with this type of sensors, due to its ability to stabilize the hydrated ion pair ammonium quaternary-indicator basic form due to interactions with the hydrophilic sites [43].

Although the I_{100}/I_0 ratio is commonly used to represent the sensitivity of a sensing membrane [14], where I_0 and I_{100} represent the measured phosphorescence intensities from the sensing film exposed from 100% nitrogen to 100% CO_2, respectively, in our case we preferred to use the I_{100}-I_0 parameter because it is a more suitable indication of the width of the measurement range of the membrane [16]. However, when using the I_{100}/I_0 parameter, the results are similar and higher than the usual minimum value of 3 for all selected membranes [14]. The I_{100}-I_0 value for these membranes containing $2.80 \cdot 10^{-2}$ mol·kg^{-1} polymer indicator concentration were 61 for Sudan III (I_{100}/I_0 = 1.10), 365 for thymol blue (I_{100}/I_0 = 3.67) and 470 for α-naphtholphthalein (I_{100}/I_0 = 9.00) using in all cases a membrane configuration with opposite sides. In the end, the indicator selected was α-naphtholphthalein because it shows the highest sensitivity for CO_2.

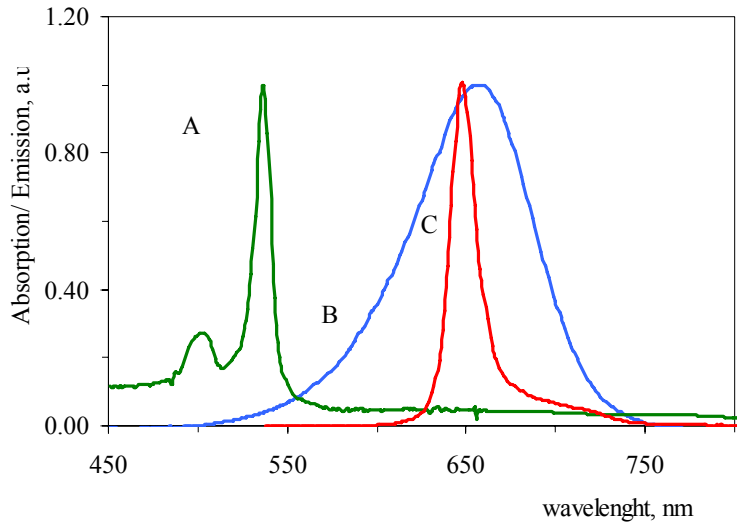

Figure 9. Spectral properties of the chemicals used in the CO_2 sensor (normalized spectra). Excitation (A) and phosphorescence emission spectra (B) of PtOEP membrane in PVCD. (C) absorption spectrum of α-naphtholphthalein. This figure shows the overlap of donor and acceptor spectra.

Additionally, α-naphtholphthalein in EC was used as the pH-dependent acceptor because its deprotonated form is blue and its absorption spectrum strongly overlaps the phosphorescence emission spectrum of PtOEP (Figure 9). When the PtOEP complex in PVCD was excited at 537 nm, the emission occurred at 650 nm overlapping the absorbance maximum of the basic form of α-naphtholphthalein paired with TOA that appeared at 655 nm, permitting the luminescence quenching. Consequently, increasing the CO_2 concentration increases the measured phosphorescence from the sensing membrane, allowing optical sensing of CO_2.

As a consequence of the instability of PtOEP in membranes containing both luminophore as the indicator chemistry, as discussed above, different arrangements for CO_2 sensing membranes were studied. A double layer configuration with the indicator membrane covering the luminophore could be used but with poor response to CO_2 (I_{100}-I_0 = 100) and very low stability (less than 1 day), probably due to the diffusion of TOAOH into the PtOEP layer and subsequent reaction. The inclusion of an inert layer (D4 and D6 polyurethane, PVCD and

Nafion were tested) between the two sensing membranes improved both stability (1 day) and response to CO_2 (I_{100}-I_0 = 333), with respect to the previous configuration, but not enough for sensing purposes.

The best solution was making the deposit on two opposite sides of the same support. In that case, we found a good response (I_{100}-I_0 = 524; I_{100}/I_0 = 9.31) and much more stability, which is studied on other section of this paper. For this reason, this configuration was selected for further studies.

The composition of the sensing membranes with the configuration on opposite sides was optimized, checking that an increase in the PtOEP concentration up to $6.84 \cdot 10^{-3}$ mol·kg^{-1} polymer (0.5%) enhances the signal intensity and the signal-to-noise ratio (S/N). This concentration was selected because at higher concentrations PtOEP self-quenching occurs. The concentration of the indicator is an important factor to adjust the sensitivity of sensing membrane that works by inner filter. Different indicator membranes were prepared varying the α-naphtholphthalein concentration between $6.37 \cdot 10^{-3}$ and $3.10 \cdot 10^{-2}$ mol·kg^{-1} polymer, and examining the I_{100}-I_0 response. The value grows up to $1.40 \cdot 10^{-2}$ mol·kg^{-1} polymer, and then decreases, probably due to some primary inner-filter effect on the excitation band of PtOEP at 537 nm from the increase in the bandwidth of the α-naphtholphthalein band (centered at 655 nm) with the concentration. Thus, a $1.40 \cdot 10^{-2}$ mol·kg^{-1} polymer α-naphtholphthalein concentration was selected. TBP was used to prepare the plasticized membrane and the amount of 3.85 mol·kg^{-1} polymer was selected. The sensitivity to CO_2 may be fine-tuned as usual by varying the TOAOH concentration in the sensing membrane [26]. In this case, we used a high concentration (1.12 mol·kg^{-1} polymer) in order to enhance the storage stability [43,44].

Additionally, the CO_2 sensing membranes were prepared using PtOEP in PVCD microparticles instead of homogeneously dissolved in PVCD. Different membranes containing PtOEP microparticles were prepared from a dispersion of these microparticles in EC dissolved in toluene/ethanol 80:20 v/v. The I_{100}-I_0 values increases with the particle percentage (2.0 %, 59; 4.0 %, 196; 11.3 %, 360) up to 11.3%, which was selected for subsequent experiments (I_{100}/I_0 =

15.8), because higher percentages make it difficult to handle the dispersion and membrane preparation. Different configurations were tested, observing that as with the homogeneous membranes discussed above, the only possible configuration was on opposed sides. Any other configuration (single membrane, double membrane and sandwich membrane) results in low stability due to the PtOEP reaction.

3.3. *Sensing and transduction mechanism*

One of the sensing mechanisms for optical sensors for CO_2 relies on fluorescence intensity or quantum yield variation by interactions (quenching) with other chemical species. The most used quenching mechanisms are resonance energy transfer (RET) [30] and inner-filter effects [14]. In the first case, the transfer of excited-state energy takes place from a donor to an acceptor sensitive to CO_2 without the appearance of a photon and mainly as result of dipole-dipole interactions between the donor and acceptor. In the case of inner-filter effects, the quenching is due to absorption of the excitation and/or emission radiation by the quencher.

Among the different inner-filter effects, the most common is a secondary inner-filter that involves the absorption of the emitted luminescent radiation by a CO_2-sensitive chromophore, typically the basic form of a liphophilic acid-base indicator [45]. With the membrane configurations used in this paper, placed on opposite sides of the same transparent support, RET quenching is not possible due to the long distance between the donor and acceptor, although Burke *et al.* [46] in their study of phosphorescent Pt(II) coproporphyrin labelled oligonucleotides suggest that porphyrin–porphyrin quenching by RET mechanism can be ruled out, being predominantly static. In any case, the no RET quenching is confirmed by measuring the phosphorescence lifetime of the membranes before and after exposure to CO_2 atmosphere (at 100% nitrogen: τ_1 96.0 μs (SD 1.85); at 100% CO_2: τ_1 97.9 μs (SD 0.77) .

The attenuation factor for luminescent intensity due to the secondary inner filter can be calculated according to Leese and Wehry [8] and Yuan and Walt

[7] procedures, considering a front-surface illumination case according to equation 1:

$$\frac{I}{I_0} = \frac{1-10^{-\varepsilon[N^-]b}}{2.303\varepsilon[N^-]b} \qquad \text{(Equation 1)}$$

where ε is the molar absorptivity of the acceptor, the basic form of α-naphtholphthalein N^- at the emission wavelength of luminophore ($8.65 \cdot 10^3$ $l \cdot mol^{-1} \cdot cm^{-1}$) and b the effective path length of the membrane (25 μm).

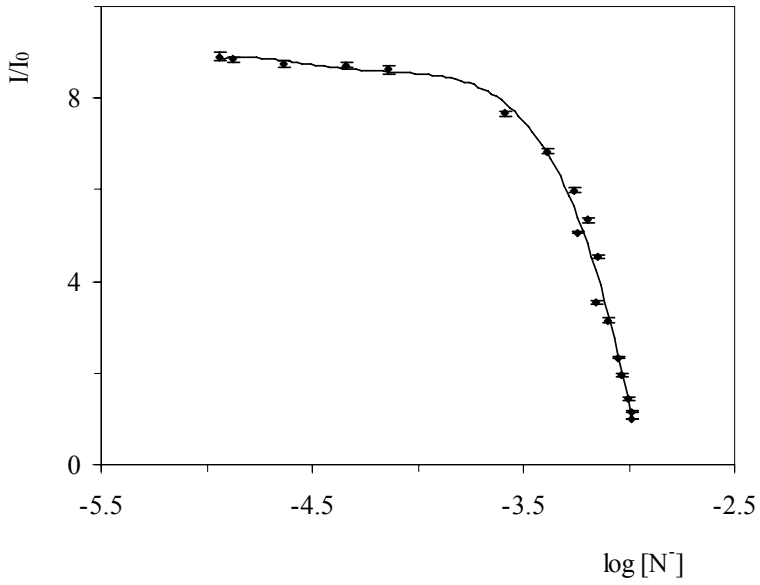

Figure 10. Calculated curve (best fit using eq.1) and experimental values of basic form of α-naphtholphthalein concentration versus the phosphorescent intensity of PtOEP in a membrane on an opposite side configuration by varying the concentration of CO2 from 0% to 100%.

Figure 10 shows a good agreement (r^2 = 0.9913) between the calculated curve and experimental values of the basic form of α-naphtholphthalein concentration on the phosphorescent intensity of PtOEP in the membrane, which corroborates the use of a secondary inner-filter mechanism for this CO_2 sensor.

The sensor mechanism is based on the reaction between α-naphtholphthalein and CO_2 according to:

$$TOA^+N^- \cdot xH_2O + CO_2 \xleftrightarrow{K} TOA^+HCO_3^- \cdot (x-1)H_2O \cdot HN \quad \text{(Equation 2)}$$

where $TOA^+N^- \cdot xH_2O$ is the ion pair formed between tetraoctylammonium cation TOA^+ and the deprotonated form of α-naphtholphthalein N^- and K is the equilibrium constant. We used a proposed approximate equation [47] to model the CO_2 concentration dependence:

$$\frac{I}{I_0} = 10^{\{-C(1/(K+[CO_2])+1/K)\}} \quad \text{(Equation 3)}$$

where $C = K\varepsilon b\left[TOA^+N^- \cdot xH_2O\right]$. In Figure 11, the normalized intensity change I/I_0 versus the CO_2 concentration is presented both for homogeneous membranes (Figure 11A) and microparticle containing membranes (Figure 11B), with the solid line being the best-fit to equation 3 and K = 1.30 and C = 1.17 (r^2 = 0.977) for homogeneous membranes and K = 0.12 and C = 0.15 (r^2 = 0.986) for microparticle containing membranes.

3.4. *Sensing membrane characterization*

The sensing membrane configuration used here responds to CO_2 concentration varying the ratio of protonated to deprotonated forms of the α-naphtholphthalein indicator, which results in a gradual change in phosphorescence intensity from luminophore proportionally to the CO_2 concentration. In order to linearize the relationship between the phosphorescence intensity and CO_2 percentage, we used the inverse of a relative phosphorescence intensity $(I_{100} - I_0)/(I - I_0)$, where I_0 and I_{100} were the intensities at 0 and 100% gaseous CO_2, versus the inverse of CO_2 concentration (Equation 4) as suggested Amao *et al.* [29], with A and B being the two proportionality constants.

$$\frac{I_{100} - I_0}{I - I_0} = A \cdot \frac{1}{[CO_2]} + B \qquad \text{(Equation 4)}$$

A good fit in the whole range, derived from threefold replicas at room temperature, 20 ºC, is observed both for homogeneous membranes (r^2 = 0.9989) and microparticle containing membranes (r^2 = 0.9961). As the sensitivity is higher for membranes with a smaller slope A value, the homogeneous membranes are more sensitive to CO_2 than microparticle membranes by a factor of 1.4. Taking into account the type of calibration function used, we considered the minimum CO_2 concentration tested, 0.02 %, as the detection limit (Table 1).

Table 1. Characteristics of sensing membranes for CO_2.

Parameter	Membrane type	
	Homogeneous	Microparticles
Slope	1.028 ±0.0081	1.43 ± 0.023
Intercept	0.82±0.099	0.08 ± 0.28
R^2	0.9989	0.9961
Measurement range (%)	0-100	0-100
Precision (DER; n = 15) at 0.6 % CO_2	0.56	0.50
Precision (DER; n = 15) at 16.7 % CO_2	0.25	0.43
LOD (% CO_2)	0.02	0.02
Response time (t_{90}) (s)	9.3 ± 0.47	11.7 ± 0.10
Recovery time (t_{10}) (s)	115 ± 2.3	127 ± 4.3

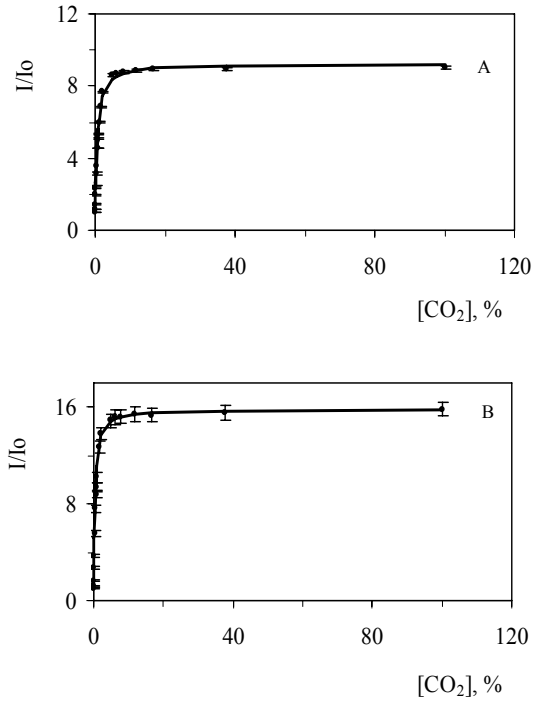

Figure 11. I/I_0 versus CO_2 concentration of a membrane with an opposite side configuration: (A) with PtOEP in PVCD and (B) with PtOEP in PVCD microparticles. The excitation and emission wavelengths are 537 and 650 nm, respectively. The solid line is the best-fit using Eq. 3.

Compared to the fluorescent pH indicator 8-hydroxypyrene-1,3,6-trisulfonic acid (HPTS) (τ_0 ~ 5 ns) widely used for plastic films CO_2 sensors, the long wavelength excitation and emission properties of PtOEP may be considered as an advantage over HPTS based ones. The detection limits reported for HPTS sensors depend on the sensor configuration, membrane material and type of measurement (steady state, time resolved, energy transfer), but typically range between 0.023% [48] and 0.1% [49,50], and thus are comparable to the described sensor (Table 2).

Table 2. Some selected luminescence-based sensors for gaseous CO_2 sensing.

Sensing Chemistry	Type of Measurem.	Detection limit	Resp time	Storage lifetime	Ref.
HPTS/EC	I	0.1%	15 s	16.2%/5 days	[49]
HPTS/IL/EC	I/R	--	20-54 s	3 months	[28]
HPTS/$(TOA)_4$/ SG	I	0.1%	30 s	6 months	[50]
HPTS$(CTA)_4$/ $Ru(dpp)_3$/O	LT/DLR	0.08%	20-30 s	7 weeks	[23]
HPTS/$(TOA)_4$/ PFO	I	0.03%	1.7 s	-	[51]
$Ru(dpp)_3$/$(TMS)_2$ /TB/EC	LT/F	0.015 hPa	15 s	2 months	[43]
$Ru(dpp)_3(TMS)_2$/ Sudan III/SG	LT/F	0.06%	20-30 s	3 months	[30]
$Ru(pzth)_3(PF_6)_2$/ PTFE	I	$9x10^{-6}$ MPa	2 min	4 months	[52]
$Eu(tta)_3$/TB/ EC	I	--	4 s	--	[29]
NA/TPP/EC	I	--	5 s	--	[14]
PtOEP/N/EC/ PVCD	I	0.02%	9 s	4 months	Our study

HPTS: 8-hydroxypyrene-1,3,6-trisulfonate; EC: ethyl cellulose; IL: Ionic liquid I : Intensity based;; R: ratiometric; TOA: tetraoctylammonium; CTA: Cetyltrimethylammonium; $Ru(dpp)_3$: Ruthenium(II) tris(4,7-diphenyl-1,10-phenanthroline); LT: Lifetime based; PFO: perfluoroalkyl ormosil; TMS: 3-trimethylsilyl-1-propane sulfonate ; TB : Thymol Blue; F: FRET; NA: α-naphtholphthalein; TPP: Tetraphenylporphyrin; SG: Sol-gel; $Eu(tta)_3$: tris(thenoyltrifluoroacetonato) europium(III) dihydrate; $Ru(pzth)_3(PF_6)_2$: tris[2-(2-pyrazinyl)-1,3-thiazole]ruthenium(II) dihexafluorophosphate; PTFE: poly(tetrafluoroethylene).

The precision in the measurement of CO_2 with the proposed sensing membranes was evaluated at two CO_2 concentrations (0.60 and 16.70 %), performing 15 measurements each, obtaining relative standard deviations of 0.56 and 0.25% in the case of the homogeneous membranes and 0.50 and 0.43% for microparticle containing membranes.

3.5. *Reversibility and response time*

The dynamic response of the sensing membranes when exposed to alternating atmospheres of pure CO_2 and pure nitrogen is shown in Figure 12. The response time from between 10% and 90% of the maximum signal of 9.0 s and,

a recovery time from 90% to 10% of 115.2 s were obtained for homogeneous membranes (Figure 12A) and 11.7 and 126.9 s for microparticle containing membranes (Figure 12B).

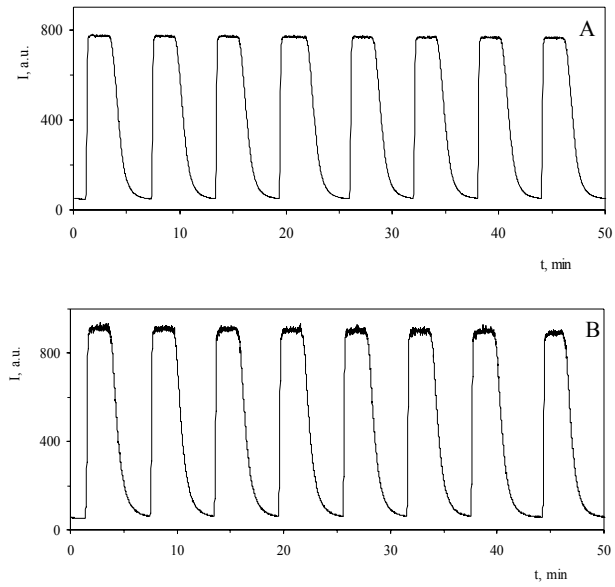

Figure 12. Response and recovery characteristics of CO_2 sensing membrane when increasing and decreasing CO_2 concentrations (from 0 to 100% and vice versa) change with membranes with opposed side configuration with PtOEP (A) and PtOEP containing microparticles (B). The excitation and emission wavelengths are 537 and 650 nm, respectively

The inclusion of luminophore in microparticles raises both the response (some 30%) and the recovery times (some 10%), despite the fact that the membrane containing the indicator is the same. In all cases, the signal changes were fully reversible and hysteresis was not observed during the measurements. The response and recovery times are higher, between 3 and 4 times, than other fluorescence-based sensors that use the same indicator, α-naphtholphthalein in ethyl cellulose TBP-plasticised membrane [14]. The reason for such discrepancies may lie in differences in temperature and membrane thickness that are not indicated in the cited papers and is of great importance in determining the rate of

response and the operational lifetime [53]. The difference between the response time and recovery time is common in CO_2 sensors as a result of the slow kinetic of the hydratation process for CO_2 and the differences between the rate constant for direct (0.040 s^{-1}) and reverse reaction (30 s^{-1}) [54]. Additionally, we checked that the prepared CO_2 membranes are able to continuously monitor increases and decreases in CO_2 concentration in a gas mixture.

The response and recovery behaviour of a homogeneous CO_2 sensing membrane on opposite sides is shown in Figure 13. It was performed by increasing and decreasing CO_2 concentrations, and six different concentrations were studied. The signal changes are fully reversible and measurement hysteresis of the CO_2 sensing film was not observed.

Compared to other sensing schemes widely used for CO_2 sensing, such as those based on the above cited HPTS, both response times and recovery times are in the same order of magnitude [48-50], although depending on the matrix, the response time can raise between 2 and 20 times [18,27,28] (Table 2).

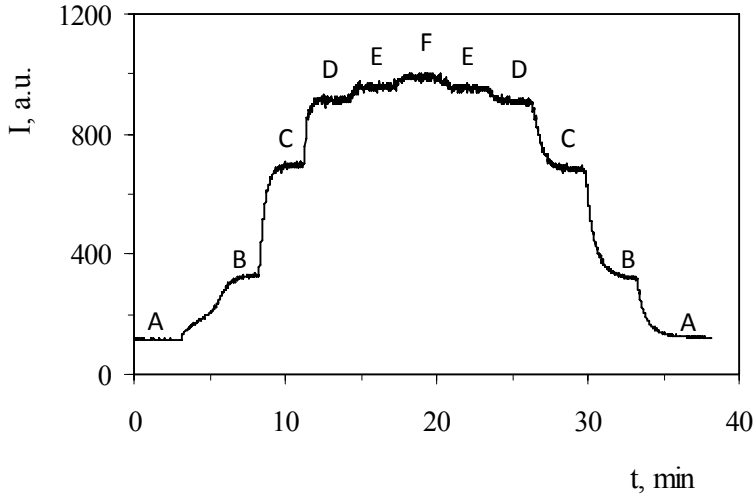

Figure 13. Response and recovery characteristic of CO_2 sensing film when increasing and decreasing CO_2 concentrations change. The excitation and emission wavelengths are 537 and 650 nm, respectively. (A) 0%; (B) 0.4 %; (C) 1.5%; (D) 6.2%; (E) 16.7% and (F) 100% of CO_2.

3.6. *Stability study*

The stability, both short-term and long-term, of sensing membranes is a very important issue for any real application. The long-term stability of luminophore membranes was studied at a good distance for 210 days, maintained in darkness at room temperature, and measuring the phosphorescence periodically. A constant increase in the signal (some 60%) was observed until the 9^{th} day, probably due to a curing process of the PVCD membrane containing PtOEP. Afterwards, the phosphorescence decreases slowly by some 20% at the end of the 210 days studied. The long-term stability of the indicator containing membrane, prepared from cocktail B, was studied for 120 days, keeping some membranes in a 33% RH atmosphere and others in 94% RH conditions. Additionally, and for membranes in high RH conditions, the influence of light was tested preparing two subsets in darkness and under ordinary, not direct, lab lighting conditions. The influence of the amount of TOAOH in the membrane was considered, preparing a set of membranes with 5 different concentrations (0.20, 0.39, 1.12, 1.67 and 2.23 mol·Kg^{-1} polymer). The stability of the membranes for CO_2 sensing was measured by the I_{100}-I_0 parameter using an independent PtOEP membrane, simply kept in darkness for the same time as the indicator membranes.

There was a significant difference between the half-life of the membranes (time it takes to reduce to one-half the initial I_{100}-I_0 value) preserved in high and low RH atmospheres. As usual, storage in air and exposure to light had a pronounced destroying effect on membranes. In 33% RH atmosphere, the half-life is between 1-2 weeks and very similar in 94% RH conditions under illumination, but in 94% RH and in darkness, it is longer than 4 months, the maximum time of the study (Figure 14). An increase in the base TOAOH concentration results in an increase in the lifetime of the membrane up to a concentration of 1.12 mol·Kg^{-1} polymer (see inset Figure 14), which confirms our previous selection for TOAOH concentration.

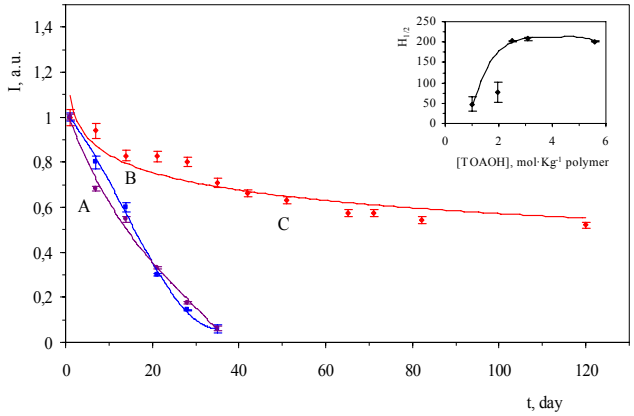

Figure 14. Stability of cocktail B under different conditions. (A) 94% RH atmosphere with sunlight (B) 33% RH atmosphere in darkness and (C) 94% RH atmosphere in darkness. Inset, $H_{1/2}$ (half-life) versus concentration of TOAOH shows the influence of the amount of TOAOH in the membrane.

As the study shows, the degradation of the indicator sensing membranes that results in a loss in sensitivity expressed as I_{100}-I_0 can be attributed to several factors: 1) loss of water from the ionic pair TOA^+N^- which reduces the response to CO_2, as shown by experiments in 33% RH atmosphere and darkness; 2) photodegradation of α-naphtholphthalein seen in experiments in 94% RH atmosphere and under illumination; and c) slow thermal decomposition of TOAOH caused by the Hoffman elimination reaction along with the neutralization of TOAOH by acidic gases and vapors present in the lab as shown by the results in 94% RH atmosphere and in darkness.

Similarly, we studied the short-term stability of the membranes prepared, with the optimal composition studying the evolution of the signal when measuring under constant irradiation at 537 nm in an atmosphere of 6.25% CO_2 for 12 h. The initial increase in signal could be ascribed to some curing process previously observed for PtOEP membranes. The decrease in phosphorescence intensity (9% in total for homogeneous membranes and 11% for microparticle containing membranes) indicates that this can be a serious problem when long-time measurements are performed with prepared sensing membranes.

Compared to HPTS based sensors, the stability of the sensor studied here seems somewhat worse, although this depends considerably on the matrix, membrane composition and storage method, with the best case being between 90 and 120 days [18,28].

3.7. *Interference study*

As noted above, this sensor is sensitive to different gases with acid-base properties in addition to CO_2, like all sensing strategies for this gas based on acid-base transduction [21]. Thus, interference from different gaseous species on CO_2 sensing membrane performance was studied. The strong quenching in luminescence caused by oxygen is prevented by a low oxygen permeability polymer. Using PVCD, both in homogeneous membranes and prepared as microparticles, a decrease in phosphorescence intensity as low as 1.2% is observed from an nitrogen atmosphere to atmospheric O_2 (21%) in the first case and 7.0% when working with microparticle membranes, due to the higher surface exposed in this case. Consequently, the presence of O_2 produces only slight changes in the sensitivity of the sensing membrane while other non-acidic gases such as CO and inert gases do not affect phosphorescence intensity. As usual [31], acidic gases and vapours such as HCl, SO_2, NO_2 and acetic acid cause interference, making the membrane non-operative.

4. CONCLUSIONS

An optical sensor for gaseous CO_2 based on phosphorescence intensity measurement of the PtOEP complex trapped both in PVCD membranes and in PVCD microparticles due to the displacement of the α-naphtholphthalein acid-base equilibrium was developed. The use of an opposite side configuration for both luminophore and pH indicator membranes prevents the observed degradation of the PtOEP complex in the presence of the phase transfer agent used, TOAOH. The observed phosphorescence intensity from PtOEP at 537 nm increased with the increase in the CO_2 concentration. A secondary inner-filter

mechanism was tested for this sensor and a full range linearized calibration was obtained by plotting $(I_{100} - I_0)/(I - I_0)$ versus the inverse of the CO_2 concentration.

The presented sensor shows a fast response (less than 9 s with a full range swing) and a suitable reproducibility of 0.5% in CO_2 concentration, accounting for analytical calibration curve fitting, interferents and lifetime.

The sensors prepared with homogeneous membranes were more sensitive (by a factor of 1.4) and accurate (1.7 times) than microparticle containing membranes, and additionally, the response and recovery times were slightly higher in microparticle containing membranes.

The presented sensor is the first room-temperature phosphorescent sensor described based on the long-life PtOEP complex described. The analyte-sensitive configurations studied based on homogeneous and microparticle membranes show good permeation selectivities and optical and adhesive properties. The studied sensing membranes can be of interest for the development of portable electronic room-temperature phosphorescence-based instrumentation for CO_2.

ACKNOWLEDGEMENTS

We acknowledge financial support from *Ministerio de Educación y Ciencia, Dirección General de Enseñanza Superior* (Spain) (Projects CTQ2005-09060-CO2-01 and CTQ2005-09060-CO2-02) and *Junta de Andalucia* (Spain) (Projects P06-FQM-01467, P08-FQM-3535).

5. CONCLUSIONES

En este capítulo se ha detallado el estudio llevado a cabo sobre un sensor para dióxido de carbono basado en sus propiedades ácido Lewis. Este sensor efectúa la medida mediante un efecto de filtro interno en el que un indicador ácido-base actúa sobre la intensidad de fosforescencia de un luminóforo de características complementarias. Para la detección de este gas se han medido los cambios en la intensidad de fosforescencia obtenida a distintas concentraciones de dióxido de carbono.

El objetivo de este estudio fue preparar un sensor para dióxido de carbono para el rango completo, esto es de 0 a 100%. Para ello se ensayaron cuatro configuraciones de membrana diferentes en las que se incluyó el luminóforo tanto disuelto en el polímero como contenido en micropartículas de PVCD preparadas mediante la técnica de *flow-focusing* para así evitar la atenuación producida por el oxígeno ambiental.

De los resultados obtenidos con cada una de las configuraciones estudiadas se deduce que el empleo de la configuración de membranas en caras opuestas, utilizando el luminóforo disuelto en PVCD, es el que ofrece mejores resultados en términos de sensibilidad y estabilidad.

Del estudio del mecanismo de sensado de dióxido de carbono podemos concluir que el modelo de transferencia de energía de resonancia no era aplicable aquí debido a la gran distancia de separación entre donor y aceptor, que se encuentran en membranas separadas por el soporte usado, y además lo corroboramos mediante el estudio del tiempo de vida de fosforescencia que se mantiene constante para diferentes concentraciones de dióxido de carbono. Además se procedió a la linealización de la respuesta exponencial creciente de forma que se pudiera emplear como función de calibrado lineal.

El sensor seleccionado además, presenta un tiempo de respuesta y recuperación cortos, lo que es una ventaja para su utilización.

La estabilidad del sensor ha sido ampliamente estudiada bajo diferentes ambientes, tanto con luz ambiental como en oscuridad y tanto en atmósfera

húmeda como en atmósfera del laboratorio. Podemos decir que las membranas, guardadas bajo oscuridad y en atmósfera húmeda se pueden utilizar durante más de cuatro meses.

El siguiente paso será la inclusión de estas membranas en una instrumentación portátil para la determinación de dióxido de carbono, lo cual será abordado en el siguiente capítulo.

6. REFERENCES

1. L.F. Capitan-Vallvey, L.J. Asensio, J. Lopez-Gonzalez, M.D. Fernandez-Ramos, A.J. Palma, Anal.Chim.Acta 583 (2007) 166.

2. A.J. Palma, J. López-González, L.J. Asensio, M.D. Fernandez-Ramos, L.F. Capitan-Vallvey, Sens.Actuators B 121 (2007) 629.

3. L. Martin-Banderas, M. Flores-Mosquera, P. Riesco-Chueca, A. Rodriguez-Gil, A. Cebolla, S. Chavez, A.M. Ganan-Calvo, Small 1 (2005) 688.

4. L. Martin-Banderas, A. Rodriguez-Gil, A. Cebolla, S. Chavez, T. Berdun-Alvarez, J.M.F. Garcia, M. Flores-Mosquera, A.M. Ganan-Calvo, Adv.Mater. 18 (2006) 559.

5. T. Förster, Ann.Phys. 2 (1948) 55.

6. J. R. Lakowicz Principles of Fluorescence Spectroscopy, 2nd ed.; Springer: 1999.

7. P. Yuan, D.R. Walt, Anal.Chem. 59 (1987) 2391.

8. R.A. Leese, E.L. Wehry, Anal.Chem. 50 (1978) 1193.

9. G. Gabor, D.R. Walt, Anal.Chem. 63 (1991) 793.

10. G. J. Mohr. Optical sensor for aqueous ethanol based on inner filter effect between a trifluoroacetylazobenzene dye and a fluorophore. 2009. Friedrich-Schiller-Universität Jena.

11. M.R. Shortreed, E. Bakker, R. Kopelman, Anal.Chem. 68 (1996) 2656.

12. X. Yang, K. Wang, C. Guo, Anal.Chim.Acta 407 (2000) 45.

13. T. Werner, I. Klimant, O.S. Wolfbeis, J.Fluoresc. 4 (1994) 41.

14. Y. Amao, N. Nakamura, Sens.Actuators B 100 (2004) 351.

15. F. Baldini, A. Giannetti, A.A. Mencaglia, C. Trono, Curr.Anal.Chem. 4 (2008) 378.

16. J.F. Fernandez-Sanchez, R. Cannas, S. Spichiger, R. Steiger, U.E. Spichiger-Keller, Sens.Actuators B 128 (2007) 145.

17. G. Neurauter, O. Kilmant, O.S. Wolfbeis, Fresenius J.Anal.Chem. 366 (2000) 481.

18. X. Ge, Y. Kostov, G. Rao, Biosensors Bioelectron. 18 (2003) 857.

19. M. Will, T. Martan, R. Mueller, O. Brodersen, G.J. Mohr, Proc.SPIE 7138 (2008) 71380A/1.

20. C. Guillaume, P. Chalier, N. Gontard, Environ.Compat.Food Packag. (2008) 396.

21. A. Mills, K. Eaton, Quim.Anal. 19 (2000) 75.

22. S.M. Borisov, C. Krause, S. Arain, O.S. Wolfbeis, Adv.Mater. 18 (2006) 1511.

23. C.v. Bültzingslöwen, A.K. McEvoy, C. McDonagh, B.D. MacCraith, I. Klimant, K. Christian, O.S. Wolfbeis, Analyst 127 (2002) 1478.

24. D.W. Lubbers, N. Opitz, Naturforsch., C: J.Biosci. 30c (1975) 532.

25. M.J.P. Leiner, Anal.Chim.Acta 255 (1991) 209.

26. B.H. Weigl, O.S. Wolfbeis, Sens.Actuators B 28 (1995) 151.

27. S.M. Borisov, M.C. Waldhier, I. Klimant, O.S. Wolfbeis, Chem.Mater. 19 (2007) 6187.

28. O. Oter, K. Ertekin, S. Derinkuyu, Talanta 76 (2008) 557.

29. N. Nakamura, Y. Amao, Anal.Bioanal.Chem. 376 (2003) 642.

30. C.v. Bültzingslöwen, A.K. McEvoy, C. McDonagh, B.D. MacCraith, Anal.Chim.Acta 480 (2003) 275.

31. B.H. Weigl, O.S. Wolfbeis, Anal.Chim.Acta 302 (1995) 249.

32. B.H. Weigl, A. Holobar, N.V. Rodriguez, O.S. Wolfbeis, Anal.Chim.Acta 282 (1993) 335.

33. M. Uttamlal, D.R. Walt, Bio/Technology 13 (1995) 597.

34. M. Cajlakovic, A. Bizzarri, V. Ribitsch, Anal.Chim.Acta 573+574 (2006) 57.

35. I. Sanchez-Barragan, J.M. Costa-Fernandez, A. Sanz-Medel, M. Valledor, J.C. Campo, TrAC, Trends Anal.Chem. 25 (2006) 958.

36. L.F. Capitan-Vallvey, M.D. Fernandez-Ramos, R. Avidad-Castañeda, M. Deheidel, Anal.Chim.Acta 440 (2001) 131.

37. L.F. Capitan-Vallvey, P. Alvarez de Cienfuegos, M.D. Fernandez-Ramos, R. Avidad-Castañeda, Sens.Actuators B 71 (2000) 140.

38. R.S. Barratt, Analyst 106 (1981) 817.

39. A.K. Bansal, W. Holzer, A. Penzkofer, T. Tsuboi, Chem.Phys. 330 (2006) 118.

40. Y. Amao, Microchim.Acta 143 (2003) 1.

41. P. Douglas, K. Eaton, Sens.Actuators B 82 (2002) 200.

42. S. Aiba, M. Ohashi, S.Y. Huang, Ind.Eng.Chem., Fundam. 7 (1968) 497.

43. G. Neurauter, I. Klimant, O.S. Wolfbeis, Anal.Chim.Acta 382 (1999) 67.

44. A. Mills, Q. Chang, N. McMurray, Anal.Chem. 64 (1992) 1383.

45. Y. Amao, T. Komori, Y. Tabuchi, Y. Yamashita, K. Kimura, Sensor Letters 3 (2005) 168.

46. M. Burke, P.J. O'Sullivan, G.V. Ponomarev, D.V. Yashunsky, D.B. Papkovsky, Anal.Chim.Acta 585 (2007) 139.

47. Y. Amao, T. Komori, H. Nishide, React.Funct.Polym. 63 (2005) 35.

48. D.A. Nivens, M.V. Schiza, S.M. Angel, Talanta 58 (2002) 543.

49. K. Ertekin, I. Klimant, G. Neurauter, O.S. Wolfbeis, Talanta 59 (2003) 261.

50. C. Malins, B.D. MacCraith, Analyst 123 (1998) 2373.

51. C.S. Chu, Y.L. Lo, Sens.Actuators B B129 (2008) 120.

52. M.P. Xavier, G. Orellana, M.C. Moreno-Bondi, J. Diaz-Puente, Quim.Anal. 19 (2000) 118.

53. A. Mills, A. Lepre, L. Wild, Sens.Actuators B 39 (1997) 419.

54. M.D. Marazuela, M.C. Moreno-Bondi, G. Orellana, Sens.Actuators B B29 (1995) 126.

Capítulo 3

Instrumento portátil para dióxido de carbono basado en componentes optoelectrónicos recubiertos con fases sensoras

Planteamiento

El objetivo de este capítulo es implementar las membranas para dióxido de carbono preparadas y caracterizadas utilizando instrumentación de sobremesa en el capítulo anterior, en una instrumentación portátil de diseño propio, de manera que se obtenga una instrumentación portátil fácil de usar, de reponer elementos sensores y de bajo coste para la determinación de este gas.

Existen diferentes tipos de instrumentos comerciales para la determinación de dióxido de carbono en distintas situaciones y para diferentes problemas basados en sensores ópticos, aunque los fabricantes no suelen indicar muchos datos acerca de los esquemas instrumentales y operacionales usados. En la introducción de esta Tesis se recogen diversos ejemplos de instrumentación existente. Un ejemplo de sensor óptico comercial es YSI 8500 que se utiliza para dióxido de carbono disuelto. Este es fabricado por la empresa YSI Corporation (www.ysi.com). Se basa en medidas de intensidad de fluorescencia del ácido 8-hidroxi-1,3,6-pirenotrisulfónico en tampón hidrógenocarbonato y cubierto con una membrana de silicona negra para evitar interferencia de la luz ambiente. Es capaz de medir en un rango de 1 a 25% de dióxido de carbono y en un rango de temperatura de 20 a 40ºC. Otro ejemplo de sensor óptico para este gas, ahora para uso médico es el denominado Colibrí (ICOR, Bromma, Suecia), que está basado en sensores de membrana homogénea y se utiliza para identificar la correcta intubación traqueal de pacientes hospitalizados. Este sensor consta de un indicador colorimétrico de pH, que tiene un color inicial azul en ausencia de CO_2 que cambia a amarillo con los niveles normales de exhalación de este gas [1].

En la Introducción de esta Tesis Doctoral se señalan los diferentes tipos de sensores de tipo óptico existentes para la determinación de dióxido de carbono y especialmente la instrumentación asociada desarrollada. Como allí queda de manifiesto, existe en el mercado poca instrumentación portátil para dióxido de carbono de tipo óptico basada en absorción de radiación en el visible o en luminiscencia, aunque sí descrita en bibliografía basada toda ella en el carácter ácido de este gas y en medidas de absorción de radiación o de fluorescencia,

por lo que es de interés el estudio que se aborda en esta Memoria de Doctorado y que emplea medidas de fosforescencia.

El equipo portátil utilizado fue desarrollado dentro del equipo multidisciplinar integrado en ECSens por el grupo de electrónica dirigido por el Dr. Palma López para la medida de oxígeno gaseoso [2] formando parte de la Memoria de Doctorado presentada por D. Javier López [3,4]. Este instrumento está basado en la atenuación de la fosforescencia de una membrana sensora por parte del oxígeno atmosférico, siendo además capaz de compensar la influencia de la temperatura y de recalibrarse con un solo punto [5]. Este desarrollo instrumental presenta un diseño compacto, buena disposición en la alineación óptica y una reducción de componentes optoelectrónicos necesarios, junto con una mayor eficacia en la recogida y procesado de la información, resultando en un instrumento portátil de medida de alta fiabilidad y de bajo coste.

El instrumento portátil para oxígeno está gobernado por un microcontrolador de gama media capaz de gestionar y controlar las múltiples interfases del equipo. Dispone de teclado para elegir distintos modos de funcionamiento, puerto para comunicación con ordenador, posibilidad de alimentación de la red o con baterías comerciales y pantalla LCD retroiluminada para la lectura directa de concentración de oxígeno y temperatura.

Brevemente, las características técnicas y funcionales de este instrumento son:

a) Fuente de luz de características adecuadas, como es un diodo emisor de luz (LED), para la excitación de la fosforescencia del luminóforo.
b) Un fotodetector que genera una señal de salida binaria, es decir, caracterizada por dos niveles de tensión, dependiendo de que la intensidad de la emisión fosforescente mencionada que reciba éste, esté por encima o no de un cierto umbral. Este dispositivo está situado a pocos milímetros de la fuente de excitación mencionada.
c) Una película sensora conteniendo las sustancias necesarias para producir una señal luminiscente estable en el tiempo y dependiente de la concentración de oxígeno. Dicha película, que es permeable al analito, se dispone en contacto con la cara activa (lente colectora) del fotode-

tector de manera que la radiación emitida por el luminóforo dependa de la concentración de dicho analito.

d) Un sensor de temperatura situado a pocos milímetros del conjunto película sensora-fotodetector.

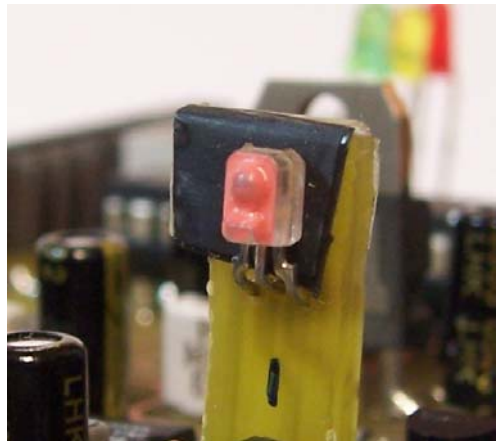

Figura 1. Fotodetector recubierto con la membrana sensora de oxígeno

La diferencia entre el equipo portátil para dióxido de carbono aquí presentado y el previamente desarrollado para oxígeno es que el parámetro analítico estudiado está relacionado con la intensidad de luminiscencia que es atenuada por el indicador de pH utilizado y no por la variación en el tiempo de vida de fosforescencia por atenuación colisional, puesto que ahora no hay variación de este parámetro de tiempo de vida.

En este capítulo se estudiaron diferentes estrategias para incluir las membranas sensoras para dióxido de carbono dentro de la instrumentación portátil desarrollada. Tras elegir la configuración óptima se modela la respuesta al gas analito y estudia la influencia de la temperatura, la estabilidad y el comportamiento dinámico del equipo desarrollado.

Sensors and Actuators B 144 (2010) 232–238

Contents lists available at ScienceDirect

Sensors and Actuators B: Chemical

journal homepage: www.elsevier.com/locate/snb

Hand-held optical instrument for CO_2 in gas phase based on sensing film coating optoelectronic elements

M.A. Carvajal[a], I.M. Pérez de Vargas-Sansalvador[b], A.J. Palma[a], M.D. Fernández-Ramos[b], L.F. Capitán-Vallvey[b,*]

[a] ECsens, Department of Electronics and Computer Technology, Campus Fuentenueva, Faculty of Sciences, University of Granada, E-18071 Granada, Spain
[b] ECsens, Department of Analytical Chemistry, Campus Fuentenueva, Faculty of Sciences, University of Granada, E-18071 Granada, Spain

ARTICLE INFO

Article history:
Received 29 June 2009
Received in revised form 17 October 2009
Accepted 26 October 2009
Available online 30 October 2009

Keywords:
Carbon dioxide
Gas sensor
Phosphorescence
Portable instrumentation
Optoelectronic coated components

ABSTRACT

Different strategies have been tested in order to include a CO_2 optical gas sensor in a low-cost portable electronic instrument. Plastic solid-state sensor membranes are based on the quenching of a phosphorescent dye by the deprotonated form of a non-luminescent pH indicator. As a result of this study, the configuration with both optoelectronic components coated with sensing chemistry (LED with the luminophore and photodetector with the pH-active dye) presents a better CO_2 response in terms of sensitivity and reproducibility than the other configurations studied by us. The portable measurement system resulting from the integration of coated LED with the luminophore and photodetector with the pH indicator was characterized in terms of calibration, sensitivity, short and long-term stability, transient response and thermal dependence with results comparable to laboratory instrumentation and other sensing films described in literature. The sensor calibration curve has been modelled according to a theoretical model, reported in the literature, with two coefficients, which has been included in the microcontroller of the measurement system to provide a direct reading of the gas concentration in the display. The sensor's full range is from 0% to 100% CO_2 concentration. The study of the response time of the membranes was made, obtaining response t_{90} and recovery t_{10} times of 31 and 117 s, respectively. Temperature dependence was successfully fitted to an Arrhenius type function that has been included in the microcontroller of the instrument, to calculate and display the CO_2 concentration, correcting the temperature dependence. The characterization demonstrated the reliability and good performance of this type of solution aimed at integrating chemical sensors in electronic and optoelectronic devices. The localization of the sensing film on the detector and on the light source makes any additional optical element unnecessary, thus reducing system costs, avoiding alignment problems, optimizing the efficiency of the signal collection and making it possible to replace the sensor easily.

1. Introduction

The determination of gaseous and dissolved carbon dioxide is of great importance in diverse areas such as environmental analysis (atmospheric pollution control, water monitoring) [1], medicine, clinical and biological investigations [2], biotechnological processes including modified atmosphere packaging [3] and industrial safety.

Conventional methods for CO_2 determination include, among others, infrared spectrometry or electrochemical measurements in buffer solutions using Severinghaus-type electrodes [4].

Different optical sensors for CO_2 have been developed based on the pH changes induced in an aqueous solution upon exposure to the gas. Usually they are based on the interrogation of either a colour or fluorescence-based pH indicator in an aqueous hydrogen carbonate buffer, thus a solution covered by a gas-permeable membrane [5] or a dye-doped layer of hydrophilic material maintained beneath a gas-permeable hydrophobic membrane [6]. The limitations of this design, due to the need to maintain the moisture level in the membrane, led to the appearance of so-called solid sensor membranes, where the aqueous buffer was replaced with an organic base, usually a quaternary ammonium hydroxide. This organic base is used for the ion pairing of the basic form of the pH indicator and to provide the water for the ion-pair hydration needed for the uptake of CO_2 from the atmosphere by forming a lipophilic hydrogencarbonate buffer [7].

There is an urgent demand today for the development of compact and low-cost analytical systems able to measure *in situ* concentrations of a given analyte in the sample in different fields. For example, determining CO_2 concentration in confined environments such as sewers, tanks and submarines, or continuously

* Corresponding author.
E-mail address: lcapitan@ugr.es (L.F. Capitán-Vallvey).

0925-4005/$ – see front matter © 2009 Elsevier B.V. All rights reserved.
doi:10.1016/j.snb.2009.10.061

HAND-HELD OPTICAL INSTRUMENT FOR CO_2 IN GAS PHASE BASED ON SENSING FILM COATING OPTOELECTRONIC ELEMENTS

M.A. Carvajal[a], I.M. Pérez de Vargas-Sansalvador[b], A. J. Palma[a], M.D. Fernández-Ramos[b] and L.F. Capitán-Vallvey[b]*

ECsens. [a] Department of Electronics and Computer Technology. [b] Department of Analytical Chemistry. Campus Fuentenueva, Faculty of Sciences, University of Granada, E-18071 Granada, Spain.

Abstract

Different strategies have been tested in order to include a CO_2 optical gas sensor in a low-cost portable electronic instrument. Plastic solid state sensor membranes are based on the quenching of a phosphorescent dye by the deprotonated form of a non-luminescent pH indicator. As a result of this study, the configuration with both optoelectronic components coated with sensing chemistry (LED with the luminophore and photodetector with the pH-active dye) presents a better CO_2 response in terms of sensitivity and reproducibility than the other configurations studied by us. The portable measurement system resulting from the integration of coated LED with the luminophore and photodetector with the pH indicator was characterised in terms of calibration, sensitivity, short and long term stability, transient response and thermal dependence with results comparable to laboratory instrumentation and other sensing films described in literature. The sensor calibration curve has been modelled according to a theoretical model, reported in the literature, with two coefficients, which has been included in the microcontroller of the measurement system to provide a direct reading of the gas concentration in the display. The sensor's full range is from 0 to 100% CO_2 concentration. The study of the response time of the membranes was made, obtaining response t_{90} and recovery t_{10} times of 31 s and 117 s, respectively. Temperature dependence was successfully fitted to an Arrhenius type function that has been included in the microcontroller of the instrument, to

calculate and display the CO_2 concentration, correcting the temperature dependence. The characterisation demonstrated the reliability and good performance of this type of solution aimed at integrating chemical sensors in electronic and optoelectronic devices. The localization of the sensing film on the detector and on the light source makes any additional optical element unnecessary, thus reducing system costs, avoiding alignment problems, optimizing the efficiency of the signal collection and making it possible to replace the sensor easily.

Key words. Carbon dioxide; gas sensor; phosphorescence; portable instrumentation; optoelectronic coated components.

* Corresponding author; *e-mail:* lcapitan@ugr.es

1. INTRODUCTION

The determination of gaseous and dissolved carbon dioxide are of great importance in diverse areas such as environmental analysis (atmospheric pollution control, water monitoring) [6], medicine, clinical and biological investigations [7], biotechnological processes including modified atmosphere packaging [8] and industrial safety.

Conventional methods for CO_2 determination include, among others, infrared spectrometry or electrochemical measurements in buffer solutions using Severinghaus-type electrodes [9].

Different optical sensors for CO_2 have been developed based on the pH changes induced in an aqueous solution upon exposure to the gas. Usually they are based on the interrogation of either a colour or fluorescence-based pH indicator in an aqueous hydrogen carbonate buffer, thus a solution covered by a gas-permeable membrane [10] or a dye-doped layer of hydrophilic material maintained beneath a gas-permeable hydrophobic membrane [11]. The limitations of this design, due to the need to maintain the moisture level in the membrane, led to the appearance of so-called solid sensor membranes, where the aqueous buffer was replaced with an organic base, usually a quaternary ammonium hydroxide. This organic base is used for the ion pairing of the basic form of the pH indicator and to provide the water for the ion-pair hydration needed for the uptake of CO_2 from the atmosphere by forming a lipophilic hydrogencarbonate buffer [12].

There is an urgent demand today for the development of compact and low-cost analytical systems able to measure *in situ* concentrations of a given analyte in the sample in different fields. For example, determining CO_2 concentration in confined environments such as sewers, tanks and submarines, or continuously analysing the gas produced during combustion in industrial or domestic boilers, would be very advisable for controlling the level of gas and respecting the safety rules. Different electronic instrumentation for gas or vapor chemical sensors has been developed [13-15], most notably amperometric sensors such as the Clark oxygen sensor [16] and low selectivity metallic oxides sensors [17].

In these cases, auxiliary systems made portable instrument design very difficult. Additional drawbacks such as complex calibration, the long time needed for stable measurements, quick sensor degradation and high energy consumption have prevented any major development in the portable instrumentation manufacture with this type of sensors. Optical sensors can provide such information with high sensitivity and selectivity, avoiding almost all these drawbacks. Moreover, the fast technological development of new light-emitting diodes (LED) and solid-state photodetectors makes it possible to design more compact optical instrumentation [18]. The first results were mainly based on lifetime measurements of fluorescence quenching by dissolved and/or gas phase oxygen [19-22]. The oxygen sensor based on phosphorescence quenching allowed very simple electronic signal processing [2]. Some prototypes required connection to a laptop computer [23]. For CO_2 sensing, similar strategies have been implemented in portable instrumentation [19], but much work remains to be done. Therefore, there is a wide research field for designing portable instrumentation for optical CO_2 sensing.

In this work, a portable instrument has been developed to measure CO_2 in the gas phase. The sensing chemistry is based on a plastic solid state sensor film that works on the secondary inner filter effect, where a luminescent dye, the platinum octaethylporphyrin complex (PtOEP), is quenched by the deprotonated form of a non-luminescent pH indicator, α-naphtholphthalein [24]. For optimal CO_2 detection by this type of sensor, the absorption band of the basic form of α-naphtholphthalein must overlap with an emission band of the luminophore.

The selected luminophore was the PtOEP complex due to its very long lifetime (τ_0 ~ 100-200 μs depending on the chemical nature of the polymer matrix), visible absorption (B(0), the Soret band, at 380 nm and Q(0) at 533 nm), Stokes displacement (emission at 650 nm), phosphorescence quantum yield (~0.2 under ambient conditions) [25] and a reasonable photostability in the conditions studied. Their long lifetime (tenths of microseconds) made it possible to develop microcontroller-based portable instrumentation for O_2 based on the measurement of a time parameter related to gas concentration [2]. This measurement system has been redesigned and optimized with a similar strategy with

regard to the membrane configuration for CO_2 sensing in the optoelectronic components [22,26,27], achieving a robust, compact and efficient sensor configuration. Our goal was a reliable, simple, low-cost prototype including a highly stabilized sensing membrane coating the optoelectronic devices. We report on an easy-to-use measurement system with high optical and electrical interference immunity, extremely simple digital signal processing circuitry, low power consumption and enough accuracy for *in situ* CO_2 determination. We have designed an instrument to overcome some of the drawbacks of previous portable designs, based on simple electronics and one signal channel without any reference channel.

2. EXPERIMENTAL

2.1. Reagents, materials and apparatus.

Platinum octaethylporphyrin complex (PtOEP) was obtained from Porphyrin Products Inc. (Logan, UT, USA). The polymers used were: poly(vinylidene chloride-co-vinyl chloride) (PVCD, particle size 240-320 μm) and ethylcellulose (EC, ethoxyl content 49%) from Sigma–Aldrich Química S.A. (Madrid, Spain). Tetrahydrofuran (THF), tributyl phosphate (TBP), toluene and ethanol were supplied by Sigma.

Other reagents used were α-naphtholphthalein and tetraoctyl ammonium hydroxide (TOAOH) (0.335 M in methanol) both from Sigma. Sheets of Mylar-type polyester from Goodfellow (Cambridge, UK) were used as a support for membranes. The gases CO_2, O_2 and N_2 used were of a high purity (>99%) and were supplied in gas cylinders by Air Liquid S.A. (Madrid, Spain). The water used was reverse-osmosis type quality from Milli-RO 12 plus Milli-Q purification system (Millipore, Bedford, MA, USA).

Luminescence decay measurements were obtained using the time-correlated single photon counting technique with an OB 920 spectrometer with a μF 900-HP microsecond flash lamp and S900 single photon photomultiplier detection system (Edinburgh Instruments Ltd, Livingston, UK).

For electrical and optical characterization of the prototype, the following instrumentation has been used: a compact minispectrometer (C9407MA Hamamatsu, Japan) for the LED spectrum measurement and a mixed signal oscilloscope (MSO4101, Tektronix, USA) for electrical measurements.

2.2. Sensing membrane preparation and configuration

An exhaustive study of different membrane compositions and configurations on a Mylar support, and their responses to CO_2 with laboratory instrumentation, has been previously carried out [24]. The sensing film composition for the portable instrumentation was taken as a result of this optimization study. Sensing films were prepared from cocktails A and B; cocktail A containing 100 mg of PVCD dissolved in 1 mL of freshly distilled THF using an ultrasonic bath and 0.5 mg PtOEP. Cocktail B is composed of 64 µL TBP, 320 µL of a solution containing 2.2 mg of α-naphtholphthalein in 2 mL of toluene/EtOH (80:20 v/v), 1 mL of toluene containing 60 mg of previously dissolved EC and finally 200 µL of 0.335 M TOAOH. All cocktails were prepared by weighing the chemicals in a 4 mL flask with a DV215CD balance (Ohaus Co., Pine Brook, NJ, USA) with a precision of ±0.01 mg.

As indicated above, one of the aims of this work was to optimize the configuration of these films obtained with the A and B cocktails placed between the LED and photodetector inside the electronic measurement system according to our previous experience with oxygen sensing [26]. In that report, the design was aimed at simplifying the sensor module of the oxygen optical sensor. We were able to improve the luminescence collecting efficiency by directly coating the detector element with the optical oxygen sensing film, thus reducing the sensor module to two elements: the light source and the coated light detector with no optical filter. In brief, no sensing membrane support was needed apart from the detector itself. That configuration resulted in fast response, low energy consumption and reduced the alignment error [5]. Here, we applied this strategy to the detection of CO_2, using the two sensing membranes containing the luminophore and pH indicator, respectively. As shown in Figure 1, three sensor

configurations, with increasing levels of sensor-electronic integration, were tested:

1) Configuration 1: A double membrane configuration on opposite sides of the Mylar support (10mm x 8 mm). One side of a Mylar support has been spin-coated with two successive volumes of 5 µl of cocktail A and after drying in saturated THF atmosphere for 1 h, 5 µL of cocktail B was placed onto the opposite side of the support with the same technique and in the same position and drying under vacuum for 12 h.

2) Configuration 2: The LED coated directly with the PtOEP sensing film and the Mylar support with the pH indicator. The LED was first polished to present a circular flat surface with a 4 mm diameter in order to prevent the cocktail solution from spilling off the flat surface of the LED. Afterwards, the PtOEP gravity-spread film was cast by placing two successive volumes of 5 µL of cocktail A on the top of the LED dome. After each addition, the device was left to dry in darkness in a dryer with saturated THF atmosphere for 1 h at room temperature. This sensing film was cured for 9 days before use. This transparent and pink film has a calculated average thickness of about 80 μm. The pH indicator membrane was prepared in the same way as described for Configuration 1 on one side of a 15 mm x 8 mm Mylar support.

3) Configuration 3: The LED coated with sensing film containing PtOEP and the photodetector with a sensing film containing the pH indicator. The PtOEP membrane was cast as in configuration 2 and the α-naphtholphthalein indicator membrane was cast onto the active face of a photodetector with the aid of a micropipette using 5 μL of cocktail B. After preparation, the photodetector was dried in darkness and at vacuum in a dryer for 12 h at room temperature. In this case the transparent and blue film has an average thickness of about 105 μm.

In all cases, the membranes containing PtOEP in PVCD were stored for curing in darkness for 9 days before their use.

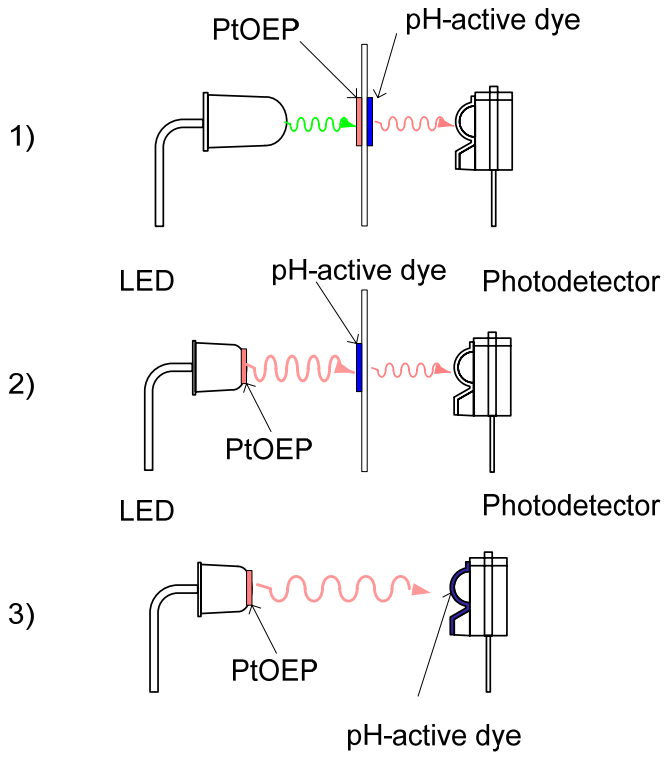

Figure 1. Different sensor configurations. 1) Both sensing membranes placed on opposite sides of the polyester support. 2) PtOEP sensing film on the LED and pH indicator film on one side of the polyester support. 3) PtOEP sensing film on the LED and pH indicator film on the photodetector.

In the last two configurations, the complete contact between the sensing films and the optoelectronic components achieves optimal luminescence and an efficient filter. Moreover, neither lens nor optical filters are required, resulting in a compact and robust sensing module. The distance between the LED and the photodetector was always less than 5 mm.

2.3. Portable electronic instrument

The luminophore and the pH-active dye described above were included in a portable electronic instrument with a low cost microcontroller (MCU) as a

control unit (PIC16F876, Microchip, Chandler, Arizona, USA), based on an earlier development used to measure oxygen [2,26]. MCU performs the control of the excitation and detection of the optical signals, includes the algorithm for the signal processing and controls all the instrument interfaces and a FT232 (Future Technology Devices International Ltd, ShangHai, China) for USB port for computer communication. The functional block diagram of the electronic system is composed of different modules: sensor module, logic circuits, timing circuits, microcontroller, power management circuits and interfaces. The instrument developed is portable and the CO_2 concentration is directly read from the display. A photograph of the sensor module is displayed in Figure 2, showing the coated LED and photodiode according to configuration 3, and the temperature sensor.

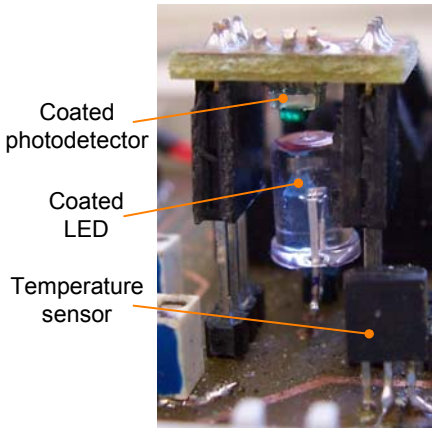

Figure 2. Photograph of sensor module in the portable instrument showing the coated optoelectronic elements in the case of configuration 3 and the temperature sensor.

In the sensor module with a single optical channel, the luminophore is optically excited by a ultra-bright green light-emitting diode, LED (110104, Marl International Ltd., Ulverston, UK) with an emission maximum at 525 nm. In Figure 3, the LED emission spectrum, the PtOEP absorption and emission spectra and the absorption band of the basic form of the pH indicator are displayed, showing very efficient spectral overlapping for the inner filter effect. To improve

excitation stability, the LED is biased with a built-in thermal-stabilised current source, providing negligible optical intensity drift. For the light collection, a photodetector, with a built-in Schmidt trigger circuit was used (IS486, Sharp, Japan). This gives a logic output depending on the light intensity: a high-level output under incident light and a low-level output under light below an intensity light threshold. At the moment that the signal decays below the threshold, the photodetector changes to low-level output. Typical values for main specifications are: illuminance for output change, 15 lx; rise time, 100 ns; and fall time, 50 ns. The pulse duration of this digital signal is processed by a time-count of pulses algorithm[2], and the result displayed in the LCD screen with no analog processing. Sensor thermal drift is also corrected by temperature monitoring with a digital output sensor (DS1820, Maxim, Sunnyvale, CA, USA) next to the sensing zone (see Figure 2). The sensor module was designed to be able to make measurements in the three different arrangements studied. A small holder was included between the LED and the photodetector to house the membrane in the first and second configurations.

The signal-to-noise ratio was improved by means of repeating the measurement procedure and subsequent result averaging. The last step would be to calculate and include the calibration function that relates the CO_2 concentration to the analytical parameter in the MCU. In this work, our aim was to test the three mentioned configurations, to analyze in detail the response of each one and to indicate the best arrangement for measuring the gas under study.

Unlike the instrumentation previously developed for oxygen, in this case for CO_2 the analytical parameter measured with this instrument is closely related to the luminescence intensity quenched by the pH-active dye. Now, there is no luminescence lifetime decay variation, because of the working mechanism of this sensor, an inner filter, and the fact that the PtOEP is trapped in a polymer which is not permeable to oxygen. Therefore the photodetector makes simple intensity integration over the time in which the final illuminance is above an established threshold.

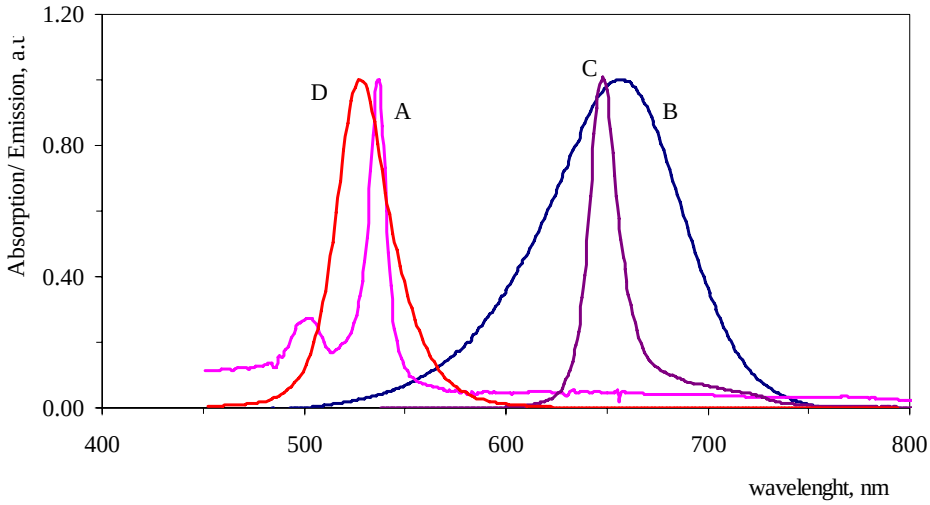

Figure 3. Spectral properties of the chemicals used in the CO_2 sensor and the excitation source (normalized spectra). Excitation (A) and phosphorescence emission spectra (C) of PtOEP membrane; (B) absorption spectrum of basic form of α-naphtholphthalein. (D) emission spectra of the 525 nm green LED. The figure shows the overlapping of donor and acceptor spectra.

2.4. Measurement conditions

The standard mixtures of CO_2 in N_2 and CO_2 and O_2 in N_2 were produced using N_2 as the inert gas component and O_2 by controlling the flow rates of the different high purity gases CO_2, N_2 and O_2, in each case, entering a mixing chamber using a computer-controlled mass flow controller (Air Liquid España S.A., Madrid, Spain) operating at a total pressure of 760 Torr and a flow rate between 100 and 500 $cm^3 \cdot min^{-1}$. For the preparation of the gas mixture lower than 0.40% CO_2, a standard of 5% CO_2 in N_2 was used, with the lowest CO_2 concentration tested being 0.02%. For the portable instrument characterization, the CO_2 measurements were performed after equilibration of the atmosphere of the instrument with the gas mixtures obtained by the gas blender indicated above.

Data were saved in a computer through a USB port connexion and ad hoc developed control software. All the room temperature measurements were

performed at 20 ºC. A thermostatic chamber (Figure 4), with a lateral hole for the connexion to a computer, made it possible to maintain a controlled temperature between −50 ºC and +50 ºC with an accuracy of ±0.5 ºC for thermal characterization.

Five membranes were prepared for the sensor configurations 1 and 2 to carry out a preliminary calibration. Twelve photodetectors were coated for configuration 3 (both components coated), six with a concentration of TOAOH of 1.12 mol·Kg^{-1} polymer and the rest with 1.67 mol·Kg^{-1} polymer of TOAOH. The coated photodetectors were welded in a small printed circuit board (PCB) with connectors to be attached to the instrument mainframe. In this last case, several studies were done: calibrations, dynamic response, thermal characterization and short and long-term stabilities. The short-term stability was studied by measuring continuously during a period of 24 h in an atmosphere of 6.25% CO_2. The long term stability of the pH-sensitive dye coated on photodetectors (configuration 3) was studied separately by storing them in a desiccator in darkness both in an atmosphere of 33% relative humidity (RH) (20±0.5ºC) and in a 94% RH atmosphere (20±0.5ºC). In all cases, the desiccators contained sodium carbonate to protect the membranes from any acidic gases from the lab. Each sensing element was tested periodically performing a CO_2 calibration.

All measurements were made replicated six times, except when stated otherwise, to check for experimental error.

Figure 4. Chamber used for thermal characterization of the instrument

3. RESULTS AND DISCUSSION

With the aforementioned configurations included in the developed instrument, resonance energy transfer (RET) quenching is not possible, due to the long distance between the luminophore and the pH indicator placed on opposite sides of the same support or in different optoelectronic elements. Moreover, Burke *et al.* [28], in their study of phosphorescent Pt(II) coproporphyrin labelled oligonucleotides, suggest that porphyrin–porphyrin quenching by RET mechanism can be ruled out, being predominantly static. Therefore, a secondary inner-filter effect occurs that involves the absorption of the phosphorescence emitted by the CO_2-insensitive luminophore by the basic form of the liphophilised acid-base indicator.

This was confirmed by measuring the phosphorescence lifetime of the membranes in configuration 1 before and after exposure to a CO_2 atmosphere (at 100% nitrogen: τ_1 96.0 μs (SD 1.85); at 100% CO_2: τ_1 97.9 μs (SD 0.77) [24]. The sensor mechanism is based on the reaction between the α-naphtholphthalein ion-pair and CO_2 according to:

$$TOA^+N^- \cdot xH_2O + CO_2 \xleftrightarrow{K} TOA^+HCO_3^- \cdot (x-1)H_2O \cdot HN \quad \text{(Equation1)}$$

where $TOA^+N^- \cdot xH_2O$ is the ion pair formed between tetraoctylammonium TOA^+ and the deprotonated form of α-naphtholphthalein N^- and K is the equilibrium constant. We used the approximate equation proposed by Amao *et al.* [29] for calibration purposes:

$$\frac{I}{I_0} = 10^{\{-C(1/(K+[CO_2])+1/K)\}} \quad \text{(Equation 2)}$$

where $C = K\varepsilon b\left[TOA^+N^- \cdot xH_2O\right]$, ε is the molar extinction coefficient of acceptor ($8.65 \cdot 10^3$ $l \cdot mol^{-1} \cdot cm^{-1}$), the basic form of α-naphtholphthalein at the emission wavelength of luminophore and b the effective pathlength of membrane (105 μm). All these assumptions are proven by the experimental results shown below.

3.1. Choice of the sensor configuration

The first task was a preliminary study of the instrument response to CO_2 for the three proposed sensor configurations, in order to choose the one with the best gas sensitivity and reproducibility. To do that, calibrations using six replicates of the three configurations were carried out at room temperature. All of them showed good fits to the model in Equation 2. However, a great dispersion of the results was obtained between the different configurations. Although the I_{100}/I_0 ratio is commonly used to represent the sensitivity of the sensing film, where I_0 and I_{100} represent the detected luminescence intensities from a sensor

film exposed to 100% N_2 and 100% CO_2, respectively [30], we prefer in our case to use the I_{100}-I_0 parameter because it is a more suitable indication of the width of the measurement range. The experimental results are summarized in Table 1, where the highest value is reached for configuration 3. The values found for configurations 1 and 2 were 53% and 92% with respect to configuration 3. Therefore, configuration 1 was rejected due to its thinner span signal. Configuration 2 presented a value of I_{100}-I_0, slightly less than configuration 1, but was rejected due to a greater experimental error. Therefore, the best $I_{100} - I_0$ value obtained, providing the highest sensitivity and the best reproducibility led us to select the last configuration for the portable instrument design. In this case, the I_{100}/I_0 ratio is approximately 15.5. Below, a detailed characterization of this sensor configuration is presented.

Table 1. Experimental results of I_{100}-I_0 for the different sensor configurations tested.

Sensor configuration	I_{100}-I_0		
	Average	SD*	Normalized
1	60257	243	53%
2	104927	2667	92%
3	114066	703	100%

*SD represents the standard deviation of six consecutive measurements. The values have been normalized to the highest value, found for configuration 3.

3.2. Portable instrument calibration

Measurements of the response of the portable instrument with sensor configuration 3 were carried out as a function of CO_2 concentration using twelve coated photodetectors and the same PtOEP coated LED (see Figure 2). Figure 5 presents a typical normalized I/I_0 change versus CO_2 concentration, with the solid line being the best-fit to Equation 2 (R^2 = 0.970), resulting in coefficient values of K = 1.10 and C = 0.704 at room temperature. Similar fits were obtained

for the rest of the experimental data (RSD 10%). This result indicates that the instrument can be calibrated using Equation 2. The sensor answer covers the full range (0-100%) although sensitivity reduces with CO_2 concentration as predicted by the experimental calibration function. The relative errors (considered as one standard deviation of six experimental measurements, normalized at the averaged value) at low (<8%) and high (>8%) CO_2 concentrations found were 2.6% and 3.6%, respectively.

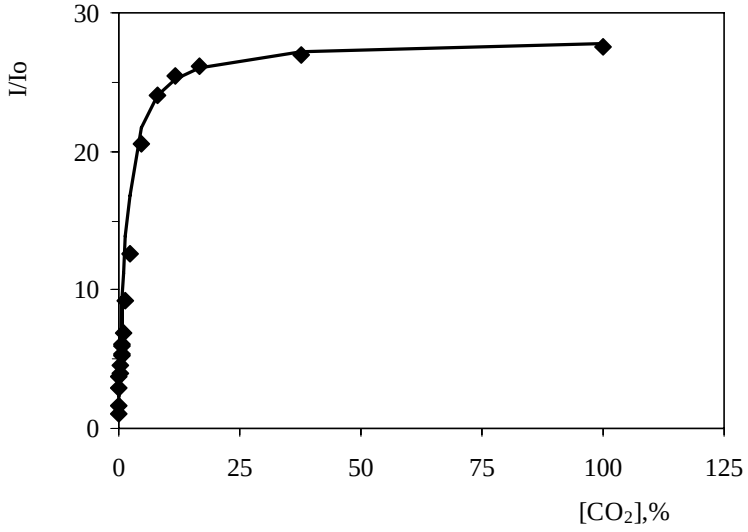

Figure 5. Instrument calibration curve at room temperature. Symbols show experimental results and line is the best fit to the model given by Eq. 2. I/I0 versus CO2 concentration of a coated optoelectronics elements configuration. The excitation and emission wavelengths are 525 and 650 nm, respectively.

Temperature has an influence on the sensitivity of these solid-type CO_2 sensors [31,32]. Therefore we studied the thermal dependence of the described sensing membranes and instrument by acquiring the calibration function at temperatures between 8 ºC and 35 ºC. As in previous papers [31-33], we observed a decrease in sensitivity with the increase in temperature, which can be ascribed to the lower solubility of CO_2 in the sensing membrane [34]. By fitting the ex-

perimental data to Equation 2, the equilibrium constants K were determined. As in spontaneous reactions, the equilibrium constant of equation 1 decreases with temperature and a linear correlation was found between 1/T and ln K (R^2 = 0.9269), and according to the Arrhenius equation an activation enthalpy ΔH = -1.7 kJ·mol^{-1} and an entropic term of 161 J·mol^{-1} was calculated (Figure 6).

The temperature dependence of K introduced in Equation 2 was included into the MCU of the instrument, to calculate and display the CO_2 concentration, correcting the temperature dependence.

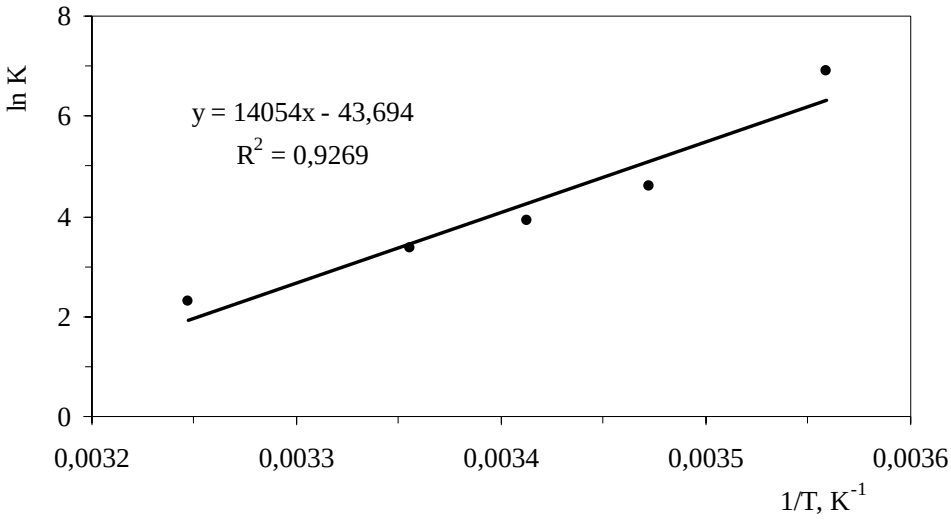

Figure 6. Arrhenius-type thermal dependence for equilibrium constant K.

3.3. Response and recovery properties and operational stability

The dynamic response of our system was also studied measuring the response at different concentrations continuously and transmitting the data to computer via a USB port. Figure 7 displays the instrument response to alternating atmospheres of pure CO_2 and pure N_2 with the sensor configuration under study. Short response times are obtained with values similar to those extracted from the sensing membrane characterisation [24]. The response time, t_{90}, was 31 s for switching from N_2 to CO_2, and the recovery time, t_{10}, 117 s for switching from CO_2 to N_2. The signal changes are fully reversible and hysteresis was not observed during the measurements.

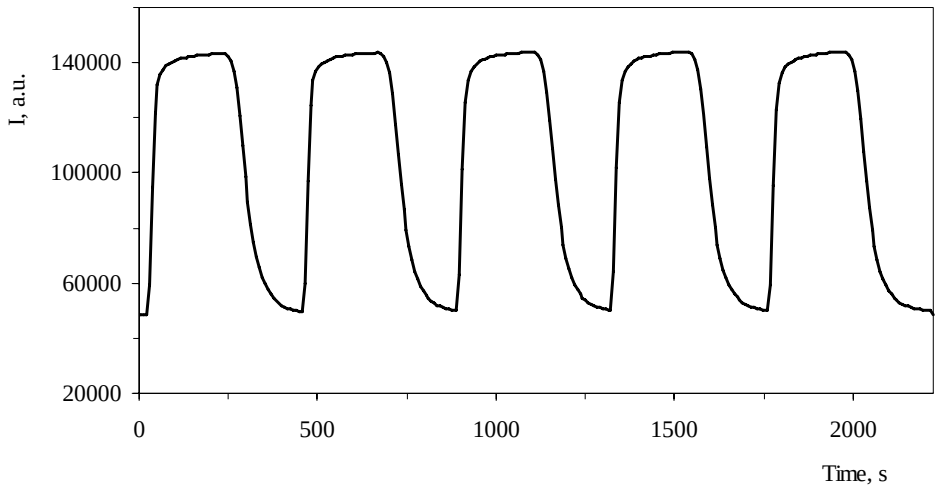

Figure 7. Dynamic response of portable instrument for changes in CO_2 concentration from 0% to 100%.

The long-term stability of the indicator membrane was studied for 330 days, keeping six photodetectors coated with the pH indicator in a 33% RH atmosphere and another six in 94% RH conditions. In the case of coated

photodetectors stored in 94% RH conditions, the influence of light was tested preparing two subsets in darkness and under ordinary, not direct, lab lighting conditions.

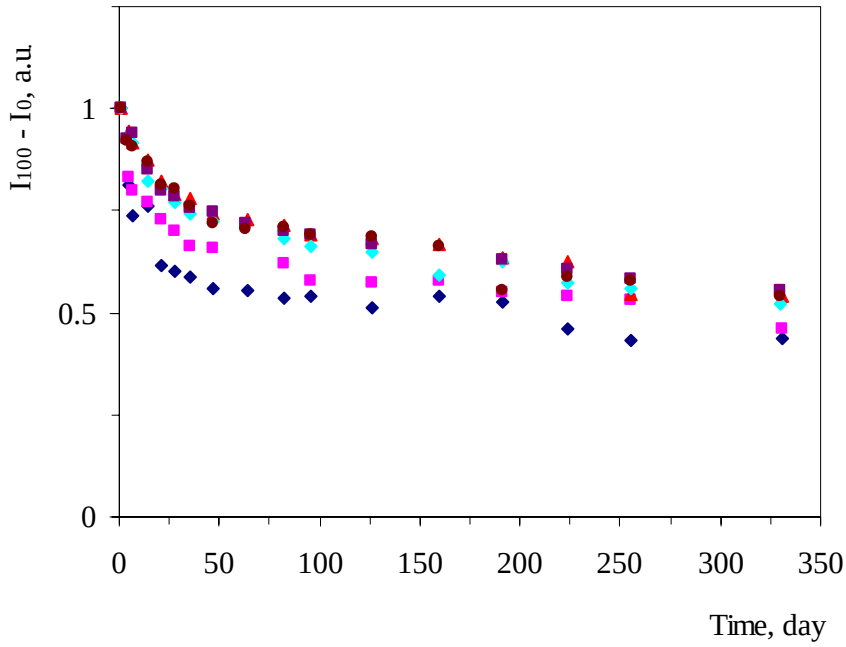

Figure 8. Long-term stability. Stability of six coated photodetectors in 94% RH atmosphere and darkness. Normalized $I_{100} – I_0$ signal versus time in days from sensor coating.

There was a significant difference between the half-life of the membranes (the time it takes to reduce to one-half the initial I_{100}-I_0 value) preserved in high and low RH atmosphere. As usual, storage in air and exposure to light had a pronounced destroying effect on the sensing elements. In 33% RH atmosphere, the half-life was between 4-7 days and very similar in 94% RH conditions under illumination, but in 94% RH and darkness, it was longer than 11 months, the maximum time of the study (Figure 8). As can be seen for the six photodetectors in Figure 8, a slow decrease in the signal can be observed up to approximately 60% of the initial values, stabilizing at this point. The results

shown in Figure 8 can be fitted to a logarithmic function curve and by extrapolation we obtained a half-life for the coated photodetectors of some 1000 days; thus this sensor can be used after more than 33 months to measure CO_2 after recalibration. Therefore, due to the initial signal decay observed, in order to obtain better stability, a period of 10 days has to pass. After this time, a decay of 5% will occur 7 days later at which time a new calibration will be needed.

Figure 9. Portable instrumentation for gaseous carbon dioxide determination

To investigate the short-term stability, the instrument response was studied at 6.25% CO_2 for 24 hours with measurements every 8 seconds. We found a mean drift of -0.16% CO_2 concentration per hour. With an appropriate periodic recalibration, the useful life of sensor could be extended.

4. CONCLUSIONS

In this study we have shown the preparation and performance of LED coated with CO_2 insensitive luminophore PtOEP and of a photodetector with an α-naphtolphtalein pH indicator in different configurations. As a result of this study, the configuration with both coated optoelectronic components (configuration 3) presents a better CO_2 response in terms of sensitivity (70% and 10% with respect to configurations 1 and 2) and reproducibility (similar to configuration 1 and three times less than configuration 2). These coated optoelectronic components are included as the sensing part of a described portable electronic instrument for gaseous CO_2 sensing with a low-cost microcontroller as a control unit. This method for locating the sensing film on the detector itself has several advantages over the earlier arrangements of the film on a separate support: a) more compact configuration which results in size reduction; b) no need for optical filters and lenses between LED and photodetector; c) no need for alignment systems of optoelectronic components or lighting signal focalisation or collimation; d) better efficiency in luminescence signal collection, which means the use of lower excitation signals with the congruent decrease in photodegradation; e) reduction in the amount of film chemicals needed for film making to a half in cocktail A and 1/5 in cocktail B. All of these advantages facilitate a sensor/detector subsystem that is inexpensive, sturdy, lightweight, and small with easily-replaceable components when necessary.

The portable measurement system resulting from the integration of coated LED and photodetectors was characterised in terms of calibration, sensitivity, stability, transient response and thermal dependence with results comparable to laboratory instrumentation and other sensing films described in the literature. The characterisation demonstrated the reliability and good performance of this type of solution that aims to integrate chemical sensors and electronic and optoelectronic devices. Typical properties from both elements, such as high selectivity of chemical sensors and direct signal processing of optoelectronic devices, are merged in this novel configuration.

ACKNOWLEDGEMENTS

We acknowledge financial support from *Ministerio de Educación y Ciencia, Dirección General de Enseñanza Superior* (Spain) (Projects CTQ2005-09060-CO2-01 and CTQ2005-09060-CO2-02) and from the Junta de Andalucía (Spain) (Projects P06-FQM-01467 and P08-FQM-3535).

5. CONCLUSIONES

En este capítulo se ha desarrollado una instrumentación portátil para la medida de dióxido de carbono basado en la medida de fosforescencia.

Se han estudiado tres configuraciones diferentes para la inclusión de las membranas en la instrumentación portátil, originadas a partir de la configuración de caras opuestas sobre un mismo soporte, que es la que seleccionamos como óptima en el capítulo anterior:

1. En la primera se depositaron las membranas sensoras en caras opuestas de una lámina de Mylar que se introdujo en una ranura mecanizada, situada en la carcasa del fotodetector, quedando esta fija y situada entre LED y PD.

2. En la segunda se limó el LED depositando la membrana que contiene PtOEP sobre la superficie circular plana resultante. La membrana que contiene el indicador de pH se depositó sobre una lámina de Mylar.

3. En la última configuración las membranas sensoras se depositaron directamente sobre los componentes optoelectrónicos, La membrana con PtOEP sobre el LED y la que contiene el indicador de pH sobre el fotodetector.

Esta última configuración fue seleccionada porque ofrecía mayor sensibilidad y reproducibilidad, además de ofrecer una serie de ventajas adicionales frente a las demás, pudiendo incluso facilitar el reemplazamiento del fotodetector con la película sensora de dióxido de carbono, que es la que presenta menor estabilidad. Ello da como resultado una instrumentación compacta y de fácil uso siendo factible el poder reemplazar sus componentes de manera sencilla.

Una vez seleccionada la configuración óptima para sensado de dióxido de carbono con este equipo se caracterizó en términos de respuesta a este gas, comportamiento dinámico, influencia de la temperatura y estabilidad de membrana.

La curva de calibración se programó en el microcontrolador del equipo, para así obtener en la pantalla del instrumento la respuesta directa de concentración de dióxido de carbono. Se estudió y modeló la influencia de la temperatura, introduciendo la dependencia térmica en la MCU, para así efectuar la corrección necesaria en función de la temperatura ambiente.

Se estudiaron los tiempos de respuesta y de recuperación del equipo, siendo estos algo mayores que los encontrados utilizando instrumentación de sobremesa, aún así estos son comparables con los de otros sensores basados en las propiedades ácido Lewis del dióxido de carbono. A pesar de ser algo mayores estos tiempos que los encontrados utilizando instrumentación de sobremesa siguen siendo suficientemente bajos como para dar lugar a un sistema de medida rápido.

Se analizó la estabilidad encontrando que si se conservan los fotodetectores en oscuridad y atmósfera húmeda pueden ser utilizados durante aproximadamente mil días. El equipo puede utilizarse continuamente, recomendando una recalibración cada siete días.

Como resultado podemos decir que hemos desarrollado una instrumentación portátil para dióxido de carbono en rango completo hasta un 100% con las películas sensoras recubriendo tanto LED como fotodetector, lo que constituye una configuración novedosa y ventajosa.

6. REFERENCES

1. C.E. Araujo-Preza, M.E. Melhado, F.J. Gutierrez, T. Maniatis, M.A. Castellano, Use of capnometry to verify feeding tube placement, Crit Care Med 30 (2002) 2255.

2. A.J. Palma, J. López-González, L.J. Asensio, M.D. Fernandez-Ramos, L.F. Capitan-Vallvey, Microcontroller-Based Portable Instrument For Stabilised Optical Oxygen Sensor, Sens.Actuators B 121 (2007) 629.

3. J. Vukovic, S. Matsuoka, K. Yoshimura, V. Grdinic, R.J. Grubesic, O. Zupanic, Simultaneous determination of traces of heavy metals by solid-phase spectrophotometry, Talanta 71 (2007) 2085.

4. Lopez-Gonzalez, J., Ph.D. Universidad de Granada, 2005.

5. A.J. Palma, J. Lopez-Gonzalez, L.J. Asensio, M.D. Fernandez-Ramos, L.F. Capitan-Vallvey, Open Air Calibration with Temperature Compensation of a Luminescence Quenching-Based Oxygen Sensor for Portable Instrumentation, Anal.Chem. 79 (2007) 3173.

6. M.J. Molina, L.T. Molina, Megacities and atmospheric pollution, J.Air Waste Manage.Assoc. 54 (2004) 644.

7. F. Baldini, A. Giannetti, A.A. Mencaglia, C. Trono, Fiber optic sensors for biomedical applications, Curr.Anal.Chem. 4 (2008) 378.

8. C. Guillaume, P. Chalier, N. Gontard, Modified atmosphere packaging using environmentally compatible and active food packaging materials, Environ.Compat.Food Packag. (2008) 396.

9. M.A. Jensen, G.A. Rechnitz, Response time characteristics of the pCO2 electrode, Anal.Chem. 51 (1979) 1972.

10. D.W. Lubbers, N. Opitz, The pCO2-/pO2-optode. New probe for measurement of partial pressure of carbon dioxide or partial pressure of oxygen in fluids and gases, Naturforsch., C: J.Biosci. 30c (1975) 532.

11. M.J.P. Leiner, Luminescence chemical sensors for biomedical applications: scope and limitations, Anal.Chim.Acta 255 (1991) 209.

12. B.H. Weigl, O.S. Wolfbeis, Sensitivity studies on optical carbon dioxide sensors based on ion pairing, Sens.Actuators B 28 (1995) 151.

13. E.d.N. Gaiao, S.R. Bezerra dos Santos, V. Bezerra dos Santos, E.C. Lima do Nascimento, R.S. Lima, M.C. Ugulino de Araujo, An inexpensive, portable and microcontrolled near infrared LED-photometer for screening analysis of gasoline, Talanta 75 (2008) 792.

14. K. Kawamura, M. Vestergaard, M. Ishiyama, N. Nagatani, T. Hashiba, E. Tamiya, Development of a novel hand-held toluene gas sensor: Possible use in the prevention and control of sick building syndrome, Measurement 39 (2006) 490.

15. Y. Suzuki, N. Nakano, K. Suzuki, Portable Sick House Syndrome Gas Monitoring System Based on Novel Colorimetric Reagents for the Highly Selective and Sensitive Detection of Formaldehyde, Environ.Sci.Technol. 37 (2003) 5695.

16. C.L. Clark, Monitor and control of blood and tissue oxygen tension, Trans.Am.Soc.Art.Int.Organs. 2 (1956) 41.

17. W. Göpel, K.D. Schierbaum, SnO2 sensors: Current status and future prospects, Sens.Actuators B 26 (1995) 1.

18. P.K. Dasgupta, I.Y. Eom, K.J. Morris, J. Li, Light emitting diode-based detectors: Absorbance, fluorescence and spectroelectrochemical measurements in a planar flow-through cell, Anal.Chim.Acta 500 (2003) 337.

19. P.C. Hauser, A solid-state instrument for fluorescence chemical sensors using a blue light-emitting diode of high intensity, Meas.Sci.Technol. 6 (1995) 1081.

20. W. Trettnak, C. Kolle, F. Reininger, C. Dolezal, P. O'Leary, R.A. Binot, Optical oxygen sensor instrumentation based on the detection of luminescence lifetime, Adv.Space Res. 22 (1999) 1465.

21. H. Yan, Ju. Lu, A solid polymer electrolyte-based oxygen sensor for portable oxygen meters, Field Anal.Chem.Tech. 1 (1997) 175.

22. A.N. Watkins, B.R. Wenner, J.D. Jordan, W. Xu, J.N. Demas, F.V. Bright, Portable, low-cost, solid-state luminescence-based O2 sensor, Appl.Spectrosc. 52 (1998) 750.

23. D. Kieslinger, K. Trznadel, K. Oechs, S. Draxler, M.E. Lippitsch, Lifetime-based portable instrument for blood gas analysis, Proc.SPIE-Int.Soc.Opt.Eng. 2976 (1997) 71.

24. I.M. Perez de Vargas-Sansalvador, M.A. Carvajal, O.M. Roldan-Munoz, J. Banqueri, M.D. Fernandez-Ramos, L.F. Capitan-Vallvey, Phosphorescent sensing of carbon dioxide based on secondary inner-filter quenching, Anal.Chim.Acta 655 (2009) 66.

25. A.K. Bansal, W. Holzer, A. Penzkofer, T. Tsuboi, Absorption and emission spectroscopic characterization of platinum-octaethyl-porphyrin (PtOEP), Chem.Phys. 330 (2006) 118.

26. L.F. Capitan-Vallvey, L.J. Asensio, J. Lopez-Gonzalez, M.D. Fernandez-Ramos, A.J. Palma, Oxygen-sensing film coated photodetectors for portable instrumentation, Anal.Chim.Acta 583 (2007) 166.

27. A.E. Colvin, T.E. Phillips, J.A. Miragliotta, R.B. Givens, C.B. Bargeron, A novel solid-state oxygen sensor, John Hopkins APL Tech.Digest 17 (1996) 377.

28. M. Burke, P.J. O'Sullivan, G.V. Ponomarev, D.V. Yashunsky, D.B. Papkovsky, Analysis of close proximity quenching of phosphorescent metalloporphyrin labels in oligonucleotide structures, Anal.Chim.Acta 585 (2007) 139.

29. Y. Amao, T. Komori, H. Nishide, Rapid responsible optical CO2 sensor of the combination of colorimetric change of a-naphtholphthalein in poly(trimethylsiliylpropyne) layer and internal reference fluorescent porphyrin in polystyrene layer, React.Funct.Polym. 63 (2005) 35.

30. Y. Amao, N. Nakamura, Optical CO2 sensor with the combination of colorimetric change of [alpha]-naphtholphthalein and internal reference fluorescent porphyrin dye, Sens.Actuators B 100 (2004) 351.

31. A. Mills, L. Monaf, Thin Plastic Film Colorimetric Sensors for Carbon Dioxide: Effect of Plasticizer on Response, Analyst 121 (1996) 535.

32. A. Mills, A. Lepre, L. Wild, Breath-by-breath measurement of carbon dioxide using a plastic film optical sensor, Sens.Actuators B 39 (1997) 419.

33. C.v. Bültzingslöwen, A.K. McEvoy, C. McDonagh, B.D. MacCraith, I. Klimant, K. Christian, O.S. Wolfbeis, Sol-gel based optical carbon dioxide sensor employing dual luminophore referencing for application in food packaging technology, Analyst 127 (2002) 1478.

34. G. Neurauter, I. Klimant, O.S. Wolfbeis, Microsecond lifetime-based optical carbon dioxide sensor using luminescence resonance energy transfer, Anal.Chim.Acta 382 (1999) 67.

Capítulo 4

Instrumentación óptica compacta para la determinación simultánea de oxígeno y dióxido de carbono

Planteamiento

En este capítulo se va a integrar en una instrumentación portátil el sensor óptico para dióxido de carbono previamente desarrollado en esta Memoria con el sensor para oxígeno puesto a punto por el equipo ECSens en un trabajo previo. En ambos casos la propiedad a medir es la fosforescencia cuya intensidad y/o tiempo de vida es modulada por la concentración de los analitos de nuestro interés. Al ser el principio de transducción el mismo, el instrumento puede compartir bloques instrumentales, simplificando así el diseño. De esta manera el objetivo principal de este capítulo es el diseño, fabricación y validación de un instrumento portátil para la determinación simultánea de oxígeno y dióxido de carbono.

La determinación simultánea de ambos gases encuentra aplicación en gran número de áreas donde las concentraciones de ambos son variables esenciales que están altamente correlacionadas bien como reactivo o como producto en reacciones fundamentales en procesos biológicos, clínicos y biogeológicos. Por ello su determinación simultánea es relevante.

La respiración oxidativa y la fotosíntesis son los procesos biológicos más importantes para la vida en la Tierra. La producción de oxígeno ocurre de forma casi exclusiva como resultado de la fotosíntesis, mientras que el dióxido de carbono se produce, consumiéndose oxígeno, en la respiración oxidativa, así como en otros procesos de gran importancia como es la fermentación y la fotorrespiración en plantas verdes. Así, no es posible distinguir entre ambos procesos si solo se monitoriza la concentración de uno solo de los dos gases. La medida simultánea de ambos gases y en el mismo lugar es el que permite la interpretación de los procesos fisiológicos subyacentes. Por ello, el control simultáneo de oxígeno y dióxido de carbono es de la mayor importancia en biotecnología, especialmente durante la fase de crecimiento celular exponencial [1].

En medicina la valoración de los niveles de oxígeno, dióxido de carbono junto con pH en sangre arterial ha llegado a ser considerada como una

herramienta esencial para el diagnóstico y tratamiento de pacientes en unidades de cuidados intensivos así como en cirugía. La valoración clínica de los pacientes con enfermedad respiratoria agudizada puede precisar la realización de gasometrías arteriales repetidas para el control evolutivo de la enfermedad. Ello requiere la repetición de punciones arteriales, que son molestas y en ocasiones dificultosas. Para pacientes en condiciones inestables, especialmente en momentos de una crisis o para valorar la idoneidad de una intervención terapéutica es de gran interés tener información continua de los niveles de ambos gases en sangre [2,3]

En otro contexto totalmente diferente, la medida representativa de la concentración de gases en suelos y sus flujos, especialmente en suelos heterogéneos, es de gran interés cuando se analizan las interacciones entre procesos biogeoquímicos en ellos. Nuevos retos en análisis de gases, además de los ya conocidos de análisis de emisiones y seguridad, como son la captura y de almacenamiento geológico de dióxido de carbono en el subsuelo, principalmente en formaciones geológicas de tipo yacimientos de petróleo y gas, formaciones salinas profundas o capas de carbón inexplotables, han abierto nuevos campos de aplicación como es el de la monitorización de gases edáficos [4].

Como último ejemplo del interés de la monitorización simultánea de gases podemos señalar la monitorización de la calidad del aire en edificios o vehículos automóviles. El control de la calidad del aire interior se requiere para prevenir la transmisión de enfermedades propagadas por el aire así como para reducir costos. Así por ejemplo, si la concentración de oxígeno alcanza un nivel peligrosamente bajo para el confort o salud humanos, el sensor puede desencadenar un cambio en los parámetros de control. La inclusión de varios sensores en una plataforma única puede suponer una gran ventaja para esta aplicación al permitir la monitorización simultánea de diversos analitos con las ventajas que ello suponer al operar de forma coordinada y cooperativa y no sólo por la multiplicidad de información que se puede obtener con ellos, sino también por el importante papel que puede desempeñar la integración y fusión de

múltiples sensores en la operación de sistemas inteligentes [5]. En particular, se ha analizado la posibilidad de que un sensor influencie directamente la operación de otro de manera que la información combinada que proporcionan los múltiples sensores resulte mayor que la suma de la información proporcionada por cada sensor de forma separada.

Esta instrumentación que se desarrolla en el capítulo actual, adquiere la información analítica basándose en el mismo principio para ambos gases, es decir, en la atenuación de la fosforescencia. En el caso del oxígeno debido a la atenuación que produce sobre esta y en el caso del dióxido de carbono, en la atenuación de la intensidad de fosforescencia causada por la presencia de un indicador cuyo equilibrio ácido-base esta modulado por el dióxido de carbono. La diferencia entre ambos, es como hemos dicho, que para oxígeno la sustancia fosforescente es la sensible a este y para dióxido de carbono la película sensible es la que contiene el indicador de pH.

Las membranas sensoras a los dos gases van a estar dispuestas sobre diferentes canales, es decir, va a existir una separación física entra ellas. Además estas se van a depositar directamente sobre los componentes electrónicos: En el caso de los LEDs, los cuatro van a estar fijos en el instrumento, en cambio los fotodetectores van a estar en una plataforma intercambiable, de manera que permita su reemplazamiento y su conservación debido a que en el caso de las membranas sensoras de dióxido de carbono requieren unas condiciones de conservación especiales como es atmósfera húmeda y oscuridad.

Un aspecto importante a tener en cuenta cuando se trata de medir simultáneamente dos o más analitos es la sensibilidad cruzada entre ellos, es decir, si existe interferencia de un gas sobre la determinación del otro, por lo que en este capítulo llevaremos a cabo el estudio de la influencia de oxígeno en el canal de dióxido de carbono y la influencia de dióxido de carbono en el canal de oxígeno. De esta manera será posible plantear una corrección caso de que sea necesario.

En este capítulo se va a desarrollar una instrumentación portátil que va a constar de cuatro canales para la determinación de gases. Esta instrumentación va a suponer un rediseño del instrumento previamente desarrollado para oxígeno incluyendo un nuevo microprocesador de mejores prestaciones que permita una mejora en la resolución. Los cuatro canales de que constará el instrumento se van a utilizar para la determinación de oxígeno y dióxido de carbono, de manera que realicen medidas redundantes de cada uno de ellos dotando así al instrumento de mayor robustez. Esto exige el establecer la igualdad de respuesta al gas de los dos canales dedicados a cada uno o bien comprobar si existe alguna diferencia. Por otra parte, el desarrollo de esta instrumentación abre la puerta a la inclusión de futuras químicas de reconocimiento para otros gases aumentado así la capacidad de la plataforma multianalito.

A continuación, se analizará la respuesta de cada canal a su analito, modelando la respuesta e integrando la calibración en el microcontrolador del equipo y también la dependencia a temperatura, debido que tanto la luminiscencia como la disolución del gas en la membrana dependen de esta. Tras lo cual se caracterizará analíticamente el instrumento desarrollado.

Microchim Acta (2011) 172:455–464
DOI 10.1007/s00604-010-0520-0

ORIGINAL PAPER

Compact optical instrument for simultaneous determination of oxygen and carbon dioxide

Isabel M. Pérez de Vargas-Sansalvador · Antonio Martínez-Olmos · Alberto J. Palma · María Dolores Fernández-Ramos · Luis Fermín Capitán-Vallvey

Received: 22 July 2010 / Accepted: 4 December 2010 / Published online: 17 December 2010

Abstract A multi-analyte platform based on a portable instrument is presented that enables oxygen and carbon dioxide to be determined in sample gases. The use of four sensing channels (two channels for each analyte to provide redundancy) warrants high system reliability. The sensing scheme in case of oxygen is based on the quenching of the phosphorescence of the platinum octaethylporphyrin complex. In case of carbon dioxide, a secondary inner-filter effect is exploited that is caused by a pH indicator whose color is reversibly changed. The sensing membranes were placed directly on the detectors and on the light sources so to make additional optical element dispensable, reduce system costs, avoid problems related to optical alignment, optimize the efficiency of data acquisition, and enable facile replacement of sensors. The resulting microcontroller-based system is immune against optical and electrical interferences, contains simple digital signal processing circuitry, and has low power consumption. The response of the system to the two gases was modeled, and calibration curves are corrected for effects of temperature. The instrument was characterized in terms of cross-sensitivity and dynamic response. It can determine oxygen and carbon dioxide in terms of volume percentage.

I. M. Pérez de Vargas-Sansalvador · M. D. Fernández-Ramos · L. F. Capitán-Vallvey (✉)
ECsens. Department of Analytical Chemistry, Faculty of Sciences, University of Granada,
Campus Fuentenueva,
E-18071 Granada, Spain
e-mail: lcapitan@ugr.es

A. Martínez-Olmos · A. J. Palma
ECsens. Department of Electronics and Computer Technology, Faculty of Sciences, University of Granada,
Campus Fuentenueva,
E-18071 Granada, Spain

Keywords Carbon dioxide · Oxygen · Optical gas sensor · Phosphorescence · Portable instrumentation

Introduction

The determination of multiple parameters simultaneously can be approached by optical sensors which have advantages over other sensing principles [1]. One interesting example of multianalyte sensing is offered by carbon dioxide and oxygen because they are key variables that are quite interrelated in a variety of fundamental reactions in overall biological, medical and biogeochemical processes, both as reactant and product, in which their simultaneous determination is relevant.

In this area, optical chemical sensors based on the interrogation of a polymer-immobilized probe that displays analyte-dependent optical properties [1] provide an attractive alternative to the more established electrochemical sensors [2].

Different optical sensors for the simultaneous determination of O_2 and CO_2 have been used with different strategies, although in the case of oxygen they are mainly based on the quenching of the luminescence of an oxygen-sensitive dye by molecular oxygen, while in the case of CO_2 they are based on optical changes in a membrane induced by the pH modification upon exposure to the gas.

The current strategy in multianalyte O_2 and CO_2 sensing is based on multispot sensors [3] in which the individual sensors are spatially separated. Several optical chemistries have been combined using different formats, flow/probe, and configurations. A flow-system to monitor pH in addition to the two gases in bioreactors based on three independent flow cells containing sensitive membranes and measuring absorbance and fluorescence intensity quenching

COMPACT OPTICAL INSTRUMENT FOR SIMULTANEOUS DETERMINATION OF O_2 AND CO_2

*Isabel M. Pérez de Vargas-Sansalvador[a], Antonio Martinez-Olmos[b], Alberto J. Palma[b], María Dolores Fernández-Ramos[a] and Luis Fermín Capitán-Vallvey[a]**

Affiliations: ECsens. [a] Department of Analytical Chemistry. [b] Department of Electronics and Computer Technology. Campus Fuentenueva, Faculty of Sciences, University of Granada, E-18071 Granada, Spain.

Abstract

A multi-analyte platform based on a portable instrument is presented that enables oxygen and carbon dioxide to be determined in sample gases. The use of four sensing channels (two channels for each analyte to provide redundancy) warrants high system reliability. The sensing scheme in case of oxygen is based on the quenching of the phosphorescence of the platinum octaethylporphyrin complex. In case of carbon dioxide, a secondary inner-filter effect is exploited that is caused by a pH indicator whose color is reversibly changed. The sensing membranes were placed directly on the detectors and on the light sources so to make additional optical element dispensable, reduce system costs, avoid problems related to optical alignment, optimize the efficiency of data acquisition, and enable facile replacement of sensors. The resulting microcontroller-based system is immune against optical and electrical interferences, contains simple digital signal processing circuitry, and has low power consumption. The response of the system to the two gases was modeled, and calibration curves are corrected for effects of temperature. The instrument

was characterized in terms of cross-sensitivity and dynamic response. It can determine oxygen and carbon dioxide in terms of volume percentage.

Keywords. *Carbon dioxide; Oxygen; Optical gas sensor; Phosphorescence; Portable instrumentation.*

Corresponding author; e-mail: *lcapitan@ugr.es*; phone number: +34958248436; fax number: +34958243328

INTRODUCTION

The determination of multiple parameters simultaneously can be approached by optical sensors which have advantages over other sensing principles [6]. One interesting example of multianalyte sensing is offered by carbon dioxide and oxygen because they are key variables that are quite interrelated in a variety of fundamental reactions in overall biological, medical and biogeochemical processes, both as reactant and product, in which their simultaneous determination is relevant.

In this area, optical chemical sensors based on the interrogation of a polymer-immobilized probe that displays analyte-dependent optical properties [6] provide an attractive alternative to the more established electrochemical sensors [7].

Different optical sensors for the simultaneous determination of O_2 and CO_2 have been used with different strategies, although in the case of oxygen they are mainly based on the quenching of the luminescence of an oxygen-sensitive dye by molecular oxygen, while in the case of CO_2 they are based on optical changes in a membrane induced by the pH modification upon exposure to the gas.

The current strategy in multianalyte O_2 and CO_2 sensing is based on multispot sensors [8] in which the individual sensors are spatially separated. Several optical chemistries have been combined using different formats, flow/probe, and configurations. A flow-system to monitor pH in addition to the two gases in bioreactors based on three independent flow cells containing sensitive membranes and measuring absorbance and fluorescence intensity quenching was described by Weigl et al. [9]. The inclusion of three fluorescent sensing layers on a disposable plastic flow-through cell that allows the successive contact of the sample with the entire sensor simplifies the determination of blood pH, pCO_2 and pO_2 [10,11], although different design have been presented for the same purpose such as the series of sensor stripes

deposited on a substrate next to a sample chamber that transversely crosses a discrete portion of the series [12].

Another arrangement consists of locating the spots of the respective optical sensor films in titerplates as proposed by Liebsch et al. [13], containing films of Pt(II)-porphyrins and Ru(II)-polypyridyl complexes at the bottom of the wells of microtiterplates next to a fast gateable CCD camera allowing luminescence lifetime imaging and, thus, the determination of both gases, temperature and pH in solution.

Optical fiber presents advantages for multianalyte sensing especially for intravascular blood gas monitoring. The configuration with three single fibers, for pH, pCO_2 and pO_2, with fluorescent chemistries attached at the tip of each fiber, optically isolated with a permeable opaque film, and mechanically integrated within a polymer structure has been widely used. A switching procedure to address each sensor in the bundle allows the sequential measurement of analytes [2,14,15]. As a last example, the deposition of fluorescence-based sensing films on top of a poly(methyl methacrylate) waveguide permit the development of a sensor chip platform for gaseous O_2, CO_2 and humidity based on phase-sensitive detection techniques [5].

The previous multianalyte design with spatially separated sensors has limitations if the spatial resolution of analytes is needed or when the volume of the sample is limited. Two solutions can be used to overcome the drawbacks: reduce the size of each sensing element or use a single sensing element that yields multiplexed optical information that can provide simultaneous analysis for several species.

Among another solutions [16], an example of the first solution was presented by Ferguson et al. [17], using a single modified optical imaging fiber containing, at the fiber's distal end, three distinct sensing elements containing covalently immobilized fluorescent reagents within polymer matrices via photopolymerization for simultaneous monitoring using ratiometric intensities of pH, CO_2 and O_2 during beer fermentation.

Two different arrangements have been used in the second case – with only one layer element – the first to superimpose sensing layers, one for each analyte. One example uses silica beads with bipyridyl-Ru(II) complex embedded in a silica matrix with a second layer consisting of a hydrogel layer containing 8-hydroxypyrenetrisulfonate in cellulose and all attached to the distal end of the fiber. Both indicators have the same excitation wavelength and quite different emission maxima that produce a single sensor for two analytes based on an easily separated intensity measurement [18], although the use of the decay time of luminescence for optical interrogation of the dual membrane sensor using the dual-lifetime referencing method offers good results [1], especially in the field of packaging industry [19].

The second arrangements refer to single layer dual sensors containing all the chemicals incorporated in some cases as microparticles within a single embedding polymer. The combination of planar optical sensors and a time-gated imaging scheme using a CCD camera makes it possible to map pCO_2 and pO_2 within one measurement [20].

In this paper, we report on the development of a portable instrument for the simultaneous determination of O_2 and CO_2 in gaseous samples based on luminescence measurements. The use of a room-temperature phosphorescence measurement in chemical sensing offers advantages over other luminescent signals [21], such as generating long lifetime emissions, facilitating in this way the design of portable instrumentation [22]. As explained below, the developed multianalyte instrument contains one reconfigurable polarization circuitry for the light source and one signal processing channel for the luminescence signal, with a considerable electronic reduction compared with other similar instrumentation [23,24]. The solution of using the same transduction principle was carried out previously by Choi and Hawkins [25], although not as a sensor, for O_2 and CO_2 monitoring based on a fluorescence in charge transfer band for O_2 and fluorescence in acid-base character for CO_2.

For design simplification, we use a scheme based on spatially separated individual sensors for both gases, but using the same transduction principle:

phosphorescent emission coming from platinum octaethylporphyrin complex (PtOEP). Its long lifetime (tenths of microseconds) made it possible to develop previous microcontroller-based portable instrumentation for individual gases such as O_2 and CO_2 based on the measurement of a time parameter related to gas concentration [22,26].

EXPERIMENTAL

Reagents, materials and apparatus

The reagents used were platinum octaethylporphyrin complex (PtOEP, Porphyrin Products Inc., Logan, UT, USA), tributyl phosphate (TBP), 1,4-diazabicyclo[2.2.2]octane (DABCO; 98%), α-naphtholphthalein, and tetraoctyl ammonium hydroxide (TOAOH; 0.335 M in methanol) all from Sigma–Aldrich Química S.A. (Madrid, Spain). The solvents used, tetrahydrofuran (THF), toluene and ethanol, were supplied by Sigma as well. As polymers, poly (vinylidene chloride-co-vinyl chloride) (PVCD, particle size 240-320 μm), polystyrene (PS, average MW 280,000, Tg: 100 ◦C, GPC grade) and ethylcellulose (EC, ethoxyl content 49%), all from Sigma, were used. All cocktails were prepared by weighing the chemicals with a DV215CD balance (Ohaus Co., Pine Brook, NJ, USA) with a precision of ±0.01 mg. The gases CO_2, O_2 and N_2 used were of a high purity (>99%) and were supplied in gas cylinders by Air Liquid S.A. (Madrid, Spain).

For the electrical characterization of the prototype, the following instrumentation was used: a mixed signal oscilloscope (MSO4101, Tektronix, USA), a 6½ digit multimeter (34410A, Agilent Technologies, USA), a 15 MHz waveform generator (33120A, Agilent Technologies, USA) and a DC power supply (E3630A, Agilent Technologies, USA).

Portable electronic instrument and signal processing

The scheme of the signal processing electronics for the portable instrument developed is presented in Figure 1. The core of the system is the 18F2550 microcontroller (Microchip Technology Inc., USA; www.microchip.com). This model was selected due to the integration of a 10 bit analog-digital converter and a USB module in this chip, which makes it possible to communicate with the computer.

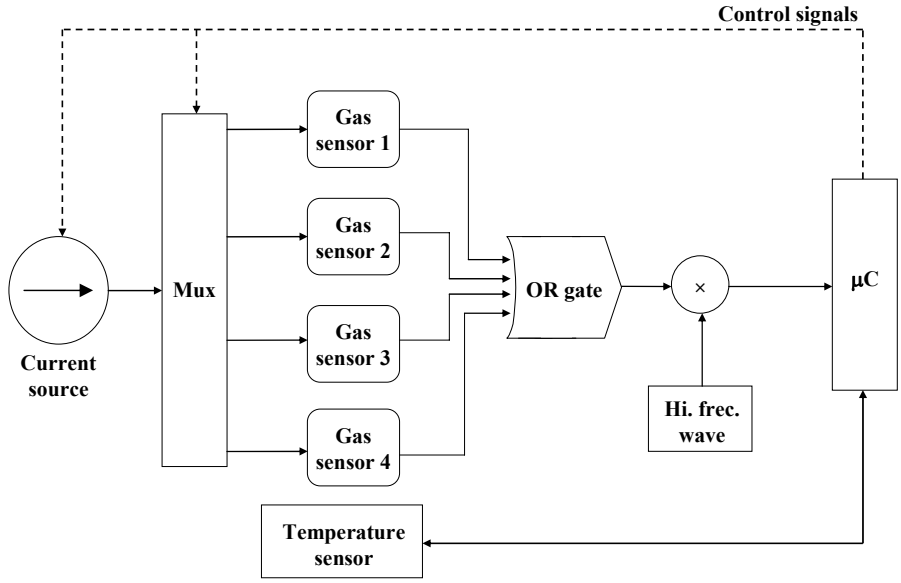

Figure 1. Block diagram of the signal processing electronics.

For the purposes of multianalyte measurement, the design of this system includes a sensing area with four channels which can be used to detect four different gases. Each sensing channel is formed by the combination of a LED (100047, Marl International Ltd., Ulverston, UK; www.leds.co.uk) for

phosphorescence excitation and a solid-state photodetector for luminescence detection, placed facing each other, with the different sensing cocktails as indicated in Figure 2a. Each LED emits at a dominant wavelength of 525 nm. The LEDs were directly soldered on the main printed circuit board with the rest of the electronic components, while the photodetectors were soldered on an auxiliary circuit board which is inserted over the LED area as shown in the photograph in Figure 2b. Each photodetector (IS486, Sharp, Japan; sharp-word.com), with a built-in Schmidt trigger circuit, gives a binary output depending on an illuminance threshold. Since four photodetectors are used, the same quantity of LED is included in the design. All the LEDs are biased by a unique thermal-stabilized current source, which has also four outputs (see Figure 1). In the present prototype, the current of every output can be individually configured by the user in the range of 0 to 20 mA, which can be used for the particular configuration of the phosphorescence of each sensor and the correction of the response deviations due to displacement in the alignment and the distance between the LED and the photodetector. The four gas sensors make concentration measurements of four different gases possible, although in this work they were used for the redundant determination of the concentrations of O_2 and CO_2 using two channels for each gas.

The thermal drift of the measurements was compensated by the integration of the DS1624 temperature sensor (Maxim, USA; www.maxim-ic.com) in the prototype which provides the temperature value, in digital format, with resolution of 0.03125 ºC through a two-wire serial interface with the microcontroller as indicated in Figure 1. This sensor allows the thermal calibration of the system. In addition, to improve the air circulation inside the instrument, a micro-fan was arranged in this new prototype, and is activated before every measurement, forcing the external air to flow in the direction of the gas sensors, performing the measurements with the fan turned off (Figure 2b). This forced ventilation is switched off before the measurement process. Finally, the result of the measurements is displayed in an LCD, or can be transmitted to a computer via the USB connection. Moreover, this USB port can be used to power the instrument as an alternative to batteries.

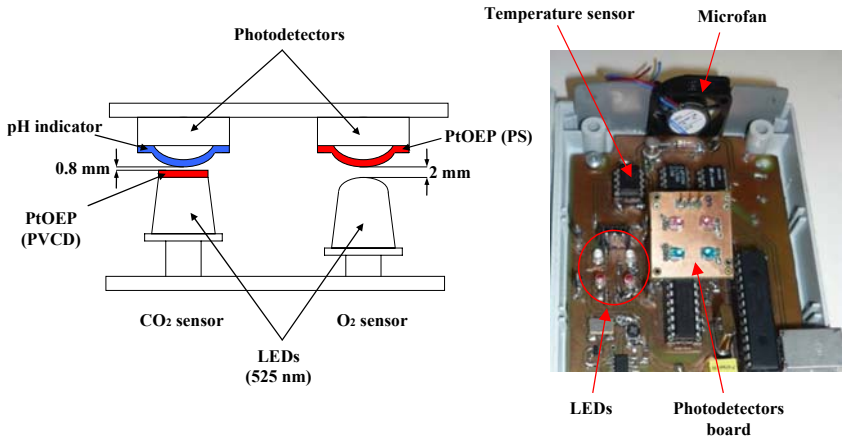

Figure 2. Sensing module. a) Gas sensor arrangement showing two channels, one for O_2 and the second for CO_2. b) Photograph of the electronics of the instrument showing the main PCB with the four LED, the micro-fan in the upper part and the auxiliary PCB with the four photodetectors.

When the gas-sensitive membrane is deposited on the surface of the photodetectors and excited by the LED, as shown in Figure 2a, it emits phosphorescence which produces a pulse at the output of the photodetector. The width of this pulse is related to the concentration of the sensed gas [22]. In addition, the availability of a programmable current source allows the implementation of an auto-zero of the measurement as follows: the photodetector used in this design has a propagation time delay of several μs, typically 3-5 μs, which means that the measured pulse width includes a component which is not produced by the sensor phosphorescence, but for the photodetector itself. This offset time can be measured by polarizing the LED with a low current (< 1 mA), which is not enough to produce an excitation of the deposited membrane and, therefore, the output signal is only due to the propagation delay. After this measurement is carried out, the LED is now biased with a high squared-shape current pulse to obtain signal from the sensing

membrane. If these two signals are subtracted, a measurement of the component of the pulse width caused only by the response of the membrane is obtained. This procedure allows the correction of the time delay introduced by the photodetector. Moreover, as this is done in each measurement, thermal and other environmental drifts of this delay time are also cancelled.

Until now, the method used to measure the duration of the pulse has been to multiply it with a high-frequency signal and to count the number of resulting pulses, N [22]. In this prototype, the analytical parameter does not count the number of pulses, N, as in our previous work, but directly counts the pulse width in seconds, t^N, which is calculated by multiplying the number of pulses N by the duration of each pulse (time resolution of the system). This factor for converting the number of pulses in a time magnitude does not affect the analytical and empirical models used until now for instrument calibration for both oxygen and carbon dioxide concentrations.

In this case, a 100 MHz clock is used, which implies a resolution of 10 ns in the time measurement. This represents a significant improving in this parameter with respect to the previously developed system [26] where the frequency of the square signal was 20 MHz and therefore the time-resolution was 50 ns. Below, technical specification will be compared between our previous and this development.

For each sensing channel, the excitation of the sensing membrane is produced by the corresponding LED 2000 times in 1 second, and the final result is an average of the measured pulse widths, which allows a reduction of the noise in the measurement and therefore an increase in the signal-to-noise ratio. Since the measurement procedure is the same for both gases, i.e., the gas concentration is related to the pulse width produced at the output of the photodetector as a consequence of the phosphorescence that reaches it coming from the sensing area, the electronics required for the measurement of that pulse width is also common for the four channels, with the only constraint being that the gas measurements must be carried out sequentially. However, this should not be an important disadvantage, because the measurement of the four

channels can be completed in only 4 seconds. This fact means a reduction in the complexity of the system and therefore, in the overall cost, which is a very desirable characteristic for a portable instrument.

Sensing channel preparation

The sensing channels were prepared by casting the sensitive membranes directly on the optoelectronic elements using a coating technique. In this way, the luminescence collecting efficiency is improved by directly coating the detector or the emitter element with the optical sensing membrane with no optical filter as indicated in previous reports [26].

Mixtures for the preparation of the oxygen-sensitive membrane were made by dissolving 0.5 mg of PtOEP and 12 mg of DABCO in 1 mL of a solution of 5% (w/v) of PS in freshly distilled THF. In the case of O_2, the sensitive membranes were cast by placing two successive volumes of 5 μL of the O_2 cocktail on the active face of the photodetector with the aid of a micropipette (Figure 2a). After each addition, the device was left to dry in darkness in a THF atmosphere for 1 hour. The obtained coated photodiodes show the lens covered with a homogeneous, transparent and pink film with an estimated average thickness of about 75 μm and an approximate PtOEP concentration of 0.055 $mol \cdot kg^{-1}$ polymer. The module containing coated photodiodes was stored in darkness until use to prevent photodegradation.

The sensing membranes for CO_2 were prepared from cocktails A and B. Cocktail A contained 100 mg of PVCD dissolved in 1 mL of freshly distilled THF using an ultrasonic bath and 0.5 mg PtOEP. Cocktail B is composed of 64 μL TBP, 320 μL of a solution containing 2.2 mg of α-naphtholphthalein in 2 mL of toluene/EtOH (80:20 v/v), 1 mL of toluene containing 60 mg of previously dissolved EC and finally 200 μL of 0.335 M TOAOH. The sensor configuration used for CO_2 consists of coating the LED with the sensing membrane containing PtOEP (cocktail A) and the photodetector with a sensing membrane containing the pH indicator (cocktail B) as shown Figure 2A. The PtOEP membrane was cast on a previously polished LED to present a circular flat surface with a 3mm

diameter in order to prevent the cocktail solution from spilling off the LED surface. Afterwards, the PtOEP membrane was cast by placing two successive volumes of 5 µL of cocktail A on the top of LED. After each addition, the module was left to dry in darkness in a dryer with a saturated THF atmosphere for 1 h at room temperature. The resulting pink membrane has an average thickness of 141 µm. The α-naphtholphthalein indicator membrane was cast onto the active face of a photodetector with the aid of a micropipette using 5 µL of cocktail B. After preparation, the module containing photodetectors was dried in darkness and at vacuum in a dryer for 12 h at room temperature. In this case, the photodiode is coated with a transparent blue film with an average thickness of about 105 µm.

The photodetectors with O_2 sensing membranes containing PtOEP in PS as well as the LED with PtOEP in PVCD need to be cured in darkness for 9 days before their use. As the photodetector module contains four elements of which two are coated for O_2 sensing (PtOEP in PVCD) and the other two are coated for CO_2 sensing (pH indicator in EC), firstly, two photodetectors were prepared for O_2 sensing and on the ninth day, the other two photodetectors were prepared for CO_2. The module containing half of the photodetectors coated with pH indicator membrane and the other half with PtOEP in PS were stored in a desiccator containing sodium carbonate to protect the membranes from any acidic gases from the lab; in darkness and in an atmosphere of 94% RH (20±0.5ºC).

Measurement conditions

The standard mixtures for instrument calibration and characterization (CO_2 in N_2 and O_2 in N_2) and cross-sensitivity studies (CO_2 and O_2 in N_2) were produced using N_2 as the inert gas component and by controlling the flow rates of the different high purity gases CO_2, N_2 and O_2, in each case, entering a mixing chamber using a computer-controlled mass flow controller (Air Liquid España S.A., Madrid, Spain) operating at a total pressure of 760 Torr and a flow rate of 500 $cm^3 \cdot min^{-1}$. For the preparation of gas mixtures lower than 2% in CO_2,

a standard mixture of 5% CO_2 in N_2 was used, with the lowest CO_2 concentration tested being 0.1%. For the portable instrument characterization, the measurements were performed after equilibration for 2 min of the instrument atmosphere with the gas mixtures obtained with the gas blender indicated above.

All measurements were replicated six times, except when stated otherwise, to check for experimental error. A homemade thermostatic chamber, with a lateral hole for the connexion to a computer and gas tubing entrance, made it possible to maintain a controlled temperature between −50 ºC and +50 ºC with an accuracy of ±0.5 ºC for thermal characterization of instrument.

RESULTS AND DISCUSSION

Instrument response modelling

The aim of this study is the integration of optical sensing membranes for O_2 and CO_2 in a battery-operated portable instrument.

In the first case, the oxygen sensitivity is due to a dynamic quenching that changes both phosphorescence intensity and the lifetime of the PtOEP [27]. As the membrane polymer used to encapsulate the platinum complex, PS was selected because of its resulting high phosphorescence (lifetime of 99.9 μs at 0 % O_2) with maximum at 647 nm when it is excited at the wavelength of the metalloporphyrin Q-band (534 nm). The photostability of the membrane is increased through the elimination of the singlet oxygen intermediate generated as a consequence of the quenching process of the luminophore by oxygen. As singlet oxygen scavenger, the heterocyclic amine DABCO was selected. The resulting membranes with 25 % of the stabilizer DABCO show enough sensitivity and suitable stability to sense oxygen with good resolution (lifetime 104.4 μs at 0 % O_2 and 13.7 μs at 100 % O_2 for membranes with 25 % DABCO) and low drift (0.01 %/day) [22].

The oxygen-sensitive photodiodes exhibit changes in the pulse width of their output at the high level, t^N, the parameter measured by this portable instrument, with the amount of oxygen due to dynamic quenching of the luminescent emission of PtOEP. As the calibration function for O_2, we used the empirical equation (eq. 1), which provided good results with previous O_2 prototypes [28]

$$[O_2] = C_0 + \frac{C_1}{\sqrt{t^N}}, \qquad \text{(eq. 1)}$$

where C_0 and C_1 are fitting parameters which include the thermal dependence.

In the second case, a secondary inner-filter effect accounts for CO_2 sensitivity that involves the absorption of the phosphorescence emitted from the CO_2-insensitive luminophore (PtOEP) by the basic form of a liphophilised acid-base indicator [29]. The sensor mechanism is based on the reaction between CO_2 and the deprotonated form of α-naphtholphthalein present in the membrane as an ion pair with tetraoctylammonium cation TOA^+. The reduction in deprotonated α-naphtholphthalein N^- concentration by reaction with CO_2 increases the phosphorescence that reaches the photodetector (eq. 2).

$$TOA^+N^- \cdot xH_2O + CO_2 \xleftrightarrow{K} TOA^+HCO_3^- \cdot (x-1)H_2O \cdot HN \qquad \text{(eq. 2)}$$

The best configuration for this instrument in terms of sensitivity and reproducibility results from assembling the sensing membrane containing PtOEP coating the LED and the pH indicator membrane on the photodetector. To

reduce the luminescence quenching of PtOEP by oxygen we used as membrane polymer a non-permeable to oxygen polymer, namely PVCD.

The secondary inner-filter mechanism was confirmed by measuring the phosphorescence lifetime of a membrane before and after exposure to a CO_2 atmosphere (at 100% nitrogen: τ_1 96.0 μs (SD 1.85); at 100% CO_2: τ_1 97.9 μs (SD 0.77) which shows there is no luminescence lifetime decay variation [26].

For calibration purposes, we used the eq. 3 [26,30] where K is the equilibrium constant for eq. 2, $C = K\varepsilon b\left[TOA^{+}N^{-}\cdot xH_2O\right]$, ε is the molar extinction coefficient of acceptor ($8.65\cdot10^3$ $l\cdot mol^{-1}\cdot cm^{-1}$), the basic form of α-naphtholphthalein at the emission wavelength of luminophore and b the effective pathlength of the membrane (105 μm), t^N and t_0^N are the pulse widths related to luminescence intensity and measured in the presence and absence of CO_2, respectively. In the case of CO_2 the photodetector of the presented instrument simplifies intensity integration over the time in which the final illuminance is above an established threshold:

$$\frac{t^N}{t_0^N} = 10^{\{-C(1/(K+[CO_2])+1/K)\}}, \qquad \text{(eq. 3)}$$

where the luminescence intensity is related to the pulse width, t^N, in our instrument as explained above.

Measurement system performance

Calibration and inter-channel repetitivity

A typical calibration function for oxygen (Figure 3A) studied using the empirical model as a fitting routine, shown in eq. 1, was done with six-fold replicas at room temperature (20 ºC) as a function of the oxygen concentration up to 30%, obtaining:

$$[O_2] = -4{,}939 + \frac{1996}{\sqrt{t^N}}, \quad R^2 = 0.998 \qquad \text{(eq. 4)}$$

with the variable t^N in nanoseconds. The response of the two O_2 channels was studied and no statistical differences between them were found. One channel fits the response of the other channel with R^2 = 0.9977, which may be due to the low dependence of the geometry of the measurement system. The average value of the two channels is used to calculate the final oxygen concentration, permitting in this way the redundancy of the system and increasing the reliability.

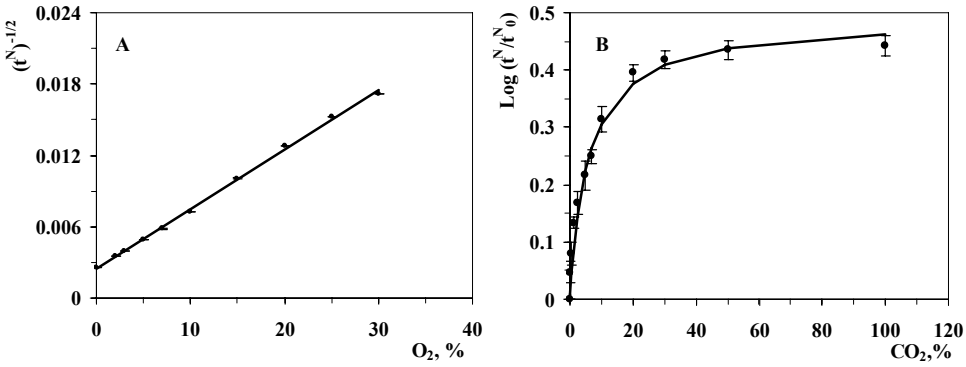

Figure 3. Calibration curves. Comparison of the experimental data (symbols) with analytical models (lines) for: A) O_2 with model of eq. 1 and B) CO_2 with model of eq. 3, both at 20ºC.

The response of the portable instrument to CO_2 was fitted according to eq. 3 used as the calibration function for the whole range studied (up to 100%). Figure 3B presents a typical normalized $\log t^N / t_0^N$ change versus CO_2 concentration, with the solid line being the best-fit to eq. 3 in logarithmic form (R^2 = 0.9878), resulting in coefficient values of K = 6.15±0.63 and C = 3.02±0.31 at 20 ºC.

The two CO_2 sensors included in the instrument show similar results, with the pulse width ratio of 1.0940. If this factor coming from one channel is included in the results from the other channel, the results adjust with R^2 = 0.9994. In any case, the CO_2 channel seems to be more sensitive to distance and alignment between the LED and photodetector than the O_2 channels. We have overcome these geometrical dependences by adjusting the LED polarization current in order to minimize the differences between the two CO_2 channels.

The module that contains the photodetectors must be kept in 94% RH conditions and darkness in a desiccator as the best way to preserve the CO_2 membranes for nearly one year; however the O_2 membranes included in the module do not need any preservation system and are not influenced by high humidity conditions [26].

The limits of detection (LOD) for the two sensors were obtained using the derivate of the calibration function and the signal obtained at 0% of gas concentration. The LOD found using this criterion were 0.001% for O_2 and 0.0003 % for CO_2.

This new configuration leads to an improvement of the instrument response, regarding to analytical and technical parameters as resolution or accuracy among others. In the Table 1 these parameters are compared to those corresponding to the previously presented prototypes [26,28].

Table 1. Technical specifications of portable instrument for simultaneous gas sensing.

Parameter	Previous prototypes	This prototype
Microcontroller	PIC 16F876	PIC 18F2550
PC Communication	Serial (RS232)	USB
Oscillator	4 MHz [28]/ 20 MHz [26]	100 MHz
Time resolution	250 ns [28] / 50 ns [26]	10 ns
Channels	1	4
Programmable current source	No [26,28]	Yes (1-20 mA / channel)
Auto-zero	No [26,28]	Yes
Alignment correction	No [26,28]	Yes
Sensed gas	O_2 [28]/ CO_2 [26]	O_2 and CO_2
Resolution	0.5% (21% O_2) [28] 0.0002% (5% CO_2) [26]	O_2: 0.05% (21%) CO_2: 0.0001 % (5%)
Detection limit	0.1% (O_2) [28] 0.002% (CO_2) [26]	0.001% (O_2) 0.0003 % (CO_2)

From this comparison it is clear that the new prototype, in addition to the capability of to measure two different gases, O_2 and CO_2, by means of a common acquisition electronics, presents a better technical performance than the previous systems, since both the resolution and the detection limit for O_2 and CO_2 are improved in more than one magnitude order due to a higher time resolution measuring the output pulse widths of the photodetectors (see Table 1).

The stability, both short-term and long-term, of sensing membranes prepared on optoelectronics elements was an issue considered in previous studied [26,31] and confirmed here. In the case of the sensitive O_2 photodetector a short-term study over 4 days at one measurement per min at 21% O_2 concentration cause a total drift of 1.5% in O_2 concentration. Aditionally a study over 20 days obtaining one measurement per day at 21% O_2 cast a mean drift of 0.02% O_2 per day. In the case of coated LED-photodetector CO_2 sensing system, the short-term stability show a mean drift of -0.16% CO_2 concentration per hour working at at 6.25% CO_2 for 24 hours measuring every 8 s. The long term stability of luminophore membranes shows a phosphorescence decreases by some 20% after 210 days and the indicator membrane show a half-life between 1-2 weeks in 33% RH atmosphere in darkness or in 94% RH conditions under illumination; although maintaining in 94% RH and in darkness it is longer than 4 months.

Temperature influence

The temperature has an influence on the O_2 sensor, as can be seen in Figure 4A, where the response of this sensor at different temperatures is depicted. From the results it can be concluded that the output signal of the sensor decreases with temperature, as well as with the O_2 concentration. This fact can be modeled with the thermal dependence of the fitting parameters C_0 and C_1 from Equation 1. From different calibrations of the oxygen sensor at several temperatures, these parameters were determined: $C_0 = -7.2479 + 0.0292 \cdot T$ ($R^2 = 0.928$), $C_1 = 7.0414 - 0.038 \cdot T + 9 \cdot 10^{-5} \cdot T^2$ ($R^2 = 0.995$) with T in Celsius degrees.

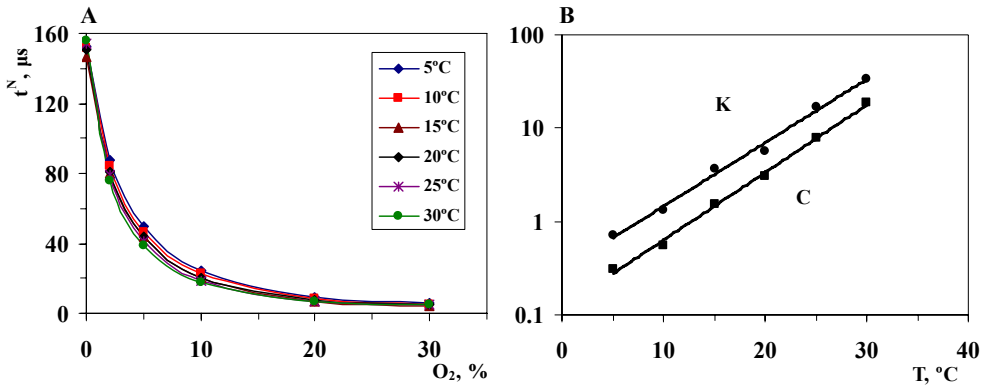

Figure 4. Thermal dependences of the instrument responses. A) O_2 thermal dependence; t^N versus % O_2 at 5, 10, 15 ,20 , 25 and 30ºC and B) CO_2 thermal dependence., between 5 a 30 ºC. Symbols represent *C* and *K* obtained from calibrations of the CO_2 sensor at different temperatures in the range 5-30 ºC and the resulting parameters were fitted to an exponential experimental curve.

As explained above, the calibration of the CO_2 sensor was carried out by means of Equation 3. Therefore, the influence of the temperature in the response of the sensor can be modeled by including the thermal dependence of the fitting parameters of that equation, i.e., by expressing *C* and *K* as a function of the temperature. This dependence was empirically determined by obtaining calibrations of the CO_2 sensor at different temperatures in the range 5-30 ºC and fitting the resulting parameters to an exponential curve, as presented in Figure 4B. From these results, the dependence of the CO_2 sensor with the temperature can be reflected by expressing the parameters as $K = 0.303e^{0.157T}$ ($R^2 = 0.9913$) and $C = 0.119e^{0.167T}$ ($R^2 = 0.9957$) with T in Celsius degrees.

Channel cross-sensitivity and dynamic behavior

Next, a cross-sensitivity study between CO_2 and O_2 sensors was performed. The influence of CO_2 in O_2 determination was investigated by means of calibrations at four CO_2 concentrations (0, 2, 25 and 70% CO_2). The results obtained show that CO_2 does not influence O_2 sensing because the calibrations curves obtained had no significant differences in all the experiments. For the

range of CO_2 concentrations from 0 % to 70 %, the oxygen result increases only 0.02 % in absolute terms at 21 % O_2 concentration.

In the case of the O_2 influence on calibration for CO_2, the problem lies in the quenching by O_2 on the PtOEP complex immobilized in a PVCD polymer despite its low O_2 permeability. Two different experiments were performed, the first one being a study only with O_2 without CO_2. This experiment consisted of measuring how the CO_2 sensor responded to increasing O_2 concentrations. In both channels, at 21% O_2, the reduction in the t^N/t_0^N signal was less than 4%. If we compared this with PtOEP immobilized in a PS membrane, the reduction in signal at 21% O_2 was 97.46% (see Figure 5A). The other experiment consisted of doing CO_2 calibrations at five concentrations of O_2 (0, 7, 14, 21 and 28%), fitting the calibration curve for each one to eq. 3. K and C coefficients can be adjusted to a straight line ($K = 0.1457 \cdot [O_2] + 5.04$; $R^2 = 0.9977$) and ($C = 0.0597 \cdot [O_2] + 2.307$; $R^2 = 0.9755$) as can be seen in the inset in Figure 5B. These dependences on C and K have been included in the calibration function (eq. 3) and programmed in the microcontroller. Consequently, it was possible to correct the O_2 influence on CO_2 detection with the equations obtained earlier.

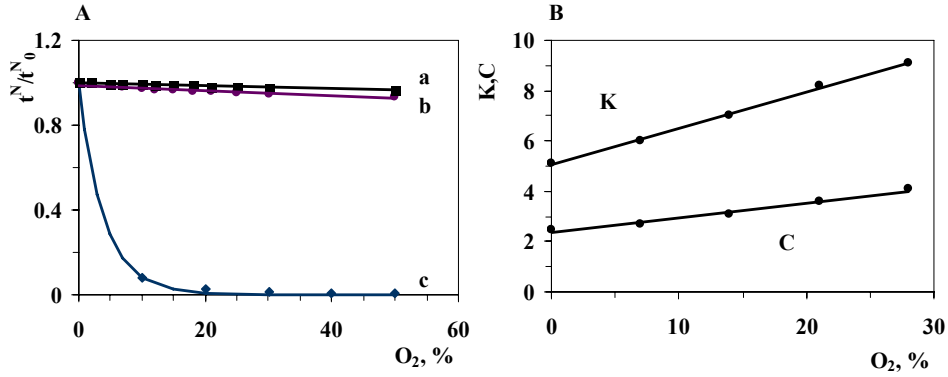

Figure 5. Influence of O_2 in CO_2 sensing. A) Responses of the CO_2 sensor to increasing O_2 concentrations using PVCD membranes (a and b) and PS membrane (c); B) Dependence of the CO_2 model parameters C and K of eq. 3 with the O_2 concentration. Symbols show experimental data and the lines show the linear fits.

The dynamic response of the instrument was studied measuring the response at different concentrations of CO_2 and O_2 continuously. Figure 6 displays the response to alternating atmospheres of pure CO_2 or O_2 and pure N_2. The differences in dynamic behavior between both gases refer to an initial low signal at 0% in the case of CO_2 to a high signal at 100% whereas the opposite behavior was observed for O_2, with a high signal at low O_2 concentrations that reduces at high concentrations. Additionally, the signal changes are fully reversible and hysteresis was not observed during the measurements. The results obtained are: response time, t_{90} s, 31.0 ± 0.9 (O_2 sensor) and 31.0 ± 2.4 (CO_2 sensor) and recovery time, t_{10} s, 149.7 ± 3.7 (O_2 sensor) and 124.9 ± 5.4 (CO_2 sensor).

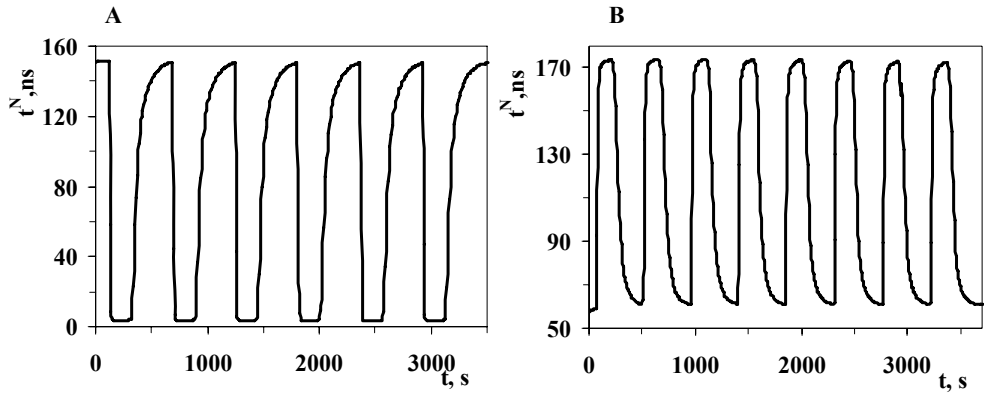

Figure 6. Dynamic response of portable instrument for changes in A) CO_2 and B) O_2 concentration from 0% to 100%.

Figure 7. Portable instrument and photodetectors board

Figure 8. Inside of the portable instrument and photodetectors board.

CONCLUSIONS

A portable multianalyte instrument with four sensing channels has been presented for the redundant determination of O_2 and CO_2. The transduction principle is common and based on phosphorescence attenuation by different mechanisms. This characteristic produces a very simplified electronic design with an important reduction in the number of the electronic components. A complete analytical and technical characterization has been carried out, showing a good agreement between the experimental data and the proposed models. A notably specifications improvement has been achieved in this prototype with respect to previous designs. Thermal compensation was included using temperature monitoring, and the cross-sensitivity responses were calculated and corrected in the case of CO_2 determination in the presence of O_2. This resulted in a microcontrolled-based easy-to-use measurement system with high optical and electrical interference immunity, extremely simple digital signal processing circuitry and low power consumption.

Acknowledgements

We acknowledge financial support from the Ministerio de Ciencia e Innovación (Spain) (Projects CTQ2009-14428-C02-01 and CTQ2009-14428-C02-02) and the Junta de Andalucía (Project P08-FQM-3535). These projects have been partially supported by European Regional Development Funds (ERDF).

CONCLUSIONES

En este capítulo hemos desarrollado una instrumentación portátil y compacta capaz de determinar simultáneamente la concentración de oxígeno y dióxido de carbono.

En este nuevo prototipo incluimos mejoras sobre el anterior instrumento usado para la determinación de oxígeno, entre ellas, un microventilador para facilitar el flujo de aire hacia dentro del equipo y principalmente la inclusión de un reloj de 100 MHz, lo que implica una resolución de 10 ns en el tiempo de medida, cinco veces mayor que la del equipo desarrollado en el capítulo anterior. Además en este prototipo tenemos un módulo USB que posibilita la comunicación con el ordenador. Al poseer 4 canales de medida permite el poder realizar medidas redundantes. Cada canal puede polarizarse con una corriente independiente, lo que permite corregir desviaciones en el alineamiento entre el LED y el fotodetector.

Se ha estudiado dos a dos la respuesta de los canales a su gas diana, encontrando que para el caso del oxígeno ambos canales dan aproximadamente la misma respuesta con lo que la concentración de oxígeno se calcula a partir de una media de la señal de cada canal. En cambio, para el dióxido de carbono sí se encontró una diferencia algo mayor, por lo que se ajustó esta diferencia con el empleo de un factor de corrección, obteniendo así resultados en ambos canales prácticamente iguales.

Se modeló la respuesta de los canales para cada gas introduciendo la función de calibrado en el microcontrolador del equipo, obteniendo así directamente en la pantalla LCD del equipo la concentración de cada uno de los gases, proveniente de la media de cada conjunto de dos canales.

Como hemos señalado anteriormente, hemos realizado un estudio de interferencia cruzada entre oxígeno y dióxido de carbono, concluyendo que este último gas no provoca interferencia alguna en la determinación del primero; sin embargo el oxígeno sí interfiere, aunque en poca extensión en la determinación de dióxido de carbono, por lo que modelamos su comportamiento a cuatro

porcentajes diferentes de oxígeno y lo introdujimos en el microcontrolador del equipo.

Se estudió la dependencia de la temperatura de 5 a 30ºC, se modeló y se introdujo la dependencia térmica de cada membrana sensora de cada gas en el microcontrolador del instrumento portátil.

Los tiempos de respuesta y recuperación encontrados, son comparables a los obtenidos anteriormente y adecuados para la determinación de ambos gases.

Por tanto, podemos concluir que hemos desarrollado una instrumentación portátil para determinación simultánea de oxígeno y dióxido de carbono que presenta gran facilidad de uso, pudiendo utilizarse como plataforma analítica muy simple de usar por parte de usuarios sin especial formación en el campo del análisis químico.

REFERENCES

1. Borisov SM, Krause C, Arain S, Wolfbeis OS (2006) Composite material for simultaneous and contactless luminescent sensing and imaging of oxygen and carbon dioxide. Adv Mater 18:1511-1516.

2. Miller WW, Yafuso M, Yan CF, Hui HK, Arick S (1987) Performance of an in-vivo, continuous blood-gas monitor with disposable probe. Clin Chem 33:1538-1542.

3. Herrejon A, Inchaurraga I, Palop J, Ponce S, Peris R, Terradez M, Blanquer R (2006) Usefulness of transcutaneous carbon dioxide pressure monitoring to measure blood gases in adults hospitalized for respiratory disease. Arch Bronconeumol 42:225-229.

4. Lazik D, Ebert S, Leuthold M, Hagenau J, Geistlinger H (2009) Membrane based measurement technology for in situ monitoring of gases in soil. Sensors 9:756-767.

5. McGaughey O, Nooney R, McEvoy AK, McDonagh C, MacCraith BD (2005) Development of a multi-analyte integrated optical sensor platform for indoor air-quality monitoring. Proc SPIE-Int Soc Opt Eng 5993:59930R-1-59930R/12.

6. Wolfbeis OS (2005) Materials for fluorescence-based optical chemical sensors. J Mater Chem 15:2657-2669.

7. Ramamoorthy R, Dutta PK, Akbar SA (2003) Oxygen sensors: Materials, methods, designs and applications. J Mat Sci 38:4271-4282.

8. Nagl S, Wolfbeis OS (2007) Optical multiple chemical sensing: status and current challenges. Analyst 132:507-511.

9. Weigl BH, Holobar A, Trettnak W, Klimant I, Kraus H, O'Leary P, Wolfbeis OS (1994) Optical triple sensor for measuring pH, oxygen and carbon dioxide. J Biotechnol 32:127-138.

10. Leiner MJP (1995) Optical sensors for in vitro blood gas analysis. Sens Actuators B B29:169-173.

11. Leiner MJP (1991) Luminescence chemical sensors for biomedical applications: scope and limitations. Anal Chim Acta 255:209-222.

12. Mason, R. W., Slovacek, R. E., and Sullivan, K. J. (2002) Optical sensor and method of operation. US 6,488,891.

13. Liebsch G, Klimant I, Frank B, Holst G, Wolfbeis OS (2000) Luminescence lifetime imaging of oxygen, pH, and carbon dioxide distribution using optical sensors. Appl Spec 54:548-559.

14. Yim, Jeffrey B., Hubbard, Todd W., Melkerson, Lori D., Sexton, Michael A., and Fieggen, Bruce M. (1991) Configuration fiber-optic blood gas sensor bundle and method of making. US 5,047,627.

15. Gehrich JL, Lubbers DW, Opitz N, Hansmann DR, Miller WW, Tusa JK, Yafuso M (1986) Optical fluorescence and its application to an intravascular blood gas monitoring system. IEEE Trans Biomed Eng 33:117-132.

16. Schiza MV, Nelson MP, Myrick ML, Angel SM (2001) Use of a 2D to 1D dimension reduction fiber-optic array for multiwavelength imaging sensors. Appl Spectrosc 55:217-226.

17. Ferguson JA, Healey BG, Bronk KS, Barnard SM, Walt DR (1997) Simultaneous monitoring of pH, CO2 and O2 using an optical imaging fiber. Anal Chim Acta 340:123-131.

18. Wolfbeis OS, Weis LJ, Leiner MJP, Ziegler WE (1988) Fiber-optics fluorosensor for oxygen and carbon dioxide. Anal Chem 60:2028-2030.

19. McEvoy, A. K., MacCraith, B. D., McDonagh, C., and von Bueltzingsloewen, C. (2010) Optical CO_2 and combined O_2/CO_2 sensors. WO/2004/077035.

20. Schroeder CR, Neurauter G, Klimant I (2007) Luminescent dual sensor for time-resolved imaging of pCO_2 and pO_2 in aquatic systems. Microchim Acta 158:205-218.

21. Sanchez-Barragan I, Costa-Fernandez JM, Sanz-Medel A, Valledor M, Campo JC (2006) Room-temperature phosphorescence (RTP) for optical sensing. TrAC, Trends Anal Chem 25:958-967.

22. Palma AJ, López-González J, Asensio LJ, Fernandez-Ramos MD, Capitan-Vallvey LF (2007) Microcontroller-Based Portable Instrument For Stabilised Optical Oxygen Sensor. Sens Actuators B 121:629-638.

23. Trettnak W, Gruber W, Reininger F, Klimant I (1995) Recent progress in optical oxygen sensor instrumentation. Sens Actuators B 29:219-225.

24. Hauser PC (1995) A solid-state instrument for fluorescence chemical sensors using a blue light-emitting diode of high intensity. Meas Sci Technol 6:1081-1085.

25. Choi MF, Hawkins P (1995) A novel oxygen and/or carbon dioxide-sensitive optical transducer. Talanta 42:483-492.

26. Carvajal MA, Perez de Vargas Sansalvador IM, Palma AJ, Fernandez-Ramos MD, Capitan-Vallvey LF (2010) Hand-held optical instrument for CO2 in gas phase based on sensing film coating optoelectronic elements. Sens Actuators B B144:232-238.

27. Bansal AK, Holzer W, Penzkofer A, Tsuboi T (2006) Absorption and emission spectroscopic characterization of platinum-octaethyl-porphyrin (PtOEP). Chem Phys 330:118-129.

28. Palma AJ, Lopez-Gonzalez J, Asensio LJ, Fernandez-Ramos MD, Capitan-Vallvey LF (2007) Open Air Calibration with Temperature Compensation of a Luminescence Quenching-Based Oxygen Sensor for Portable Instrumentation. Anal Chem 79:3173-3179.

29. Perez de Vargas-Sansalvador IM, Carvajal MA, Roldan-Munoz OM, Banqueri J, Fernandez-Ramos MD, Capitan-Vallvey LF (2009) Phosphorescent sensing of carbon dioxide based on secondary inner-filter quenching. Anal Chim Acta 655:66-74.

30. Amao Y, Komori T, Nishide H (2005) Rapid responsible optical CO_2 sensor of the combination of colorimetric change of a-naphtholphthalein in poly(trimethylsiliylpropyne) layer and internal reference fluorescent porphyrin in polystyrene layer. React Funct Polym 63:35-41.

31. Capitan-Vallvey LF, Asensio LJ, Lopez-Gonzalez J, Fernandez-Ramos MD, Palma AJ (2007) Oxygen-sensing film coated photodetectors for portable instrumentation. Anal Chim Acta 583:166-173.

Capítulo 5

Sensor portátil para dióxido de carbono basado en un sistema de membranas intercambiables para aplicaciones industriales

Planteamiento

Este capítulo fue desarrollado en la Dublin City University como resultado de la estancia predoctoral que llevé a cabo en el National Centre for Sensor Research dentro del grupo de investigación "Adaptive Sensors Group" dirigido por el Profesor Dermot Diamond.

El propósito de esta estancia fue aprender la técnica PEDD (Paired Emitter-Detector Diode) desarrollada por el grupo de investigación citado para ser utilizada en medidas de absorción de radiación en sensores. Esta técnica está basada en el concepto de que un LED puede funcionar tanto como fuente de luz o como detector.

Esta nueva técnica para el desarrollo de instrumentación optoelectrónica emplea dos LED, funcionando uno como fuente de luz y el otro como detector de la misma. La fotocorriente generada por el LED y modificada por la muestra se descarga a una velocidad proporcional a la intensidad de luz que le ha llegado y se mide con un circuito sencillo. Por tanto, en lugar de medir la fotocorriente generada directamente, lo que es difícil por su pequeño valor, se utiliza un circuito para la medida del tiempo necesario para que la fotocorriente generada por el LED emisor descargue el LED detector. De esta manera se origina una salida digital directamente sin necesidad de usar un conversor A/D o un amplificador operacional.

Esta estrategia muestra una buena sensibilidad, bajo consumo de energía, bajo coste y, por último, buena exactitud y relación S/N. Esta configuración ha sido implementada por ese grupo en diversas plataformas. Una de ellas usa una sonda preparada a partir de dos LED fusionados para lo que se emplean dos LED idénticos cortados y pegados juntos formando un ángulo de 90º de forma que se evite que un LED ilumine al otro. La presencia de especies absorbentes de radiación en la disolución donde se encuentra la sonda, modifica la luz que procedente del LED emisor llega al detector [1]. Un segundo diseño consiste en una rueda de LED que cubren el rango espectral deseado, un LED IR en el centro de ellos como detector y una celda para la muestra a medir cubierta con un reflector en la parte superior. El empleo de

técnicas de multicalibracion se ha usado para la resolución de mezclas binarias y ternarias de colorantes con errores promedio en torno al 6% [2].

En el caso de realizar el reconocimiento óptico del analito, bien por transmisión o por reflexión, mediante una reacción química de tipo reversible, se pueden situar los reactivos en una película delgada que se incluye dentro del instrumento usando diferentes estrategias. Así se puede colocar sobre un soporte inerte, como en el caso del indicador de frescura de pescado basado en el carácter básico de los compuestos aminados que se forman por putrefacción de pescado desarrollado por Diamond *et al*. [3]. En este caso se usa un instrumento que mide reflectancia basado en LED entre los que se sitúa la membrana sensora preparada por *spin coating* sobre un disco de PET. Este mismo principio de reconocimiento, un indicador ácido-base inmovilizado, se ha usado como sensor visual para empaquetado inteligente [4]. Aquí una membrana plastificada de acetato de celulosa conteniendo verde de bromocresol responde linealmente hasta 15,0 mg/l, expresado como amoniaco, con una precisión del 4% (RSD).

Una segunda posibilidad es colocar la película sensora directamente sobre los elementos optoelectrónicos. Este es el caso del detector colorimétrico de amoniaco basado nuevamente en la técnica PEDD en el que se sitúa la película sensora, compuesta por p-nitrofenilnitrosamina en PVC, por *drop coating* sobre un LED de montaje superficial. El empleo de un LED emisor verde de 574 nm permite desarrollar un procedimiento para medir entre 5 y 15 mg/l [5].

La impresión de la membrana sensora directamente sobre la lente del LED origina un sustancial aumento de precisión [6]. Así ocurre para el caso de un instrumento portátil para la medida de ácido acético gaseoso basado en una configuración PEDD con una membrana de azul de bromofenol como par iónico con bromuro de tetrahexilamonio en etil celulosa. La precisión mejora desde un 68% preparada por *drop coating* hasta un 5,6 por impresión por chorro. Este sensor para ácido acético se ha usado para diseñar una red de sensores

inalámbricos pata la detección y seguimiento en tiempo real de una pluma de ácido acético [7].

En este capítulo de la Tesis doctoral se va a desarrollar una instrumentación portátil para la medida de dióxido de carbono basada en la técnica PEDD.

Con este propósito se ha diseñado un prototipo diferente de los anteriormente reseñados en el que se utilizaron cuatro LED, enfrentados dos a dos, con lo que finalmente hay dos canales de medida, uno de ellos utilizado para la medida de dióxido de carbono y otro como canal de referencia. Estos LED se montaron sobre una pieza de LEGO, pensada para poder variar la distancia existente entre los LED. Además esta pieza consta de un portamembranas, que es una ranura donde se sitúa la membrana al objeto de dejarla completamente fija.

Se optó por depositar las membranas sensoras sobre un soporte plástico (diseñado mediante el software Autocad, Autodesk, Spain), en lugar de sobre los componentes electrónicos como en capítulos anteriores, debido a que los LED son más difíciles de reemplazar y así se hace un sistema más cómodo de uso, ya que hay que reemplazar con cierta frecuencia los soportes con la química de reconocimiento inmovilizada sobre ellos.

Se estudian dos tipos de configuraciones, una en la que tenemos por un lado el sistema que venimos utilizando y que contiene PtOEP y por otro el segundo cóctel citado con anterioridad que contiene el indicador de pH. Para ello se depositan cada uno en caras opuestas del soporte. En la segunda configuración solo vamos a utilizar el indicador de pH. En ambas configuraciones medimos dióxido de carbono basándonos en las propiedades ácidas de este, lo que provocará cambios en el pH del medio y por tanto en el color del indicador ácido-base que dejará pasar más o menos radiación proveniente de PtOEP (configuración 1) o bien del propio LED emisor rojo (configuración 2).

Dependiendo de la configuración utilizada usaremos diferentes LED como fuentes de radiación. En el primer caso un LED verde, para excitar la

fosforescencia del PtOEP y en el segundo caso un LED rojo. Como LED detector se va a utilizar siempre un LED rojo. El uso de diferentes LED dependerá de las longitudes de onda de emisión y excitación de las sustancias que estamos utilizando en la química de reconocimiento.

En base a los resultados obtenidos se elegirá la configuración óptima para el reconocimiento de dióxido de carbono con este prototipo LED-LED y pasaremos a caracterizar el instrumento considerando tanto aspectos instrumentales como es la distancia LED-LED a el modelado de la respuesta y la caracterización analítica del instrumento portátil.

A NEW LED-LED PORTABLE CO_2 GAS SENSOR BASED ON AN INTERCHANGEABLE MEMBRANE SYSTEM FOR INDUSTRIAL APPLICATIONS

I.M. Pérez de Vargas-Sansalvador[a], C. Fay[b], T. Phelan[b], M.D. Fernández-Ramos[a], L.F. Capitán-Vallvey[a,], D. Diamond[b], F. Benito-Lopez[b,*]*

[a] ECsens. Department of Analytical Chemistry, Faculty of Sciences, Campus Fuentenueva, University of Granada, E-18071 Granada, Spain

[b]CLARITY: Centre for Sensor Web Technologies, National Centre for Sensor Research, Dublin City University, Dublin 9, Ireland

Abstract

A new system for CO_2 measurement (0-100%) based on a paired emitter-detector diode arrangement as a colorimetric detection system is described. Two different configurations were tested: *configuration 1* (an opposite side configuration) where a secondary inner-filter effect accounts for CO_2 sensitivity. This configuration involves the absorption of the phosphorescence emitted from a CO_2-insensitive luminophore by an acid-base indicator and *configuration 2* wherein the membrane containing the luminophore is removed, simplifying the sensing membrane that now only contains the acid-base indicator. In addition, two different instrumental configurations have been studied, using a paired emitter-detector diode system, consisting of two LEDs wherein one is used as the light source (emitter) and the other is used in reverse bias mode as the light detector. The first configuration uses a green LED as emitter and a red LED as detector, whereas in the second case two identical red LEDs are used as emitter and detector. The system was characterised in terms of sensitivity, dynamic response, reproducibility, stability and temperature

influence. We found that configuration 2 presented a better CO_2 response in terms of sensitivity.

Key words. Carbon dioxide sensor; Gas sensor; Optical sensor; Paired emitter detector-diode sensor; Portable instrumentation.

* Corresponding authors:

Prof. Luis Fermin Capitán-Vallvey, Department of Analytical Chemistry, University of Granada, Faculty of Sciences, Avda. Fuentenueva s/n, E-18071 Granada, Spain, Tel.: +34 958248436, Fax: +34 958 243 328, E-mail: lcapitan@ugr.es.

Dr. Fernando Benito-Lopez, CLARITY: Centre for Sensor Web Technology, National Centre for Sensor Research, Dublin City University, Glasnevin, Dublin 9, Dublin-Ireland, Tel.: + 353 1 700 7603, Fax: + 353 1 700 7995, E-mail: fernando.lopez@dcu.ie.

Enviado para su publicación a la revista Analytica Chimica Acta (Ms. No.: ACA-11-600) y actualmente en revisión por los autores (*major revision*).

1. INTRODUCTION

CO_2 is an important industrial gas for many different uses that include production of chemicals (e.g. urea), inert agent for food packaging (to extend the shelf-life of meat, cheese, etc.), beverages, refrigeration systems, welding systems, fire extinguishers, water treatment processes, and many other smaller scale applications [8,9].

In the agro-food industry CO_2 is widely used in modified-atmosphere packaging where its task is to inhibit growth of spoilage bacteria [10,11]. For instance, in active packaging technologies a CO_2 generating system can be considered as a technique complimentary to oxygen scavenging [12]. High CO_2 levels (10-80 %) are desirable for foods such as meat and poultry in order to inhibit surface microbial growth and to extend their lifetime. The maintenance of CO_2 concentration within packages in food [13], as for instance using inserted sachets [14,15], must be carefully monitored since CO_2 permeability is 3-5 times higher than that of oxygen for most of the plastic films and because CO_2 is absorbed by many foods like meat and poultry.

Real-time process monitoring is fundamental for effective process control [16-19]. The rapid development of bioprocess applications together with the agro-food industry have led to an intensive search for new sensors capable of providing real-time information about the state of the processes.

Conventional methods for CO_2 determination include, among others, infrared spectrometry [20] or electrochemical sensors based on liquid (Severinghaus-type electrodes) or solid electrolytes [21,22]. The most popular sensors used for CO_2 gas sensing in biotechnological applications are based on electrochemical measurements that can be prepared with different materials. Optical based CO_2 sensors, with low limits of detection, find applications in a variety of industrial processes, environmental monitoring, pollution control, biotechnology and within the food industry [23]. They are based on the Lewis acid character of CO_2 that, through reaction with the Lewis donor water, causes a change in pH that can be monitored using absorbance or fluorescence-based pH indicators. Typically, the acid-base indicators are immobilised in so-called

solid sensor membranes [24], made from gas-permeable polymers such as ethyl cellulose [25], sol-gels [26], silicones [27], composite materials [28] or directly attached to the tip at the end of, or in the core, of an optical fiber [29]. In addition to indicator, the membrane often contains quaternary ammonium hydroxide [30] and/or room-temperature ionic liquids [31,32] for ion pairing with the basic form of the pH indicator, and to provide the water that is needed to form the hydrated ionic pair to uptake the CO_2 from the atmosphere, by forming a lipophilic hydrogencarbonate buffer.

Sensing CO_2 schemes based on luminescence typically result in higher sensitivity than those based on absorption or reflection, although the small number of luminescent acid-base indicators require other strategies such as FRET (fluorescence resonance energy transfer) from an inert fluorescent dye to a colorimetric acid-base indicator, converting the color change in intensity or lifetime information [24,26,33]. An interesting example in food industry applications is the use of a fluorescence sensor, hydroxypyrene trisulphonate, for the measurement of CO_2 in modified atmosphere packaging by a dual luminophore referencing sensing scheme [34,35].

However, portable instruments for CO_2 detection tend to employ luminescence lifetime-measurements because of their advantages (photobleaching or leaching of the dye, intrinsic sample fluorescence, changes in the light source intensity do not affect the signal) over intensity-based schemes. Phase modulation techniques can be used to implement lifetime-based measurement in portable instrumentation based on phase measurement electronics in conjunction with LEDs and photodiodes [36-39].

Another strategy for CO_2 sensing is based on a colour change conversion to luminescence. It exploits a secondary inner-filter effect of a long lifetime luminophore dye, platinum octaethyl-porphyrin, inmobilised on PVCD (poly (vinylidene chloride-co-vinyl chloride) membranes, by a pH indicator, α-naphtholphthalein. It is implemented in a portable instrumentation with both optoelectronic components coated with sensing chemistry (LED with the

luminophore and photodetector with the pH-active dye) [40], and later integrated into a multi-analyte platform for oxygen and CO_2 [41].

Contributing factors from both the chemical layer fabrication process and the optical detection system have significant impact on the sensitivity and reproducibility of the sensing device. By employing the most suitable optical detection method sensitivity issues can be addressed. Methods such as charge coupled devices [42], light wave multimeters [30], flat bed scanners [43-45] and photodiodes [3,4,46] have been explored previously. While functional, not all are suitable for the applications outlined earlier in terms of practicality, portability and scalability. Previous reports by Lau [47], Shepherd [7] and O'Toole *et al.* [6] have reported the advantages of implementing a paired emitter-detector diode (PEDD) arrangement as a colorimetric chemical detection system. A PEDD system consists of two LEDs wherein one is used as the light source (emitter) and the other is used in reverse bias as the light detector.

In this paper we explore the PEDD method along with the α-naphtholphthalein-platinum octaethylporphyrin chemistry to develop a portable, low-power optical system for CO_2 detection. In this technique the photocurrent generated by the emitter LED and later modified by the sample, discharges the detector LED at a rate which is related to the intensity of light that reaches the detector, which can be tracked by a simple microprocessor circuit. Therefore, instead of measuring the photocurrent directly, a simple timer circuit is used to measure the time taken for the photocurrent generated by the emitter LED to discharge the detector LED to give a digital output directly without using an A/D converter or operation amplifier [1,5,48].

2. EXPERIMENTAL

Reagents, materials and apparatus

The reagents used were platinum octaethylporphyrin complex (PtOEP, Porphyrin Products Inc., Logan, UT, USA), tributyl phosphate (TBP), α-naphtholphthalein, and tetraoctyl ammonium hydroxide (TOAOH; 0.335 M in

methanol) all from Sigma–Aldrich Química S.A. (Madrid, Spain). The solvents used, tetrahydrofuran (THF), toluene and ethanol, were supplied by Sigma as well. PVCD (particle size 240-320 μm) and ethylcellulose (EC, ethoxyl content 49%), were obtained from Sigma. All cocktails were prepared by weighing the chemicals with a DV215CD balance (Ohaus Co., Pine Brook, NJ, USA) which had a precision of ±0.01 mg. The gases CO_2 and N_2 were of a high purity (>99%) and were supplied in gas cylinders by Air Liquid S.A. (Madrid, Spain).

The interchangeable membrane platform was fabricated using a laser ablation system-excimer/CO_2 laser, Optec Laser Micromachining Systems, Belgium and a laminator system Titan-110, GBC, USA. 150 μm PMMA (poly(methylmethacrylate)) sheets were purchased from Goodfellow, UK; 50 μm double-sided pressure sensitive adhesive film (AR8890) was obtained from Adhesives Research, Ireland and Mylar-type polyester from Goodfellow, UK.

The red LEDs used were obtained from Digi-Key, Ireland Part No. 67-1612-ND and the green LED, L-7113GC was obtained from Kingbright manufacture, Radionics.

Portable electronic instrument and signal processing

The realisation of a PEDD instrument for this study consisted of two key elements: 1) Mechanical testing rig; 2) Electronics and control.

Firstly, a test rig was constructed to ensure the accurate alignment of the two LED pair channels, the secure placement of the chemical sensing membrane and to investigate the effect of the distance between the emitter and detector LEDs. Figure 1 illustrates the experimental setup. The membrane housing (constructed using a Dimension SST 768 rapid prototyper) contained two sensing chambers wherein each was fitted with one LED emitter/detector pair. The rig was designed with a reference channel (with nothing between the emitter and the detector) coupled with an active channel (equipped with the optical sensing layer). This setup allows to correlate the detectors and accounts for any potential noise effects. Alternatively, reference channel allows performing two parallel measurements to investigate batch processing.

Furthermore, the chambers were designed with hollow through-hole sections to allow for a flow of gas to react with the sensing membrane. The LEDs were polished and flattened down, and placed within threaded housings, so that the rotation of the housing inside the tapped holder varied the distance between the emitter and the detector. The distance was adjusted by inserting different sized washers, each of a pre-set designed thickness. Finally, the membrane holder allows the sensing surface to be directly aligned with both the emitter and detector LEDs. This design was chosen in order to enable the distance between the emitter and detector to be accurately adjusted.

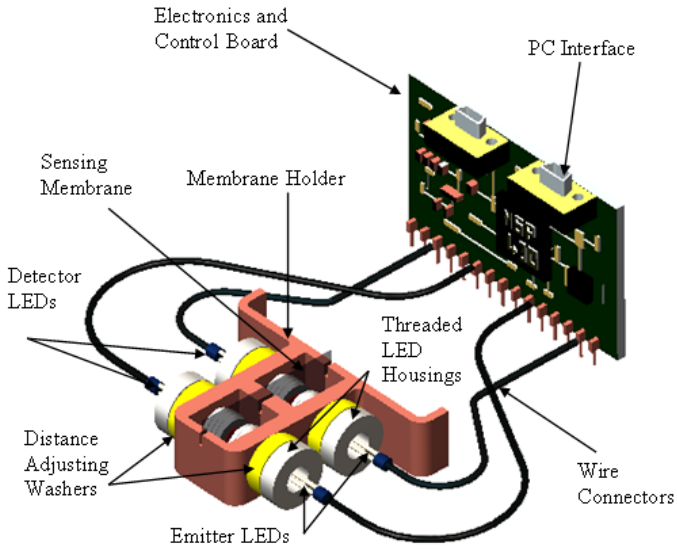

Figure 1. Instrumentation setup for the PEDD system. The sensing membrane, equipped with the chemical sensing layer, is held in place by the Membrane Holder and aligned on one axis with the detector/emitter LEDs for absorbance measurements. The LED distances are adjusted via screw threads and/or washers. The control board connects via shielded wiring to the LEDs and reports the measurement values to a PC via the PC interface.

An appropriate electronic design was put in place to realise the operation of a PEDD analysis system. Figure 2 shows that the microcontroller

has full control over the operational timing of both detector and emitter LEDs (via IO ports).

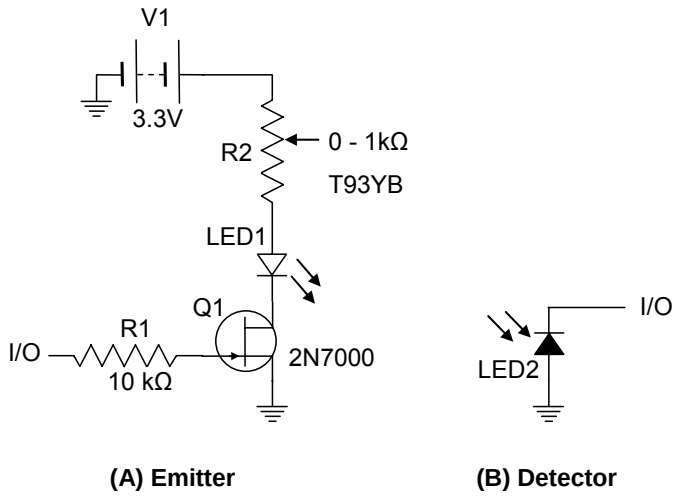

Figure 2. Electronic design for the LED emitter and detector system connected to input output (I/O) ports on the MSP430F449 micro-controller. (A) Emitter electronic and control design showing the LED light source powered by a 3.3V regulator, protected by an adjustable resistor (VISHAY T93YB 0-1kΩ Trimmer) and controlled by a NFET transistor (STMICRO-ELECTRONICS NFET 2N7000) via a micro-controller pin. (B) Detector electronic design showing how the cathode of the LED is charged and analysed by an IO pin on the micro-controller.

The measurement procedure was programmed as follows:

1. Set the software counter variable to 0;
2. Set the detector IO pin to output mode;
3. Charge the detector LED's internal capacitance (cathode), by setting the IO output register high (i.e. 3.3V);

4. Switch the IO register to input mode once the LEDs capacitance is fully charged;

5. Set the emitter IO high to turn on the emitter LED;

6. Check over a fixed number of processor counts (in this case 65535) and increment the software counter if the IO pin's state is above the logic threshold;

7. Output the counter value to the PC;

8. Set the emitter IO low to turn off the emitter LED;

9. Repeat the process i.e. go to step 1.

The number of counts above the threshold is proportional to the time required to discharge the detector LED to the pre-set threshold. This process was repeated and the microcontroller was programmed in a never-ending loop to achieve this. Finally, the output-sampling rate was set at 1 data point per second.

Subsequently, the chemical sensing layer was initially exposed to two extremes i.e. 100% N_2 and 100% CO_2 where the dynamic range of the detector was maximised by adjusting the variable resistor on the emitter LED (see Figure 2), which in turn maximised the resolution.

To determine the optimum distance between emitter LED and detector LED when using the prototype instrument, a study of its response at different distances to 100% N_2 (t_0) and 100% CO_2 (t_{100}) was carried out. The distances studied were measured from the tip of one LED to the tip of the other, as explained above.

The t_0-t_{100} signal increases with distance up to 0.7 mm because of the quantity of light that reaches the detector LED decreases taking into account their viewing angle and thus increasing the discharge time. The optimum operation distance was selected to be 0.7 mm (Figure 3) because the corresponding signal was the largest and independent of the LED-LED distance.

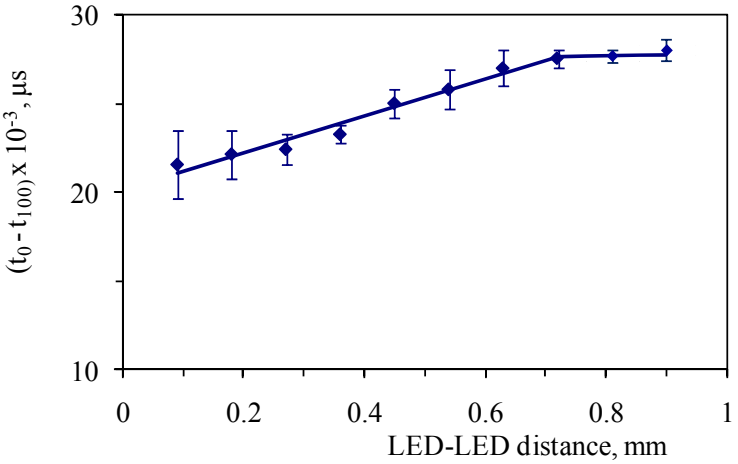

Figure 3. Influence of LED-LED distance in the instrument on t_0-t_{100} value.

Sensing interchangeable membranes preparation

In order to give an extra degree of freedom to the device and therefore provide easy handling of the membranes during preparation and subsequent device integration, it was decided to fabricate an interchangeable membrane support that contains both sensing membranes. The platform was easily fabricated in poly(methyl methacrylate), pressure-sensitive adhesive and Mylar in five layers designed in AutoCAD (2002), cut using CO_2 laser and laminated, see Figure 4.

Configuration 1: Sensing membranes with luminophore for CO_2 were prepared from cocktails A and B. Cocktail A contains 100 mg of PVCD dissolved in 1 mL of freshly distilled THF, using an ultrasonic bath, and 0.5 mg PtOEP. Cocktail B has 64 µL TBP, 320 µL of a solution containing 2.2 mg of α-naphtholphthalein in 2 mL of toluene/EtOH (80:20 v/v), 1 mL of toluene containing 60 mg of previously dissolved EC, and 200 µL of 0.335 M TOAOH. The sensor preparation consists of the casting on one side of the support with 10 µL of cocktail A. After that, the support was left to dry in darkness in a

desiccator that had a saturated THF atmosphere for 1 h at room temperature. The prepared PtOEP membranes need to be cured in darkness for 9 days before continuing the preparation. Then, 10 µL of cocktail B was casted on the opposite side of the support with the aid of a micropipette, followed by drying in darkness under vacuum in a desiccator for 12 h at room temperature. The supports were kept in the desiccator in darkness at 94% RH atmosphere (20±0.5ºC). The separation between the two membranes is defined by the thickness of the Mylar, 250 µm.

Configuration 2: Sensing membranes without luminophore were prepared by casting 10 µL of cocktail B onto the support, and dried and stored as indicated above.

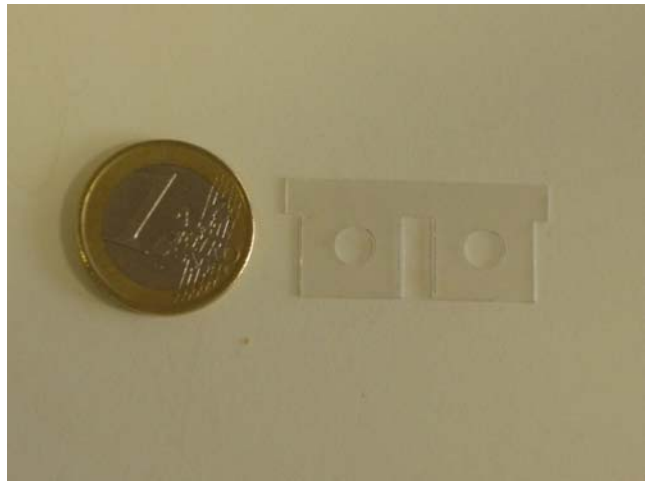

Figure 4. Interchangeable sensing membranes.

Measurement conditions

The standard mixtures for instrument calibration and characterization were prepared using N_2 as the inert gas by controlling the flow rates of the different high purity gases CO_2 and N_2, entering a mixing chamber using a

computer-controlled mass flow controller (Air Liquid España S.A., Madrid, Spain) operating at a total pressure of 760 Torr and a flow rate of 500 $cm^3 \cdot min^{-1}$. For the preparation of gas mixtures lower than 2% in CO_2, a standard mixture of 5% CO_2 in N_2 was used, with the lowest CO_2 concentration tested being 0.1%. For the portable instrument characterization, the measurements were performed after equilibration of the instrument atmosphere for 2 min with the gas mixtures obtained with the gas blender.

All measurements were replicated eight times to check for experimental error. A homemade thermostatic chamber, with a lateral hole for the connexion to a computer and gas tubing entrance, made it possible to maintain a controlled temperature between −50 ºC and +50 ºC with an accuracy of ±0.5 ºC for thermal characterization of the sensor.

3. RESULTS AND DISCUSSION

Optical response of Sensing Membranes

The optical response of the sensor upon exposure to CO_2 is based on its reaction with the deprotonated form of α-naphtholphthalein (N^-) that is as an ion-pair with tetraoctyl-ammonium (TOA^+) according to:

$$TOA^+N^- \cdot xH_2O + CO_2 \xleftrightarrow{K} TOA^+HCO_3^- \cdot (x-1)H_2O \cdot HN \qquad \text{(Eq. 1)}$$

where $TOA^+N^- \cdot xH_2O$ is the hydrated ion pair and K the equilibrium constant.

Two different systems were tested in order to find the best conditions to measure CO_2 via the PEDD technique. In the first case, a secondary inner-filter effect accounts for CO_2 sensitivity, as demonstrated previously [40]. It involves the absorption of the phosphorescence emitted from the CO_2-insensitive luminophore (PtOEP) (λ_{exc} 537 nm, λ_{em} 650 nm) by the basic form of α-naphtholphthalein (λ_{max} 655 nm). This means that a green LED (527 nm) should

be used to excite PtOEP that emits around 650 nm therefore the emitted radiation is effectively absorbed by the basic form of the indicator (Figure 5). Consequently, a red LED (657 nm) must be used as detector. The increase in CO_2 concentration displaces the equilibrium to the acid form of the indicator (λ_{max} 310 nm) increasing the amount of light, from PtOEP phosphorescence, that strikes the detector LED. This reduces the measured discharge time t, which is in turn related to the concentration of the target species.

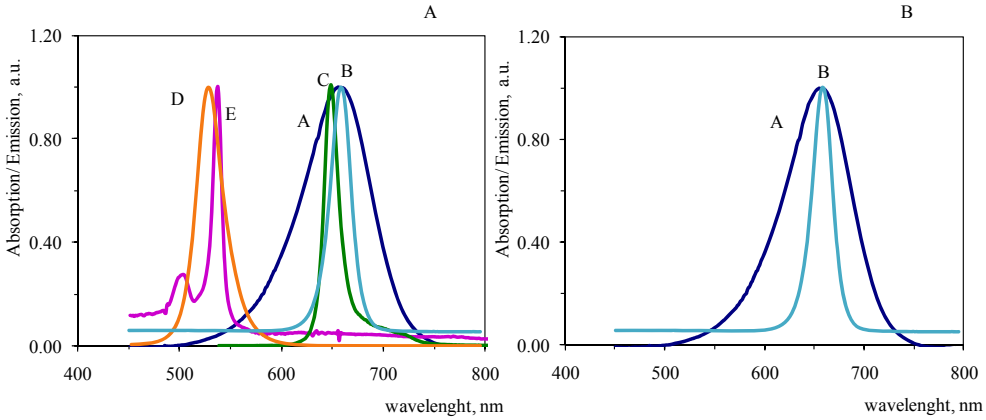

Figure 5. Spectral properties of the dyes used in the CO_2 sensing membranes and the excitation source (normalised spectra). Fig.1A. Excitation (E) and phosphorescence emission spectra (C) of PtOEP membrane; (A) absorption spectrum of basic form of α-naphtholphthalein;(D) emission spectra green LED and (B) emission spectra of red LED. The figure shows the overlapping of donor and acceptor spectra. Fig. 4B. (A) Absorption spectrum of basic form of α-naphtholphthalein and (B) emission spectra of red LED.

The opposite side configuration for both luminophore and pH indicator membranes is used to prevent the observed degradation of the PtOEP complex in the presence of the phase transfer agent, TOAOH. However, degradation is observed even if the platinum complex is included in microparticles [40]. Additionally, the immobilization of PtOEP in oxygen-insensitive PVCD membrane prevents their quenching by oxygen at atmospheric level.

In the second system tested, the membrane containing the luminophore PtOEP is eliminated, simplifying the sensing membrane that now only contains the acid-base indicator, reducing cost and completely avoiding the interference of O_2 upon the phosphorescence of the PtOEP complex. This second system is formed by mounting two identical red LEDs (657 nm) facing each other, with the holder containing the indicator membrane placed between the two LEDs

Instrument response to carbon dioxide

Both sensing membrane systems respond to CO_2 through variations of the ratio of protonated to deprotonated forms of the α-naphtholphthalein indicator which generate corresponding changes in the discharge time of the reverse biased detector LED, which are related to the CO_2 concentration. Plotting the discharge time *versus* CO_2 percentage gives a decay function that can be fitted to the exponential function $y = y_0 + Ae^{-(x/t)}$ (configuration 1: R^2=0.9983, configuration 2: R^2=0.9845).

According to Mills *et al.* [49] the ratio of concentrations of protonated to deprotonated forms of indicator is proportional to CO_2 concentration:

$$\frac{\left[TOA^+HCO_3^- \cdot (x-1)H_2O \cdot HN\right]}{\left[TOA^+N^- \cdot xH_2O\right]} = K\left[CO_2\right] = \frac{A_0 - A}{A - A_{100}} \qquad \text{(eq. 2)}$$

where A_0 and A_{100} are the absorbance at 0 (deprotonated form) and 100 % CO_2 (protonated form), respectively, and A is the absorbance at any intermediate concentration.

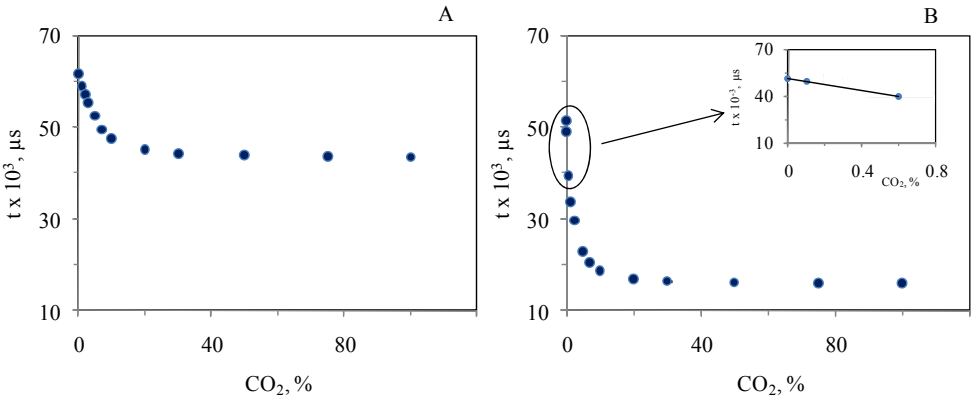

Figure 6. Response of the instrumental proto-type to CO_2. Discharge time *vs.* CO_2 percentage. A: configuration 1 and B: configuration 2. Inset: Experimental function used to calculate the LOD.

The absorbance was calculated from eq. 3 using the amount of light I reaching the detector and the amount I^0 in the absence of indicator membrane [1]. The value t^0 corresponds to the discharge time obtained in the absence of the indicator membrane and t to the discharge time of the membrane at any CO_2 concentration.

$$A = \log \frac{I^0}{I} = -\log \frac{t^0}{t} \qquad \text{(eq.3)}$$

From eq. 2 a linear relationship can be obtained with slope equal K and zero intercept. The deviations observed at higher CO_2 percentages can be attributed to non fulfillment of Beer's law due to use of a polychromatic light

source in this instrument. (Configuration 1: $\frac{A_0 - A}{A - A_{100}}$ = 0.1703[CO_2] – 0.0286; R^2= 0.9901; Configuration 2: $\frac{A_0 - A}{A - A_{100}}$ = 0.4467[CO_2] – 0.021; R^2 = 0.9857).

The slopes found show that a considerable difference in sensitivity exists between both configurations (configuration 2 is 2.6 times more sensitive than configuration 1).

Comparison between the two configurations studied

It is possible to use the above eq. 2 for calibration purposes although the linear response is limited up to *ca.* 5 %. Moreover to achieve a full calibration range, that could be included in the microcontroller of the instrument, an empirical equation was used based on a relative analytical parameter (named as R) based on the discharge time ($(t_{100} - t_0)/(t - t_0)$) *vs.* the inverse of CO_2 concentration. In this case t_0 and t_{100} are the values of discharge time at 0 and 100 % CO_2, respectively and t at any other concentration.

The limit of detection (LOD) of the instrumental procedure was obtained from exponential raw experimental data using the first three points at low CO_2 concentration because they can be adjusted to a straight line (Figure 6B inset) [50]. Using the critical level (s_0) in the signal domain (configuration 1: 50.91 μs; configuration 2: 108.73 μs) and the obtained adjustments (configuration 1: t = -2290.1[CO_2] + 61535; R^2=0.989; configuration 2: t = -19525[CO_2] + 51155; R^2=0.999) the LODs were calculated as usual by LOD = t_0 + 3 s_0, where t_0 is the average blank signal (previously defined) and s_0 is the critical level or standard deviation of the blank, which was determined from eight replicate measurements. The LODs found using this approach were 0.0082 % for configuration 1 and 0.0066 % for configuration 2 (notice that this value is less than normal atmospheric CO_2 concentration, which is ca. 0.04%).

The limit of quantification (LOQ) was obtained from the calibration function [51]. In this case the critical level s_0 is the standard deviation of t_0, the

discharge time at the LOQ as given by equation 4, and the analytical parameter at the LOQ (R_{LOQ}) as given by equation 5. Therefore, from the obtained R_{LOQ} and the calibration function the LOQ can be estimated as 5.9% and 2.6% CO_2 for configurations 1 and 2, respectively.

$$t_{LOQ} = t_0 - 10s_0 \quad \text{(eq. 4)}$$

$$R_{LOQ} = \frac{t_{100} - t_0}{10s_0} \quad \text{(eq. 5)}$$

The comparison between both configurations studied, in terms of signal range (t_0-t_{100}), and slope of calibration function, LOD and LOQ (Table 1) shows configuration 2 gives better performance. The difference between the behaviour of the two configurations can be explained by considering that the use of the luminiscent membrane in configuration 1 reduces the amount of light reaching the sensing membrane and hence the detector LED compared to configuration 2. Hence configuration 2 was selected for subsequent experiments.

Table 1. Comparison of signal range, slope, LOD an LOQ of the two sensing configurations studied.

	t_0-t_{100} (µs)	Slope	LOD (%)	LOQ (%)
Configuration 1	18,175	5.962	0.0082	5.86
Configuration 2	35,358	1.379	0.0066	2.67

Analytical characterization

The dynamic response of the sensing membranes when exposed to alternating atmospheres of pure CO_2 and pure nitrogen was carried out as shown in Figure 7. The response time was calculated from between 10% and

90% of the maximum signal, returning a value of 11 ± 1 s and, the recovery time from 90% to 10% which was found to be 55 ± 5 s.

In addition, the response and recovery behaviour of the CO_2 sensing membrane was studied at different intermediate CO_2 concentrations (0, 1, 3, 7, 20, 100% CO_2). In all cases, the signal changes were fully reversible and hysteresis was not observed during the measurements.

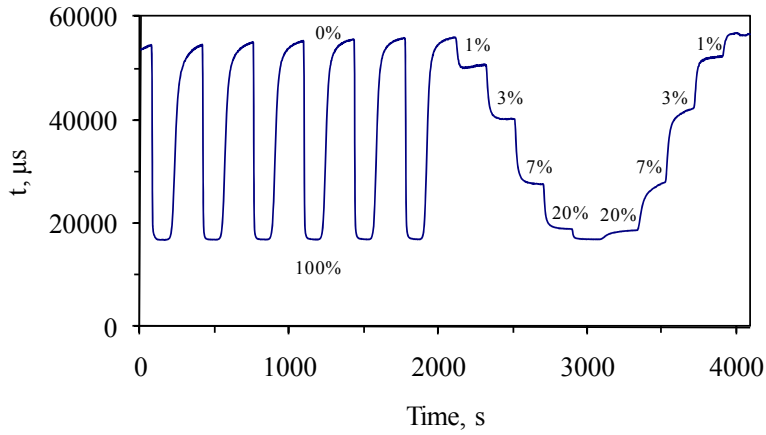

Figure 7. Dynamic response of the portable instrument to changes in CO_2 concentration from 0% to 100%. Response characteristics at 1, 3, 7, 20 and 100% CO_2.

The response and recovery times are lower than those obtained for other systems developed by us [40,41,52], especially the recovery time, which was half of that obtained before. The response and recovery times obtained here are comparable and even lower than other sensing schemes widely used for CO_2 sensing [53-55].

The precision of proposed prototype was measured by studying the intra-day reproducibility. Five measurements at 100% N_2 and 100% CO_2 were

performed using the same membrane at 45 minutes intervals with 8 replicates each. A good reproducibility with a relative standard deviation of 1.15% was obtained for t_0-t_{100}.

Stability is a very important characteristic to take into account in a sensor, and even more so if this device is going to be used for industrial applications. Stability was studied by means of an inter-day reproducibility measuring t_0 and t_{100} (with the same membrane as in the intra-day study) repeated for 5 days in a row (n=8 per day). The inter-day relative standard deviation was 1.77%, in good agreement with our previous study of the stability of α-naphtholphthalein membrane, in which a one year long-term stability of the indicator membrane was demonstrated when stored under 94% RH conditions [52].

Temperature has a considerable influence on the sensitivity of CO_2 sensors based on CO_2 acid-base character [49,56]. Therefore, we studied the thermal dependence of the sensing membranes by acquiring the calibration function at temperatures between 5 ºC and 30 ºC. From this study, we observed a decrease in sensitivity with increasing temperature (Figure 8), which can be attributed to the inverse dependence of the CO_2 solubility in the indicator layer on the temperature [57].

By using eq. 2 and 3 the value of K was calculated for each temperature (Figure 9) and the resulting ln K *vs.* T^{-1} (Kelvin degrees) plot up to 5% CO_2 was linear (R^2 = 0.995, Inset figure 6) yielding a ΔH value of -142 KJ/mol and a ΔS of -208 J/mol·K. Here $\Delta G<0$, that means that the reactions are spontaneous, due to the large negative ΔH value as was observed previously with similar sensors [49,58].

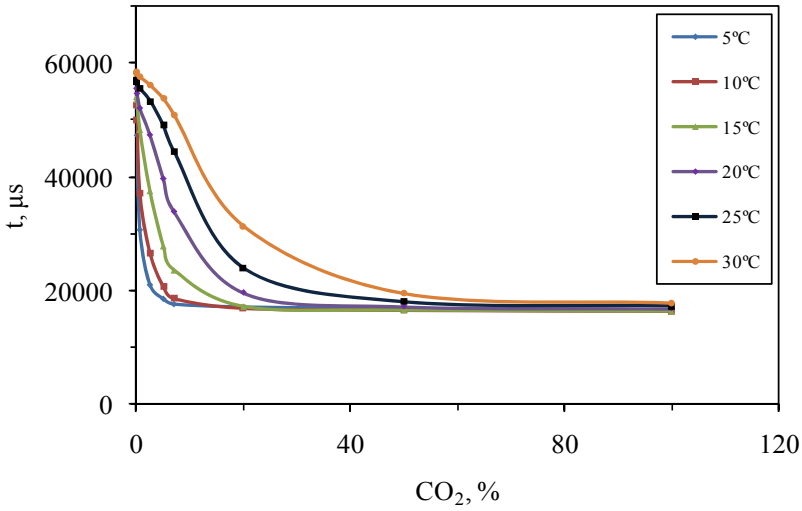

Figure 8. Temperature influence on the response of the sensing membrane at 5, 10, 15, 20, 25 and 30 ºC

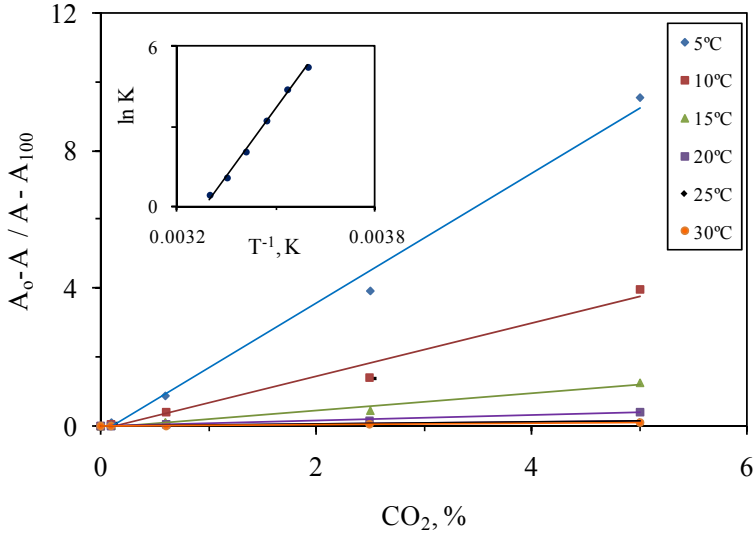

Figure 9. Thermal dependence of the sensing membranes. Main section: Plots of $\frac{A_0 - A}{A - A_{100}}$ *vs.* CO_2 percentage at each temperature studied (5-30ºC). Inset: plot of lnK *vs.* T (K) over the temperature range studied.

This sensor is sensitive to different gases with acid-base properties in addition to CO_2, like all sensing strategies for this gas based on acid-base transduction so they will cause interference in measurements. In a previous paper we studied the interference of O_2, CO HCl, SO_2, NO_2 and acetic acid [40].

Table 2 shows the comparison between both configurations of the sensing device presented here with different optical CO_2 sensing devices in literature.

Table 2. Comparison of performance of proposed instrument for CO_2 with literature.

Instrument type	Sensing membrane	Range (%)	LOD (%)	Remarks	Ref.
Commercial dedicated	HPTS	1-25	-	Ysi 8500 carbon dioxide monitor	www.ysi.com
Dedicated	HPTS in ethyl cellulose	<2	-	LED-based solid state instrument	[59]
Dedicated	PtOEP – α-naphtholphthalein	<100	0.02	Instrument with coated optoelectronic components	[52]
Multianalyte platform	HPTS sol-gel	<100	<1	CCD imaging	[38]
Multianalyte platform	HPTS	<10	---	Phase modulation technique. DLR scheme	[39]
Multianalyte platform for blood gases	Ru(II) chelate complex	---	---	Portable device fluorescence decay time based	[36]
Non dedicated	HPTS in ethyl cellulose	<100	---	B&W CCD camera	[60]
Multianalyte device	HPTS in ethyl cellulose	<10	---	Sensor array on flexible substrate	[61]
Dedicated	Configuration 1	<100	0.0082	PEDD technique	Current study
Dedicated	Configuration 2	<100	0.0066	PEDD technique	Current study

HPTS: 1-hydroxypyrene-3,6,8-trisulphonate; DLR: Dual Luminophore Referencing technique

4. CONCLUSIONS

The instrumental design studied could form the basis of a versatile handheld instrument for industrial applications, capable of measuring very low CO_2 concentrations, to below atmospheric value, and up to 1%, due to the good precision achieved. In addition, a much broader CO_2 range (from 2.6 to 100%) can be measured by means a relative signal.

Two different configurations have been tested, with configuration 2 being the most sensitive. This configuration comprises two red LEDs, one LED working as emitter and the other one as detector. The interchangeable sensor layer only contains α-naphtholphthalein (the PtOEP membrane is eliminated) which brings advantages like simplification of the sensing membrane, reduced cost and avoidance of the O_2 interference on the analytical signal arising from phosphorescence of the PtOEP complex.

Some advantages of the PEDD arrangement include the simplicity of the resulting sensor and electronics, low cost, high resolution, and excellent sensitivity.

The device has been characterised in terms of sensitivity, dynamic response, reproducibility, stability and temperature influence.

The response and recovery times found were very fast in comparison with other devices based on the acidic nature of CO_2. The signals were fully reversible, and hysteresis was not observed during measurements. Moreover, good reproducibility and stability have been found. The temperature influence was studied and modelled; an expected behaviour was found for this prototype.

The characterisation suggests that overall this is a very promising sensor for monitoring CO_2. The main advantages of this device are ease of use, versatility, rapid response, and good sensitivity and the main disadvantage is the interference of acidic vapours.

ACKNOWLEDGEMENTS

We acknowledge financial support from the *Ministerio de Ciencia e Innovación, Dirección General de Investigación y Gestión del Plan Nacional de I+D+i* (Spain) (Projects CTQ2009-14428-C02-01 and CTQ2009-14428-C02-02); *Junta de Andalucía* (*Proyecto de Excelencia* P08-FQM-3535) and Science Foundation Ireland under grant 07/CE/I1147. These projects were partially supported by European Regional Development Funds (ERDF). I.M. Pérez de Vargas-Sansalvador wants to thank Junta de Andalucía for the grant "Estancias de Excelencia 3/2009"

5. CONCLUSIONES

En este capítulo hemos desarrollado una instrumentación portátil para medida de dióxido de carbono basada en la técnica PEDD.

Esta técnica ofrece una serie de ventajas frente a la comúnmente utilizada de LED-PD como puede ser simplicidad de la electrónica a emplear, bajo coste, alta resolución y muy buena sensibilidad.

De las dos configuraciones utilizadas, se eligió como óptima la segunda configuración, debido a que presentaba mejores resultados, además así se evita la posible interferencia del O_2 sobre el sistema y se aminoran costes debido a que se utilizan menos reactivos químicos.

Se ha comprobado que la respuesta del sistema instrumental estudiado, que se basa en las propiedades ácidas del CO_2, se ajusta a este modelo hasta un 5% de CO_2, concluyendo que las posibles desviaciones del mismo se deben a la luz policromática utilizada.

Dado que la respuesta directa del instrumento frente a la concentración de CO_2 presenta la forma de un decaimiento exponencial y con objeto de calibrar propusimos el uso de una nueva ecuación que permitiera un ajuste lineal para todo el rango estudiado.

Se ha demostrado que este equipo puede detectar dióxido de carbono por debajo del valor ambiental de este gas (LOD 0,0066%.), lo que es de gran interés ya que este es uno de los problemas tradicionales del sensado óptico del gas. El límite de detección se calculó a partir de los datos directos que genera el instrumento utilizando los primeros puntos que se pueden ajustar a una línea recta. El límite de cuantificación por su parte lo calculamos a partir de la función lineal de calibrado usada, obteniendo un valor del 2,6 % de CO_2.

Podemos concluir que nos encontramos ante un equipo versátil, que va a poder utilizarse de dos maneras según la cantidad de CO_2 que queramos detectar, puede utilizarse para detectar bajas concentraciones utilizando directamente los datos brutos que proporciona el equipo o bien, para un rango

mayor (2,6-100% CO_2), mediante el uso de la ecuación de calibración propuesta.

El equipo fue caracterizado en términos de sensibilidad, respuesta dinámica, precisión, estabilidad e influencia de temperatura.

Al estudiar los tiempos de recuperación y respuesta nos encontramos con unos tiempos menores que los encontrados en la instrumentación previamente desarrollada, lo que es una ventaja sobre la instrumentación anterior.

Se estudió la precisión intra-día encontrando un resultado de precisión bastante alto, de 1,15% (n=8). El estudio inter-día se realizó durante cinco días consecutivos, obteniendo una precisión del 1,77% (n=8).

A partir del estudio de la influencia de la temperatura sobre las medidas, se realizó la modelización de esta influencia con el objetivo de poder corregirla. El comportamiento encontrado muestra unos parámetros termodinámicos, tanto entálpicos como entrópicos, habituales para este tipo de sistemas.

Se puede concluir que se ha logrado el desarrollo de una instrumentación portátil para dióxido de carbono con un potencial uso industrial.

6. REFERENCES

1. K.T. Lau, S. Baldwin, R.L. Shepherd, P.H. Dietz, W. Yerzunis, D. Diamond, Talanta 63 (2004) 167.

2. K.T. Lau, W.S. Yerazunis, R.L. Shepherd, D. Diamond, Sens.Actuators B 114 (2006) 819.

3. A. Pacquit, K.T. Lau, H. McLaughlin, J. Frisby, B. Quilty, D. Diamond, Talanta 69 (2006) 515.

4. A. Pacquit, J. Frisby, D. Diamond, K.T. Lau, A. Farrell, B. Quilty, D. Diamond, Food Chem. 102 (2007) 466.

5. R.L. Shepherd, W.S. Yerazunis, K.T. Lau, D. Diamond, IEEE Sens.J. 6 (2006) 861.

6. M. O'Toole, R. Shepherd, G.G. Wallace, D. Diamond, Anal.Chim.Acta 652 (2009) 308.

7. R. Shepherd, S. Beirne, K.T. Lau, B. Corcoran, D. Diamond, Sens.Actuators B 121 (2007) 142.

8. M. Mazzotti; J. C. Abanades; R. Allam; K. S. Lackner; F. Meunier; E. Rubin; J. C. Sanchez; K. Yogo; R. Zevenhoven *IPCC Special Report on Carbon Dioxide Capture and Storage*, B.Metz, e. a. E., Ed.; Cambridge University Press: NY, 2005.

9. M. Sivertsvik, W.K. Jeksrud, J.T. Rosnes, Int.J.Food Sci.Technol. 37 (2002) 107.

10. S. Neethirajan, D.S. Jayas, S. Sadistap, Food Bioprocess Technol. 2 (2009) 115.

11. S.C. Seideman, P.R. Durland, J.Food Qual. 6 (1984) 239.

12. P. Suppakul, J. Miltz, K. Sonneveld, S.W. Bigger, J.Food Sci. 68 (2003) 408.

13. M. Ozdemir, J.D. Floros, Crit.Rev.Food Sci.Nutr. 44 (2004) 185.

14. J.P. Kerry, M.N. O'Grady, S.A. Hogan, Meat Science 74 (2006) 113.

15. M. L. Rooney *Active food packaging,* Blackie Academic & Professional: Glasgow, 1995.

16. R.M. Balabin, R.Z. Safieva, E.I. Lomakina, Anal.Chim.Acta 671 (2010) .

17. R.M. Balabin, S.V. Smirnov, Anal.Chim.Acta In Press, Corrected Proof. DOI: DOI: 10.1016/j.aca.2011.03.006 (2011) .

18. B. Li, Z. Zhang, Y. Jin, Anal.Chim.Acta 432 (2001) .

19. R.M. Balabin, R.Z. Safieva, Anal.Chim.Acta 689 (2011) .

20. G. Zhang, X. Wu, Opt.Lasers Eng. 42 (2004) 219.

21. J.W. Fergus, Sens.Actuators B 134 (2008) 1034.

22. H.H. Moebius, J.Solid State Electrochem. 8 (2004) 94.

23. V. Vojinovic, J.M.S. Cabral, L.P. Fonseca, Sens.Actuators B 114 (2006) 1083.

24. A. Mills, K. Eaton, Quim.Anal. 19 (2000) 75.

25. N. Nakamura, Y. Amao, Anal.Bioanal.Chem. 376 (2003) 642.

26. C.v. Bültzingslöwen, A.K. McEvoy, C. McDonagh, B.D. MacCraith, Anal.Chim.Acta 480 (2003) 275.

27. X. Ge, Y. Kostov, G. Rao, Biosensors Bioelectron. 18 (2003) 857.

28. S.M. Borisov, C. Krause, S. Arain, O.S. Wolfbeis, Adv.Mater. 18 (2006) 1511.

29. F. Baldini, A. Giannetti, A.A. Mencaglia, C. Trono, Curr.Anal.Chem. 4 (2008) 378.

30. B.H. Weigl, O.S. Wolfbeis, Sens.Actuators B 28 (1995) 151.

31. S.M. Borisov, M.C. Waldhier, I. Klimant, O.S. Wolfbeis, Chem.Mater. 19 (2007) 6187.

32. O. Oter, K. Ertekin, S. Derinkuyu, Talanta 76 (2008) 557.

33. G. Neurauter, I. Klimant, O.S. Wolfbeis, Anal.Chim.Acta 382 (1999) 67.

34. C.v. Bültzingslöwen, A.K. McEvoy, C. McDonagh, B.D. MacCraith, I. Klimant, K. Christian, O.S. Wolfbeis, Analyst 127 (2002) 1478.

35. McEvoy, A. K., MacCraith, B. D., McDonagh, C., von Bueltzingsloewen, C., Optical CO_2 and combined O_2/CO_2 sensors, WO/2004/077035 (2010).

36. D. Kieslinger, K. Trznadel, K. Oechs, S. Draxler, M.E. Lippitsch, Proc.SPIE-Int.Soc.Opt.Eng. 2976 (1997) 71.

37. M.E. Lippitsch, D. Kieslinger, S. Draxler, Sens.Actuators B 38 (1997) 96.

38. C. Malins, M. Niggemann, B.D. MacCraith, Meas.Sci.Technol. 11 (2000) 1105.

39. O. McGaughey, R. Nooney, A.K. McEvoy, C. McDonagh, B.D. MacCraith, Proc.SPIE-Int.Soc.Opt.Eng. 5993 (2005) 59930R/1.

40. I.M. Perez de Vargas-Sansalvador, M.A. Carvajal, O.M. Roldan-Munoz, J. Banqueri, M.D. Fernandez-Ramos, L.F. Capitan-Vallvey, Anal.Chim.Acta 655 (2009) 66.

41. I.M. Perez de Vargas-Sansalvador, A. Martinez-Olmos, A.J. Palma, M.D. Fernandez-Ramos, L.F. Capitan-Vallvey, Mikrochim.Acta 172 (2011) 455.

42. J.C. Carter, R.M. Alvis, S.B. Brown, K.C. Langry, T.S. Wilson, M.T. McBride, M.L. Myrick, W.R. Cox, M.E. Grove, B.W. Colston, Biosensors Bioelectron. 21 (2006) 1359.

43. M.C. Janzen, J.B. Ponder, D.P. Bailey, C.K. Ingison, K.S. Suslick, Anal.Chem. 78 (2006) 3591.

44. N.A. Rakow, K.S. Suslick, Nature 406 (2000) 710.

45. N.A. Rakow, A. Sen, M.C. Janzen, J.B. Ponder, K.S. Suslick, Angew.Chem.Int.Ed. 44 (2005) 4528.

46. Crowley, K.; Pacquit, A.; Hayes, J.; King Tong, L.; Diamond, D. (2005) 30-10-2005.

47. K.-T. Lau, S. Baldwin, M. O'Toole, R. Shepherd, W.J. Yerazunis, S. Izuo, S. Ueyama, D. Diamond, Anal.Chim.Acta 557 (2006) .

48. M. O'Toole, D. Diamond, Sensors 8 (2008) No.

49. A. Mills, A. Lepre, L. Wild, Sens.Actuators B 39 (1997) 419.

50. ISO, Internacional standard.ISO11843-5 (2008) .

51. IUPAC, Pure Appl.Chem. 67 (1995) 1699.

52. M.A. Carvajal, I.M. Perez de Vargas Sansalvador, A.J. Palma, M.D. Fernandez-Ramos, L.F. Capitan-Vallvey, Sens.Actuators B B144 (2010) 232.

53. K. Ertekin, I. Klimant, G. Neurauter, O.S. Wolfbeis, Talanta 59 (2003) 261.

54. C. Malins, B.D. MacCraith, Analyst 123 (1998) 2373.

55. D.A. Nivens, M.V. Schiza, S.M. Angel, Talanta 58 (2002) 543.

56. A. Mills, L. Monaf, Analyst 121 (1996) 535.

57. M.D. Marazuela, M.C. Moreno-Bondi, G. Orellana, Sens.Actuators B 29 (1995) 126.

58. A. Mills, Q. Chang, N. McMurray, Anal.Chem. 64 (1992) 1383.

59. P.C. Hauser, Meas.Sci.Technol. 6 (1995) 1081.

60. M.I.J. Stich, S.M. Borisov, U. Henne, M. Schaeferling, Sens.Actuators, B 139 (2009) 204.

61. T. Mayr, T. Abel, E. Kraker, S. K÷stler, A. Haase, C. Konrad, M. Tscherner, B. Lamprecht, Procedia Engineering 5 (2010) 1005.

Capítulo 6

Instrumento multisensor para monitorización de oxígeno, temperatura y humedad en suelos

Planteamiento

El desarrollo de este capítulo se llevó a cabo contando con el interés mostrado por el Centro Tecnológico Forestal de Cataluña por un instrumento capaz de determinar los niveles de oxígeno edáfico pues este parámetro afecta decisivamente al crecimiento y desarrollo de cultivos.

Una baja concentración de oxígeno edáfico puede llevar al deterioro de la función de las raíces, decreciendo su productividad. Si existe falta de oxígeno, decrece la respiración mitocondrial y por tanto se limita el transporte de nutrientes minerales como N, P y K [1].

Al tratarse de una aplicación nueva para nuestro grupo, se nos plantearon una serie de variables a estudiar, tanto el tipo de suelo adecuado para llevar a cabo los experimentos como el tipo de cultivo, teniendo que cumplir una serie de características. En el caso del suelo tendrá que poseer una porosidad adecuada para la correcta difusión del oxígeno y a su vez presentar similitudes con el que se utiliza en diferentes tipos de cultivos. En el caso del cultivo, deberá de tratarse de una planta o árbol, capaz de absorber gran cantidad de oxígeno, ya que debido a que las medidas se van a realizar en el laboratorio tendremos que, con un número limitado de plantas, poder observar los cambios de concentración de oxígeno.

Al plantearnos este reto, pensamos en la inclusión no sólo de un sensor para oxígeno, sino también que esta nueva instrumentación permitiera la monitorización de temperatura y humedad, que también afectan al desarrollo de las plantas. Además, como el sensor de oxígeno a incluir es conocido por nosotros y presenta influencia de la temperatura, nos interesaba estudiar si la humedad afectaba en alguna medida al funcionamiento del sensor.

En primer lugar se pasó a diseñar la sonda, de manera que presente una forma adecuada para poder ser enterrada y que además esté herméticamente cerrada excepto por el extremo enterrado, para así evitar que el agua llegue al sensor en caso de encharcamiento por lluvia o riego.

Una vez diseñada la sonda, se plantearon los experimentos a realizar para el testeo de la sonda, tanto en el laboratorio como tratando de acercarnos en lo posible a las condiciones que tendríamos en una situación real.

En este capítulo veremos el diseño, fabricación y caracterización de esta sonda multisensora.

MULTISENSOR PROBE FOR SOIL MONITORING

A. Martinez-Olmos[a°], I.M. Pérez de Vargas-Sansalvador[b°], A. J. Palma[a], J. Banqueri[a], M.D. Fernández-Ramos[b] and L.F. Capitán-Vallvey[b]*

ECsens. [a] Department of Electronics and Computer Technology. [b] Department of Analytical Chemistry. Campus Fuentenueva, Faculty of Sciences, University of Granada, E-18071 Granada, Spain.

Abstract

In this work, a probe for soil monitoring has been developed. This instrument allows the measurement of three parameters: oxygen concentration, temperature and relative humidity of the interstitial air in soil at depth of the roots. The oxygen sensor is based on the quenching of phosphorescent octaethylporphyrin complex. A full description and characterization of the instrument are carried out.Their applications in a first step under controlled conditions in the laboratory and after that closer to real situations are also shown. First, the sensor probe was characterised inside a climatic chamber, then in a lysimeter and finally, the instrument was tested in planted soil for which it was buried in a pot containing an *Ilex x meserveae* (Blue Angel) tree. In the two first steps, effects of temperature and humidity were studied as well as response and recovery behaviour, limit of detection, limit of quantification and time drift. In the last step, the evolution in oxygen during waterlogging experiments were carried out with two different holly trees, one of three years old and the other of two years old and a comparison between the results obtained for both trees was performed.

Key words. Edaphic oxygen; gas sensor; phosphorescence; portable instrumentation; optoelectronic coated components.

° Both authors contribute equally to this work

* Corresponding author; *e-mail:* lcapitan@ugr.es

INTRODUCTION

Oxygen diffuses from the atmosphere through soil pores to plant roots, soil microbes and chemicals present at a diffusion rate rapid enough to maintain adequate oxygen availability [2]. The gas exchange is essential to plants function because roots during the respiration process take up the oxygen in the surrounding of the roots in the rhizosphere and in turn, release carbon dioxide. The movement of oxygen from the atmosphere to the root involves the diffusion through different phases: gaseous phase of the soil, gas-liquid phase boundary and liquid phase water film around the root [3]. The root oxygen bio-availability is the most important parameter in root physiology and metabolism and depend on different factors such as oxygen concentration, pore size, water content and microbial activity of the soil [1]. Lack of oxygen may lead to a reduction of root growth, availability of nutrients, evaporation, and photosynthesis rate; in short, to a reduction in plant material production.

The analysis of oxygen in soil atmosphere have been performed by using different techniques such as gas chromatography with thermal conductivity detection, although this technique is unsuitable for continuous oxygen monitoring in the field and require the use of a sampling device for soil atmosphere [4].

Among electrochemical sensors, that are very commonly used, the polarographic (Clark-type) have been used in plots subjected to flooding [5], plants in anaerobic conditions [6] and also as a portable oxygen detector for assessing wetland soil attributes [7]. They need relatively small air sample which can be analyzed in the field, however, the probe must be removed and the electrolyte changed periodically [8]. The problem of noise and drift in these polarographic sensors can be addressed by using self-referencing sensor technologies [9]. The estimation of bio-availability of oxygen to growing roots is approached by Porterfield et al. [1] using a Clark type oxygen electrode covered by a gel membrane system to allow the sensor to consume oxygen in a manner that simulates the activity of an actual root.

Galvanic cell oxygen sensor presents a small volume and consumes little oxygen and has been used in studies of gas diffusion through soil columns [10] with results in field that agree with laboratory gas analysis [11] especially for long-term *in situ* use in agricultural soil [8]. On the other hand, a solid electrolyte zirconia type oxygen sensor has been developed in a waterproof version for oxygen determination in soil by Ishii and Kadoya [12] with advantages of no recalibration and short response time.

An alternative approach refers to the use of optical sensors all based on the dynamic quenching that oxygen causes on luminescent characteristics of luminophores emission. Different results have been reported based on intensity measurement obtained with optic fibre sensor, commercial in some cases, based on miniaturized spectrometers and portable computers in sediments [13] and soils [8,14]. Problems of instability, photobleaching of luminophore and influence of temperature and humidity on calibration have been reported [8].

From the point of view of photostability and immunity to stray optical signal interference, decay time measurement are more advantageous than intensity, mainly using phase modulation techniques as is the self-referencing sensor based on platinum tetrakis(pentafluorophenyl) porphyrin as luminophore to measure molecular oxygen flux patterns from plant systems [1,15].

In this paper, we have designed and tested a portable multisensor instrument for measuring oxygen concentration, temperature and relative humidity of interstitial air of the soil near the root of plants. The optochemical sensor of oxygen, where the sensing film is based on the luminophore dye platinum octaehylporphyrin complex immobilized in a polystyrene membrane and stabilized with the heterocyclic amine DABCO, was previously developed by us [16,17]. Below a detailed description and characterization of the instrument and its application in controlled conditions of laboratory and near real situations is presented.

EXPERIMENTAL

Reagents, materials and equipment

The reagents used were platinum octaethylporphyrin complex (PtOEP, Porphyrin Products Inc., Logan, UT, USA) and 1,4-diazabicyclo[2.2.2]octane (DABCO; 98%, from Sigma–Aldrich Química S.A., Madrid, Spain). The solvent used, tetrahydrofuran (THF), was supplied by Sigma as well. As polymer, polystyrene (PS, average MW 280,000, Tg: 100 ºC, GPC grade, Sigma) was used. The cocktail was prepared by weighing the chemicals with a precision of ±0.01 mg in a DV215CD balance (Ohaus Co., Pine Brook, NJ, USA). The gases O_2 and N_2 used were of a high purity (>99%) and were supplied in gas cylinders by Air Liquid S.A. (Madrid, Spain).

For the electrical characterization of the prototype a mixed signal oscilloscope (MSO4101, Tektronix, USA), a 6½ digit multimeter (34410A, Agilent Technologies, USA), a 15 MHz waveform generator (33120A, Agilent Technologies, USA) and a DC power supply (E3630A, Agilent Technologies, USA) were used. A code in Visual Basic© has been developed for control and calibration purposes.

Instrument description

The instrumentation for soil monitoring developed is composed of two different modules. The sensing probe where takes place the measurement of the soil variables of interest and the acquisition electronics where the output signals from the probe are processed and stored. Photography of the full instrument is presented in the Figure 1 where both sensing and processing units are shown.

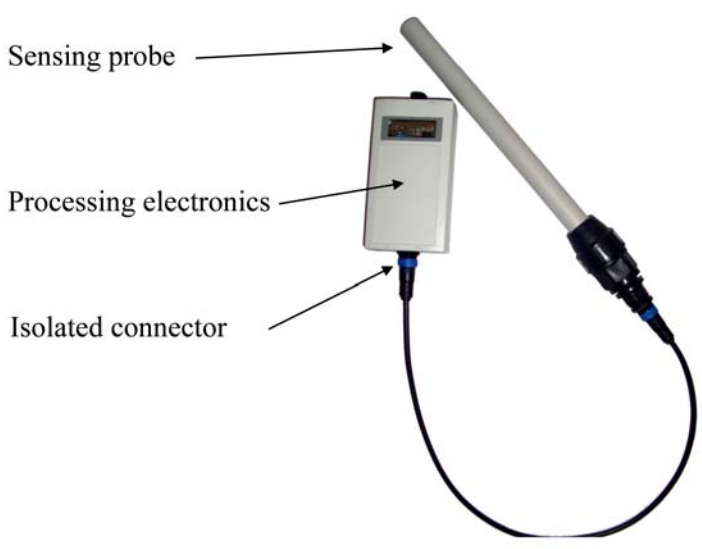

Figure 1. Multisensor prototype for soil monitoring

The sensors included in the sensing module are located into an insulating plastic pipe which is buried in the soil that is object of study, as it can be seen in Figure 1. This pipe is open at the bottom to allow the oxygen exchange with the surrounding soil, but sealed at the top to avoid the water from penetrating the probe.

Sensing probe

The sensing probe is prepared to be buried in the soil and measures temperature, humidity and oxygen concentration. It is fabricated onto a printed circuit board (PCB) of small dimensions (20×38 mm) and contains three different sensors. The temperature sensor is the commercial chip DS1624 (Dallas Semiconductor, USA) that measures temperature in the range -55 to 125 ºC with a resolution of 0.03125 ºC and generates a digital word of 13 bits that is serially sent to the processing module. The humidity sensor is the model HIH-4030 (Honeywell, USA) that can provide relative humidity measurements in the full range 0-100%. Its output signal must be corrected with the temperature

measurement into the processing module. The last of the sensors is the oxygen concentration detector that is an optical sensor developed by the authors in previous works and based on the quenching of the phosphorescence of PtOEP by the oxygen. The phosphorescence emitted by the oxygen sensitive membrane of PtOEP is collected by the photodetector IS486 (Sharp, Japan), which produces in response a high voltage pulse whose width depends on the life time of the phosphorescence and therefore on the oxygen concentration [16,17]. This pulse is transmitted to the processing electronics where it is quantified. The IS486 is highly sensitive to light at 645 nm that virtually match with the light emitted by the membrane (650nm), and presents a low delay in the response time typically about 3 μs, compensated in any case. The light source used to excite the PtOEP membrane is a green LED with illumination peak at 525 nm, the model E1S17-3G (Tayoda Gosei, Japan), a small surface mounted device (SMD) with dimensions 3.5×2.7 mm which can be placed very close to the photodetector thanks to its plane surface. The probe is connected to the external unit through a 7-wire cable from where power is supplied to the sensors and which is used to transmit all the measurement signals to the external acquisition unit.

The scheme of the sensing probe is presented in Figure 2, it can be seen how the probe is placed into the pipe. The rigid pipe is necessary to prevent the probe from damage which may be caused by the water and the direct contact with the soil. This pipe is open at the bottom and some drills have been made just below the sensing circuit to allow gases in the soil and among them oxygen to penetrate in the system, so the oxygen measurement corresponds to its concentration in the soil. The pipe counts on two sealed isolations, one at the height of the probe and another one at the top of the pipe. The aim of these seals is to prevent the water from flooding the system by maintaining a watertight atmosphere. In Figure 3 a diagram of the sensing probe is presented. As it can be seen the temperature and humidity sensors are placed on opposite sides of the PCB in order to save space. The oxygen sensor formed by the green LED and the photodetector is situated at the bottom of the board so it can be near the open extreme of the pipe. The photodetector covered by the

PtOEP membrane is not fixed in the PCB but it is inserted in a set of holes so it can be removed and replaced by other sensor at any time with no need of discarding the whole probe.

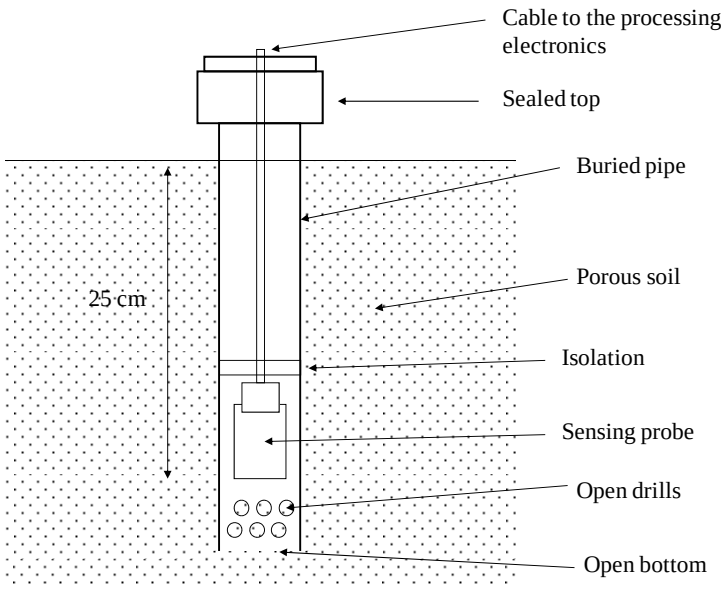

Figure 2. Disposition of the probe in the pipe

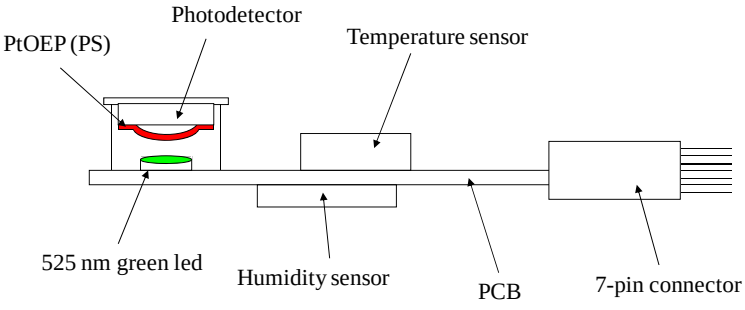

Figure 3. Scheme of the sensing probe.

Processing module

The processing module is the reading unit which is placed on the soil and connected to the buried sensing probe through an isolated IP65 connector. It contains all the electronics needed to receive and process the output signals from the sensing probe. The objective of the full instrument is to monitor a porous soil during a long time of several months. In this period, the prototype must be operating with a power supplied by batteries, so it has been designed for low power consumption administered by the processing unit. The core of this module is a microcontroller PIC16F876 (Microchip Technology, USA). This device has been selected due to its low cost and low power consumption when operating in sleep mode, about 20 μA.

The processing unit contains other modules for the signal treatment. A current source is designed to polarize the LED in the oxygen sensor with a pulsed current of 15 mA and an operation frequency of 2 kHz. By working in a pulsed mode, drifts are reduced [16]. A logic block based on NAND gates is included to perform the multiplication between the output signal from the photodetector and a high frequency wave of 12 MHz from which the life time of the phosphorescent signal is obtained. For data storage, a memory of 512 Kbit model 24LC512 (Microchip Technology, USA) is included. Finally, a module VNC1L has been integrated in the system in order to provide the microcontroller with USB host capability. This module communicates with the PIC through the UART port, and can operate with external USB devices such as flash memories. In this operation mode, the instrument is situated in the soil to be monitorized and left working for several weeks. When the user needs to check the data, it's only necessary to connect the USB memory to the prototype and the data will automatically be downloaded in the device. In this way, there is no user interface in form of keypad or buttons which are not desirable in a system that has to be as isolated as possible from environmental elements that may cause damage in the circuitry.

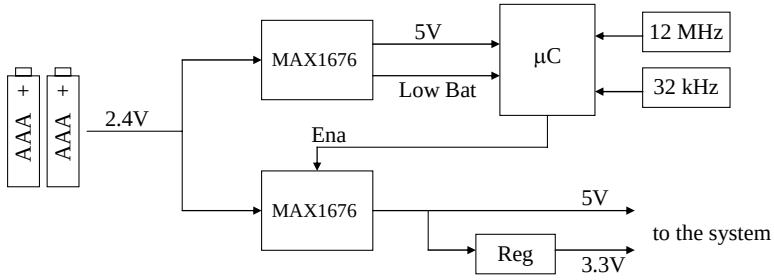

Figure 4. Power management system.

The power management in the instrument is governed by the PIC microcontroller as depicted in Figure 4. Two rechargeable batteries AAA of 1.2V and 1200 mA/h are used as primary power source, which generates a voltage of 2.4V. In the instrument, there are some components that operate at 5V and others at 3.3V, so both DC lines are required. To elevate the voltage from the batteries the DC/DC converter MAX1676 (Maxim Integrated Products, USA) is used. As it can be seen in Figure 4 one converter generates 5V only for the microcontroller, whereas other converter provides 5V and, through a regulator, 3.3V for the rest of the system. The reason for having a double converter is that the PIC needs to be supplied with 5V continuously even while operating in sleep mode, whereas the rest of the components only have to be powered at the moment of operating, that is, when taking a measurement, processing the signals or storing data. Its state is controlled by the PIC through an *enable* signal that turns the converter on and off. Therefore, a very low consumption mode can be configured when no measurement is been carried out by disconnecting the secondary DC/DC converter so no component is consuming any current and setting an state of sleep mode for the microcontroller, in which the main external clock of 12 MHz is disabled and replaced by a low frequency crystal of 32 kHz. In this mode, less than 0.5 mA is consumed. Taking into account that the measurements can be completed in 3 seconds and that the consumption when operating is 17 mA and assuming that the system is taking one measurement of the environmental variables every 10 minutes, the mean consumption per hour

is 0.58 mA which means that the system can be operating for 86 days, that is, about 3 months.

Sensing membranes preparation

Mixtures for the preparation of the oxygen-sensitive membrane were made by dissolving 0.5 mg of PtOEP and 12 mg of DABCO in 1 mL of a solution of 5% (w/v) of PS in freshly distilled THF. The sensitive membranes were cast by placing two successive volumes of 5 μL of the cocktail on the active face of the photodetector with the aid of a micropipette. After each addition, the device was left to dry in darkness in a THF atmosphere for 1 hour. The obtained coated photodiodes show the lens covered with a homogeneous, transparent and pink film with an estimated average thickness of about 75 μm and a PtOEP concentration of 0.055 mol·kg^{-1} polymer. Oxygen sensing membranes need to be cured in darkness for 9 days before their use.

Measurements conditions

We studied step by step the developed instrument measuring environment magnitudes (O_2 concentration, T and HR) in soil. First the sensor probe was characterised inside a climatic chamber to study the behaviour of the sensor at open air, after that the instrument was measured in a lysimeter to know the performance of the instrument in soil under controlled variables and finally, the instrument was studied in planted soils for which it was buried in pots that contains trees in order to obtain measurements in conditions closer to real situation.

Climatic chamber

The instrument was tested with a climatic chamber where the mixtures of gases were targeted directly to the sensor probe in open air. The standard mixtures for instrument calibration and characterization (O_2 in N_2) were produced using N_2 as the inert gas component and by controlling the flow rates of the

different high purity gases (100%) N_2 and O_2, in each case, entering a mixing chamber using a computer-controlled mass flow controller (Air Liquid España S.A., Madrid, Spain) operating at a total pressure of 760 Torr and a flow rate of 500 $cm^3 \cdot min^{-1}$,being the specified accuracy ± 0.5% of reading and ± 0.1% of full scale. For the portable instrument characterization, the measurements were performed after equilibration for 2 min of the instrument atmosphere with the gas mixtures obtained with the gas blender indicated above.

To produce different humidity conditions (from 14 to 100% RH) a CEM-system was used. This system consists of a mass flow controller for measurement and control of the carrier gas flow (N_2), a mass flow meter for liquids (MiniCoriflow) with a range of 0.4 - 20 g/h of liquid (water in this case) and a CEM 3-way mixing valve and evaporator for control of the liquid source flow and mixing the liquid with the carrier gas flow resulting in total evaporation, besides it contains a temperature controlled heat-exchanger to add heat to the mixture to produce a complete evaporation of the liquid (100ºC was selected for water).

Lysimeter

The sensor probe was buried at a depth of 15 cm in a lysimeter that is a pot 26.5 cm diameter and 27 cm height (see Figure 5). This experiment was designed to investigate the accuracy of the sensor under controlled conditions in the lab prior to *in situ* measurements in soil. The lysimeter was prepared in a plastic container filled by dry medium sand (0.1 - 1 mm particle size, 16.1 kg). The sand was collected from Getares beach in Algeciras (Cádiz, Spain), was dried in an oven and then was sieved with a 1 mm sieve. At the bottom of the container there is an inlet for gas entry connected to a circular tube placed in a plane at 4 cm of the bottom with vents regularly spaced for homogeneous gas flow. A volume at the bottom of the container of 2123.7 cm^3 provided a homogeneous gas flow. The gas inlet at the bottom was connected to the mass flow controllers. The mixtures of gases were prepared as explained above in the climatic chamber.

Figure 5. Sensing probe buried in the lysimeter

Planted soils

The instrument was buried at a depth of 15 cm in pots of 52 cm diameter and 39 cm height and with a hole of 1 cm diameter for drainage, which were filled with standard soil (characteristics: pH 6.2, conductivity 2.2 MMHO/cm, carbonates 0.42%) with a final volume of 78577.5 cm^3, which contains undecomposed organic matter and is very porous for a good oxygen diffusion. As sample bush, *Ilex x meserveae* 'Blue Angel' was selected. Two *Ilex x meserveae* specimens of 2 and 3 year old, (height 121 and 145 cm) respectively, trees were transplanted into the pots (see Figure 6) 4 days after the beginning of the experiment. After that the oxygen concentration, relative humidity and temperature in the soil were measured at intervals of 10 minutes. The pots were watered once a day and the surplus water drained. A couple of days after the beginning of measurements the waterlogging treatment was launched maintaining it until damage in the shrub was observed, draining in this moment off the water through the hole in the pot.

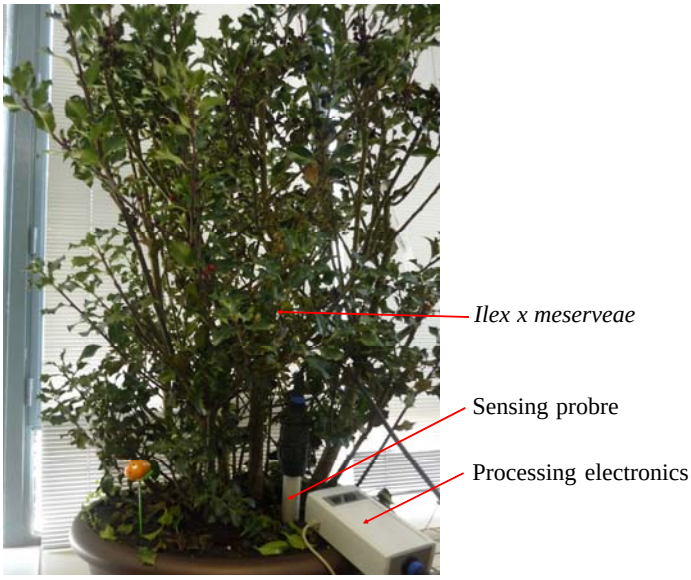

Figure 6. Instrument setup for near-root oxygen measurement.

RESULTS AND DISCUSSION

Instrument Response

The oxygen response of the probe has been modelled following the empirical model proposed in previous works [16,17] expressed by equation 1:

$$[O_2] = C_0 + \frac{C_1}{\sqrt{t^N}} \qquad \text{Eq. 1}$$

where t^N is the photodetector output pulse width in ns, and C_0 and C_1 are the fitting constants. In Figure 7 the calibration curve and the corresponding fitting to Equation 1 for fixed temperature and humidity conditions are presented. This calibration was done using six-fold replicas at room temperature (20±0.5 ºC) as a function of the oxygen concentration up to 35%, obtaining C_0 = 4037.5 and C_1 = 10.2 (R^2 = 0.997).

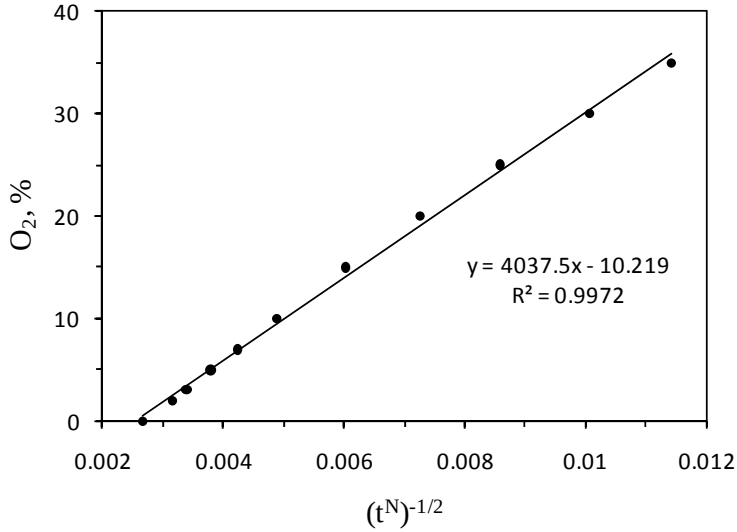

Figure 7. Oxygen calibration curve and fitting with error bars included.

The limit of detection (LOD) was calculated from the raw exponential experimental data using the first three points that can be adjusted to a straight line (t^N = -18040 [O_2] + 139304; R^2 = 0.9899) [18], by using the conventional approach defined by LOD = t^N_0 - 3 s_0, where t^N_0 is the blank or average value in the absence of oxygen and s_0 is the critical level or standard deviation of the blank, which was determined from six replicate measurements. The limit of quantification (LOQ) of the instrumental procedure was obtained from the calibration function by using LOD = t^N_0 + 10s_0.The LOD found using this approach were 0.14 and the LOQ 1.01% of O_2.

The resolution in the oxygen concentration can be obtained from eq. 1 as:

$$\Delta O_2 = \frac{C_1}{\left(t^N\right)^{\frac{3}{2}}} \Delta t^N \qquad \text{Eq. 2}$$

where Δt^N is the time resolution which is given by the period of the high frequency signal used to quantify the output pulse of the photodetector. In this case, the frequency used is 12 MHz, which implies that Δt^N = 83 ns. From Equation 2 the resolution in concentration of oxygen at 21% is 0.1%

The time drift of the measurements has been studied by measuring at a fixed concentration of 21% oxygen for 24 hours, taking measurements every 10 minutes. The result obtained is 0.05 %/day which means that the data present very low drift. The accuracy of the sensor was evaluated as the standard deviation of the reconstruction error in a set of 30 validation data, obtaining a value of 0.07%. The low values for the resolution, the time drift and the accuracy make the measurements very reliable.

Temperature has a considerable influence on the sensitivity of luminescent sensors. Therefore, the thermal dependence of the sensing membranes was evaluated by acquiring the calibration function shown in Figure 8 at temperatures between 5 ºC and 30 ºC. From this study, a decrease in sensitivity with temperature was observed that can be attributed to a diminishing of the luminescence of the PtOEP, and hence the lifetime of phosphorescence, when the temperature rises.

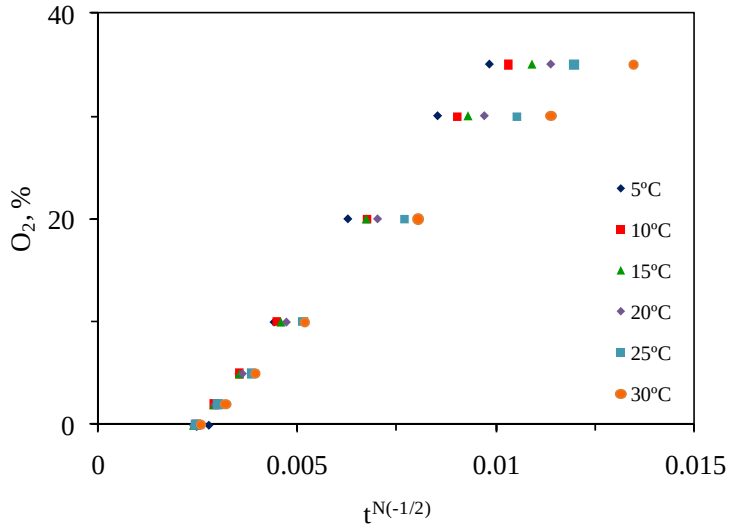

Figure 8. Oxygen calibration at different temperatures.

The calibration curves of Figure 8 have been modelled using the expression of Equation 1, obtaining different values for the fitting parameters C_0

and C_1 for each temperature. A modelling function for these fitting parameters with the temperature can be found including the thermal dependence of the oxygen sensor in these constants. In this case, a simple linear function is used for the first parameter (C_0 = -63.149T + 5218.3 ; R^2 = 0.986) and a quadratic polynomial function for the second (C_1 = 0.0123T^2 - 0.5502T + 15.295; R^2 = 0.998) with the temperature expressed in Celsius degrees.

In order to evaluate the possible effects that the humidity may produce on the measurements of the oxygen concentration, a study of the oxygen response at different humidity atmospheres (14, 19, 30, 39, 63, 77 and 98% RH) at six different oxygen concentrations (2, 5, 10, 20, 30 and 35 % O_2) has been carried out using the climatic chamber. We calculated the percentage of variation between the biggest and the smallest value of t^N at each HR finding that the variations oscillated between 1.8 and 3.1%. Because of the small difference found that can be observed in the plane lines obtained in Figure 9, it is concluded that the humidity conditions did not affect to our sensor.

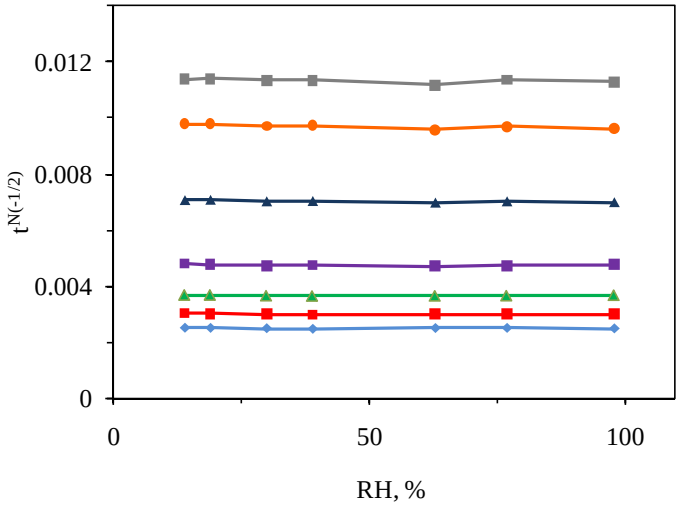

Figure 9. Oxygen calibration curves at different relative humidity values. Blue line 0% O_2, red line 2% O_2, green line 5% O_2, purple line 10% O_2, dark blue line 20% O_2, orange line 30% O_2, grey line 35% O_2.

A study of the dynamic response of the sensing membrane when exposed to alternating atmospheres of pure O_2 and pure N_2 was carried out. The response time was calculated from between 10% and 90% of the maximum signal, obtaining a value of 28.5 ± 0.6 s and, the recovery time from 90% to 10% which was found to be 59.0 ± 2.2 s in open air.

In addition, the response and recovery behaviour of the O_2 sensing membrane was studied at different intermediate O_2 concentrations (0, 2, 5, 10 and 30% O_2). In all cases, the signal changes were fully reversible and hysteresis was not observed during the measurements, as it can be seen in Figure 10.

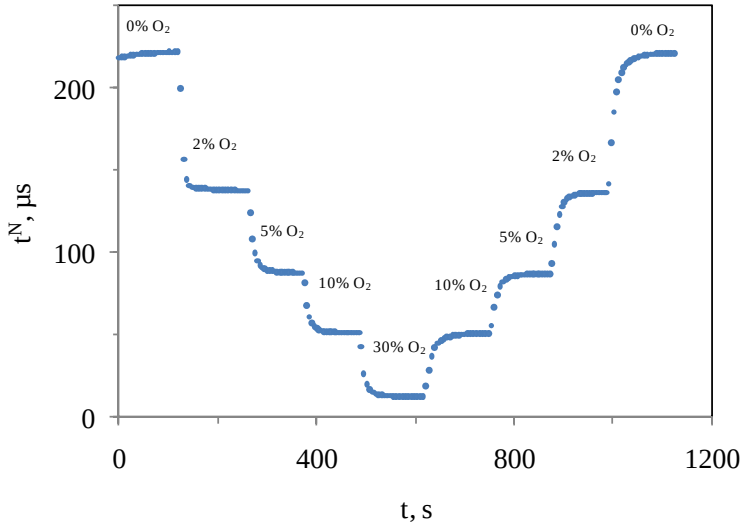

Figure 10. Dynamic response of the oxygen probe.

Multisensor probe in the lysimeter

Once the characterization of the instrument in open-air conditions has been carried out, some experiments were performed in the lysimeter with mixtures of known composition of oxygen in nitrogen to simulate groundwater-near gas composition. After check similar response to oxygen in open air, the

dynamic response, from 0 to 30% of O_2, of the oxygen sensor was again studied in order to evaluate the delay produced by the diffusion of the oxygen through the sand when injected at the bottom of the pot. The response time obtained was 7.7 ± 0.2 min and the recovery time 15.9 ± 0.2 min. As expected the times calculated here are much higher than the times calculated in the previous section, because the mixture of gases has to diffuse into the sand to arrive to the sensor.

Multisensor probe in planted soils

The instrument was used to measure oxygen concentration, RH and temperature in holly tree (*Ilex x meserveae*) planted soils near the roots. This kind of tree was selected because of its big roots which are expected to consume oxygen in soil quickly. To simulate partial anaerobic conditions in the soil, the planted trees were subjected to waterlogging cycles. Figure 11 shows the evolution in oxygen during the waterlogging experiment using a three year-old tree

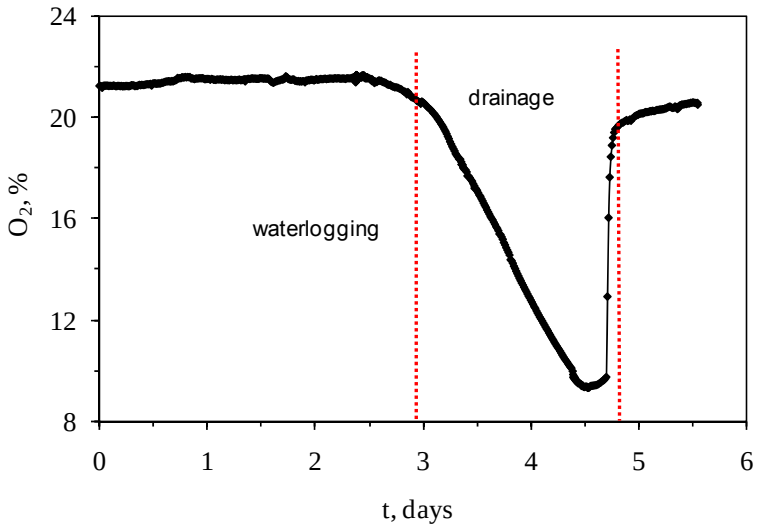

Figure 11. Variation in soil oxygen for tree 1.

These results were obtained in the month of July with a constant temperature of 27 ºC. As it can be observed from this figure, the concentration of oxygen at the sensing probe depth is about 21%, i.e. the open air oxygen level, which is expectable in a well drained porous soil [12]. After waterlogging a diminishing of the oxygen near the roots is produced due to the consumption of the plant. Since there is no exchange with the external air because of the isolation caused by the water, the oxygen is not renewed in the soil and therefore decreases. When the pot is drained the air is able to penetrate the soil rapidly thanks to its high porosity, reaching quickly the open air level at the moment that oxygen diffuses to the head of the sensing probe.

A second experiment following the previous scheme was carried out using a younger tree of the same kind (2 year-old *Ilex x meserveae*, height 121 cm) with the aim of observing the differences in oxygen consumption in a bush with roots less grown. Since the roots are smaller and therefore, less deep in the soil, the sensing probe was buried at a depth of 15 cm close to the tree. In this case, a longer register of the oxygen concentration with two waterlogging cycles was performed, for about 40 days, taking measurements every 10 minutes. The obtained results are presented in Figure 12, where both oxygen concentration (solid line) and temperature (dotted line) are shown.

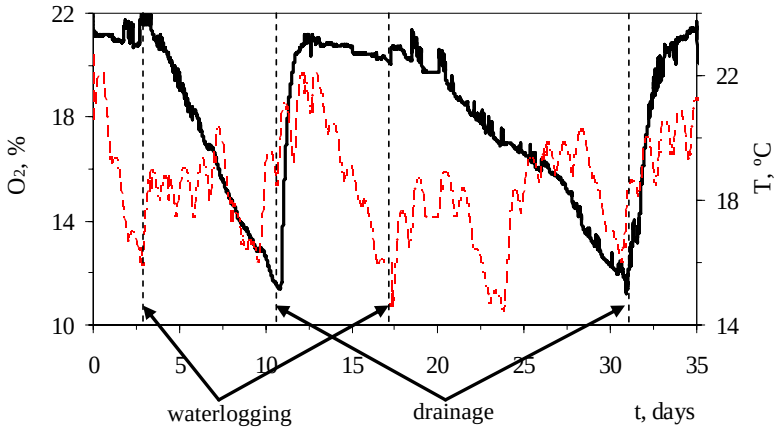

Figure 12. Variation in soil oxygen (solid line) and temperature (dotted line) for two-year old tree.

This experience was performed during the month of January with soil temperature varying from 14 to 22ºC, from where the daily variations of temperature can be seen as small peaks of higher frequency and the long time variations are observed as the baseline drift. The effect of the temperature on the measurements has been compensated using the thermal calibration explained above. As it can be seen from this figure, two consecutive cycles of waterlogging and drainage are applied to the system. Before watterlogging the oxygen concentration is about 21% as it happened in the previous study. For this bush, the concentration of oxygen after flooding decreases to 12% in approximately 5 days, while the first tree produced the same drop in only 2 days, as derived from Figure 11. Moreover, in the second waterlogging cycle of Figure 12 the same oxygen decreasing takes about 15 days which is a consequence of the first cycle: the flooding of the pot and the lack of oxygen exchange with the open air affects the tree which lost a big part of its leafs and therefore the consumption of oxygen decreased.

CONCLUSIONS

A portable sensor probe for soil monitoring has been developed and tested in different conditions. The developed instrument is capable of measuring oxygen concentration, temperature and relative humidity of the interstitial air of soil at roots depth with enough resolution, response time and limit of detection. Electronics has been carefully designed for in situ and autonomous operation during several months.

Cycles of waterlogging and drainage of controlled soils have been monitorized in a lysimeter and in planted soils. In this last case, the influence of plant age in the oxygen consumption at the root depth has been shown. The results obtained in both trees demonstrate the capability of this sensor probe to measure O_2 concentration, temperature and HR in soil.

ACKNOWLEDGEMENTS

We acknowledge financial support from Ministerio de Educación y Ciencia, Dirección General de Enseñanza Superior (Spain) (Projects CTQ2005-09060-CO2-01 and CTQ2005-09060-CO2-02) and from the Junta de Andalucía (Spain) (Projects P06-FQM-01467 and P08-FQM-3535). These projects were partially supported by European Regional Development Funds (ERDF).

CONCLUSIONES

En este capítulo hemos desarrollado una instrumentación para la determinación simultánea de concentración de oxígeno, temperatura y humedad relativa (RH) en suelos.

Tras el desarrollo de la sonda, esta se ha caracterizado mediante un conjunto de experimentos paso a paso para poder llegar a unas condiciones próximas a condiciones reales.

1. Se estudió el comportamiento del sensor en el interior de una cámara térmica, para así estudiar la respuesta del sensor de oxígeno, obteniendo la curva de calibrado a temperatura y RH contantes. Se modeló la respuesta a oxígeno en función de la temperatura y se estudió la posible influencia de la RH, concluyendo que no existe influencia de esta en la determinación de oxígeno. También se obtuvieron los tiempos de recuperación y respuesta.

2. En un segundo paso se estudió el comportamiento del instrumento en un lisímetro relleno de arena preparada para la correcta inyección de mezclas de gases por su interior. Lo que tratamos es de corroborar los resultados obtenidos en el experimento de la cámara térmica y a su vez estudiar el retardo producido en los tiempos de respuesta y recuperación al tener que difundir el gas en la arena, que como esperábamos fueron de 7.7 ± 0.2 min y 15.9 ± 0.2 min, respectivamente.

3. Como paso final se estudió el comportamiento del sensor cuando estaba enterrado cerca de las raíces de un acebo. Se utilizaron dos acebos, de dos y tres años de edad, respectivamente, los cuales se sometieron a ciclos de inundación y drenaje, para ver los cambios que se producían como consecuencia de estos ciclos. Se observó, como era de esperar, una disminución del nivel de oxígeno edáfico

al impedir la inundación la reposición del oxígeno consumido por las raíces y una recuperación al drenar el terreno.

Podemos concluir en base a los resultados obtenidos, que se ha diseñado una sonda para monitorización en suelos de tres parámetros: concentración de oxígeno, temperatura y humedad relativa con especificaciones de resolución, tiempo de respuesta y resolución adecuados para su uso in situ y de forma autónoma durante varios meses.

REFERENCES

1. D.M. Porterfield, S.S. French, A.R. DeCarlo, Biol.Eng. 1 (2008) 219.
2. H. L. Bohn; B. L. McNeal; G. A. O'Connor Soil Chemistry, 2nd Edition ed.; John Wiley Sons: New York, 2001.
3. M. B. Kirkham Principles of soil and plant water relations, Elsevier Academic Press: Burlington, MA, 2005.
4. J. Glinski; W. Stepniewski Soil aeration and its role for plants, CRC Press, Inc: Raton Boc, FL, 1985.
5. B.D. Meek, T.J. Donovan, L.E. Graham, Soil Sci.Soc.Am.J. 44 (1980) 433.
6. K. Dittert, J. Woetzel, B. Sattelmacher, Plant Biol. 8 (2006) 212.
7. S.P. Faulkner, W.H. Patrick, R.P. Gambrell, Soil Sci.Soc.Am.J. 53 (1989) 883.
8. J.C. Kallestad, T.W. Sammis, J.G. Mexal, Soil Sci.Soc.Am.J. 72 (2008) 758.
9. D.M. Porterfield, Biosensors Bioelectron. 22 (2007) 1186.
10. S.B. Jones, D. Or, G.E. Bingham, Vadose Zone Journal 2 (2003) 602.
11. D.X. Li, P.D. Lundegard, Ground Water Monit.Rem. 16 (1996) 106.
12. T. Ishii, K. Kadoya, Plant Soil 131 (1991) 53.
13. G. Holst, R.N. Glud, M. Kuehl, I. Klimant, Sens.Actuators, B B38 (1997) 122.
14. S.L. Johnson, C.R. Budinoff, J. Belnap, F. Garcia-Pichel, Environ.Microbiol. 7 (2005) 1.
15. D.M. Porterfield, J.L. Rickus, R. Kopelman, Proc.SPIE-Int.Soc.Opt.Eng. 6380 (2006) 63800S/1.
16. A.J. Palma, J. López-González, L.J. Asensio, M.D. Fernandez-Ramos, L.F. Capitan-Vallvey, Sens.Actuators B 121 (2007) 629.

17. A.J. Palma, J. Lopez-Gonzalez, L.J. Asensio, M.D. Fernandez-Ramos, L.F. Capitan-Vallvey, Anal.Chem. 79 (2007) 3173.

18. ISO, Internacional standard.ISO11843-5 (2008) .

Conclusiones

Como resultado del trabajo realizado en esta Tesis Doctoral, se deducen las siguientes conclusiones:

1. Se ha desarrollado un sensor para dióxido de carbono gaseoso que opera hasta un 100%, basado en la medida de atenuación de fosforescencia empleando instrumentación convencional. Está basado en las propiedades ácidas de la molécula de este gas. El cóctel conteniendo el luminóforo PtOEP fue empleado tanto disuelto como encapsulado en micropartículas del polímero impermeable a oxígeno PVCD. Se demostró que este sensor funciona según el modelo de filtro interno secundario. Del estudio de las diferentes configuraciones de disposición de membrana sensora sobre el soporte, se eligió como óptima aquella en la que se disponen ambas membranas en caras opuestas del mismo, ya que minimiza el deterioro del luminóforo en presencia del agente de transferencia de fase utilizado. Además, se preparó con el luminóforo disuelto y no en micropartículas, ya que origina resultados con mayor sensibilidad (1,4 veces) y exactitud (1,7 veces). Estas membranas pueden ser utilizadas durante más de cuatro meses, conservándose en condiciones de atmósfera húmeda y oscuridad.

2. Se han incluido las membranas sensoras mencionadas para dióxido de carbono en una instrumentación portátil de bajo coste y fácil manejo diseñada y construida en el grupo de investigación. De las diferentes disposiciones de membrana ensayadas, se obtuvieron los mejores resultados con aquella en la que los cócteles se depositan directamente sobre los componentes optoelectrónicos (LED y fotodetector) ya que presentaba mejor respuesta a dióxido de carbono en términos de sensibilidad y reproducibilidad. Como resultado obtuvimos un instrumento portátil capaz de medir dióxido de carbono gaseoso hasta el 100% de concentración, que permite la corrección de la temperatura, con unos tiempos de recuperación y respuesta (t_{90} = 31 s, t_{10} = 117 s) comparables a otros sensores basados en las propiedades ácidas de este gas. Además se trata de membranas estables, ya que si se conservan los fotodetectores

en oscuridad y atmósfera húmeda pueden ser utilizados durante aproximadamente mil días y si se utiliza en modo continuo, se recomienda una recalibración cada siete días

3. Se ha desarrollado un instrumento portátil para la medida simultánea de oxígeno (0-30%) y dióxido de carbono (0-100%). Esta instrumentación consta de cuatro canales, destinados dos de ellos a la medida de un gas y los otros dos a la medida del otro, con lo que es posible realizar medidas redundantes. En este dispositivo y para el caso del oxígeno no existe interferencia por parte del dióxido de carbono, pero sí en la dirección opuesta, por lo que se modeló esta dependencia y se introdujo en el microcontrolador del equipo para su corrección. Igualmente se modeló la dependencia a la temperatura de ambos sistemas con objeto de posterior compensación. De los estudios de comportamiento dinámico, se obtienen tiempo de recuperación y respuesta similares a los del equipo anterior: t_{90} 31,0 ± 0.9s (sensor O_2) y 31,0 ± 2.4s (sensor CO_2) y t_{10} 149,7 ± 3,7s (sensor O_2) y 124,9 ± 5,4s (sensor CO_2). Este prototipo presenta una serie de nuevos elementos como son un microventilador, que se apaga justo antes de realizar la medida y que facilita el flujo de aire hacia el interior del equipo y un reloj de 100 MHz, en lugar del de 20 MHz que se empleó en el equipo previo, con lo que obtuvimos una resolución cinco veces mayor. Con ello tenemos una instrumentación capaz de medir simultáneamente ambos gases con los componentes optoelectrónicos recubiertos con las películas sensoras, que son fácilmente reemplazables cuando es necesario y con un largo tiempo de vida.

4. Se ha puesto a punto un equipo portátil de medida de dióxido de carbono gaseoso hasta el 100 %, utilizando en lugar del sistema LED-fotodetector antes usado, un sistema LED-LED, que tiene una serie de ventajas como simplicidad de la electrónica empleada y por tanto de los equipos resultantes, alta sensibilidad, bajo coste y elevada resolución. De las dos configuraciones estudiadas, una en la que medimos cambios

en intensidad de fosforescencia y otra en la que medimos cambios de absorbancia, se selecciona esta última como óptima debido a que presentaba un menor límite de detección (LOD 0,0066%). Consiguiendo con este equipo un LOD por debajo del nivel de dióxido de carbono ambiental. Se obtuvo de esta manera un equipo versátil capaz de trabajar a muy baja concentración de dióxido de carbono (por debajo del valor atmosférico y hasta un 1%) utilizando para la calibración los datos brutos obtenidos debido a la gran precisión en la medida o bien, en un rango mayor mediante el uso de la ecuación de calibración propuesta (2.6 hasta 100%). Los tiempos de recuperación y respuesta (t_{90} 11 ± 1 s; t_{10} 55 ± 5 s) que encontramos con este equipo son menores a los encontrados con los otros equipos que hemos desarrollado. La precisión intra-día encontrada proporciona un resultado notable, 1,15% (n=8). El estudio inter-día se realizó durante cinco días consecutivos, obteniendo una precisión del 1,77% (n=8). En conclusión, tenemos una instrumentación capaz de medir dióxido de carbono, incluso por debajo del nivel ambiental, en la que se ha corregido la dependencia de la temperatura, con las membranas depositadas sobre soportes intercambiables para dar un grado extra de libertad al sistema.

5. Se planteó el desarrollo de un sensor para medir oxígeno edáfico (0-35%), por lo que se diseñó una nueva sonda de forma que pudiera ser enterrada cerca de las raíces permitiendo a su vez la entrada de aire, pero no la de agua para evitar un mal funcionamiento en el sistema. Además de oxígeno, también mide humedad y temperatura, parámetros que son interesantes de conocer y que en el caso de la temperatura afectan además a la respuesta del sensor de oxígeno. Se ha concluido que la humedad no afecta a este sensor de oxígeno. Se caracterizó el equipo en condiciones controladas en laboratorio (en cámara térmica y en un lisímetro) obteniendo un LOD de 0,14% y un tiempo de recuperación y respuesta de 28.5 ± 0.6 s y 59.0 ± 2.2 s en cámara térmica y de 7,7 ± 0,2 min y 15,9 ± 0,2 min en lisímetro. La aplicabilidad de la sonda se comprobó en árboles *Ilex x meserveae* (acebos) de diferente edad

(2 y 3 años) sometidos a ciclos de inundación y drenaje. Las medidas aquí obtenidas nos indican la buena capacidad de esta sonda sensora para medir concentración de oxígeno, temperatura y humedad relativa en suelo.

Publicaciones

Artículos

Artículos publicados

1. Phosphorescent sensing of carbón dioxide based on secondary inner-filter quenching Analytica Chimica Acta 655 (2009) 66-74
2. Hand-held instrument for CO_2 in gas phase based on sensing film coating optoelectronic elements. Sensors and Actuators, B: Chemical 144 (2010), B127(2), 232-238
3. Compact optical instrument for simultaneous determination of O_2 and CO_2. Microchimica acta (2011), 172: 455-464

Artículos enviados

1. A new LED-LED portable CO_2 gas sensor based on an interchangeable membrane system for industrial applications. Analytica Chimica Acta. (Ms. No.: ACA-11-600, en revisión)
2. Multisensor probe for soil monitoring. Sensors and Actuators, B: Chemical.

Aportaciones a actas de congresos

Posters

1. Participación en XIV International Symposium on luminescence spectrometry con el trabajo titulado “Phosphorescent sensing of O_2 and CO_2 using a portable instrument” celebrado en Praga (República Checa), Julio 2010

2. Participación en VII Colloquium Chemiometricum Mediterraneum con el trabajo titulado “Optimization of experimental variables by Doehlert design in a portable optical CO_2 instrumentation” celebrado en Granada, del 21 al 24 de Junio de 2010.

3. Participación en Europtrode X (European Conference on Optical Chemical Sensors and Biosensors) con el trabajo titulado: “Compact optical instrument for simultaneous O_2 and CO_2 determination” celebrado en Praga (República Checa), del 28 al 1 de Marzo de 2010

4. Participación en Euroanalysis 2009 con el trabajo: “Multy analyte imaging in one-shot format sensors for natural waters” celebrado en en Innsbruck (Austria) del 6 al 10 de Septiembre de 2009

5. Participación en Euroanalysis 2009 con el trabajo: “Use of Hue coordinate of the HSV color space as a quantitative parameter for bitonal optical sensors” celebrado en Innsbruck (Austria) del 6 al 10 de Septiembre de 2009

6. Participación en Euroanalysis 2009 con el trabajo: “Hand-held optical instrument for CO_2 in gas phase base on sensing film coating optoelectronic elements” celebrado en Innsbruck (Austria) del 6 al 10 de Septiembre de 2009

7. Participación en Europtrode IX (European Conference on Optical Chemical Sensors and Biosensors) con el trabajo:"CO_2-sensing film with nanoparticles encapsulated for portable instrumentation" en Dublin (Irlanda) del 28 al 1 de Marzo de 2010

8. Participación en GRASEQA 2008 XI Reunión del Grupo Regional Andaluz de la Sociedad Española de Química Analítica con el trabajo:" Sensor óptico para determinación de CO_2 empleando complejos de rutenio celebrado en Huelva 12-13 Junio

9. Participación en 12as Jornadas de Análisis Instrumental (JAI) con el trabajo: "Portable instrumentation for CO_2 measurement" celebrado en Barcelona del 21 al 23 de Octubre de 2008

Comunicaciones orales flash (poster + presentación oral corta)

1. Participación en GRASEQA 2010 XII Reunión del Grupo Regional Andaluz de la Sociedad Española de Química Analítica con el trabajo: "Instrumentación portátil para la determinación simultánea de O_2 y CO_2 en gases" celebrado en Córdoba del 10 al 11 de Junio de 2010

2. Participación en I Workshop sobre Nanotecnología Analítica con el trabajo: "Empleo de nanopartículas con luminóforo interno para medidas de dióxido de carbono" celebrado en Córdoba del de Julio de 2007

Comunicaciones orales

1. Participación en Conference on Analytical Sciences Ireland 2011- 6th Casi con el trabajo titulado: "A new LED-LED portable CO_2 gas sensor based on an interchangeable membrane system for industrial applications" celebrado en Dublín (Irlanda) 21-22 de Febrero de 2011

2. Participación en Jornadas Andaluzas de Formación inicial del Profesorado Universitario. El Papel de los Mentores con el trabajo titulado: “Integración de distintos tipos de actuaciones en la formación del profesorado novel: mentorización, asesoramiento y entrenamiento” celebrado en Granada en 2010